

Electronic Supporting Information

Effective stabilization of a planar phosphorus(III) center embedded in a porphyrin-based fused aromatic skeleton

Keisuke Fujimoto and Atsuhiko Osuka*

Department of Chemistry, Graduate School of Science, Kyoto University, Sakyo-ku, Kyoto 606-8502,
Japan.

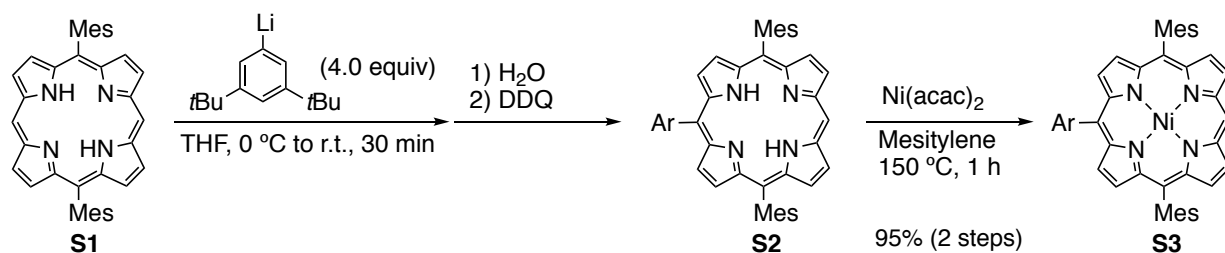
Contents

1. Instrumentation and Materials
2. Experimental Procedures and Compound Data
3. NMR Spectra
4. High Resolution Mass Spectra
5. X-Ray Crystal Structures
6. Absorption Spectra
7. Determination of Pyramidal Inversion Barriers
8. Electrochemical Properties
9. Temperature Dependent Magnetic Susceptibility
10. DFT Calculations
11. References

1. Instrumentation and Materials

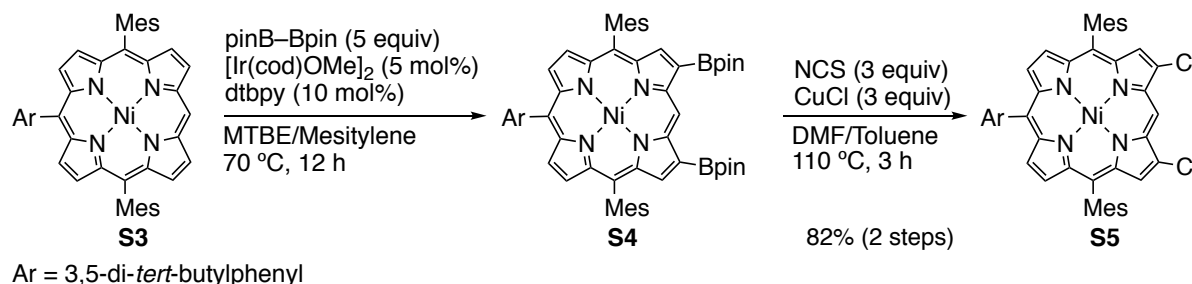
^1H NMR (600 MHz), ^{13}C NMR (151 MHz), and ^{31}P NMR (243 MHz) spectra were taken on a JEOL ECA-600 spectrometer. Chemical shifts were reported as delta scale in ppm relative to CHCl_3 ($\delta = 7.26$) and CH_2Cl_2 ($\delta = 5.31$) for ^1H NMR, to CDCl_3 ($\delta = 77.16$) for ^{13}C NMR, and to H_3PO_4 ($\delta = 0.00$) for ^{31}P NMR. UV/Vis absorption spectra were recorded on a Shimadzu UV-3600PC spectrometer. High-resolution APCI-TOF mass spectra were taken on a Bruker micrOTOF. X-Ray single crystal diffraction analyses were performed on a Rigaku XtaLAB P200 apparatus at -180 °C using two-dimensional detector PILATUS 100K/R with $\text{Cu-}K_\alpha$ radiation ($\lambda = 1.54187$ Å). The structures were solved by direct method SIR-97 and refined by SHELXL-97 program.^[S1] Redox potentials were measured by cyclic voltammetry on an ALS electrochemical analyzer model 660. Magnetic susceptibility was measured for the powder sample with the temperature range from 2 to 300 K at 0.5 T magnetic field by a Quantum Design MPMS-2S instrument. Toluene and *o*-dichlorobenzene (*o*-DCB) were distilled from CaH_2 . THF and ether was purified by passing through a neutral alumina column under N_2 . CHCl_3 was purified by passing through alumina column. Methyl *tert*-butyl ether (MTBE) and mesitylene were dried over activated MS4A under N_2 . Anhydrous dimethylacetamide (DMA) was purchased from Sigma Aldrich. Unless otherwise noted, materials obtained from commercial suppliers were used without further purification.

2. Experimental Procedures and Compound Data



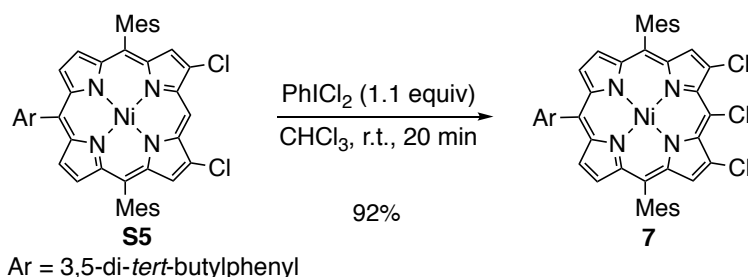
Synthesis of S3: To a Schlenk tube containing Li shot (210 mg, 30 mmol) and dry ether (6.0 mL), 1-bromo-3,5-di-*tert*-butylbenzene (2.8 g, 10 mmol in 6.0 mL of ether) was slowly added under argon atmosphere. After the solution was stirred at room temperature for 1 h, the resulting solution of 3,5-di-*tert*-butylphenyllithium was transferred to a Schlenk tube containing 5,15-dimesitylporphyrin **S1** (1.1 g, 2.0 mmol) and dry THF (60 mL) at 0 °C under argon atmosphere. After the reaction mixture was stirred at 0 °C for 10 min and then at room temperature for 30 min, H₂O (2.0 mL) was added. After stirring at room temperature for 10 min, 2,3-dichloro-5,6-dicyano-1,4-benzoquinone (DDQ) (2.3 g, 10 mmol) was added. After further stirring at room temperature for 30 min, the reaction mixture was passed through alumina column eluting with CH₂Cl₂. After removal of the solvent *in vacuo*, the residue was purified by silica gel chromatography eluting with CH₂Cl₂/hexane and then dissolved in mesitylene (70 mL). To the obtained mesitylene solution of **S2**, Ni(acac)₂ (2.1 g, 7.0 mmol) was added. After stirring at 150 °C for 1 h, the reaction mixture was passed through silica gel column eluting with CH₂Cl₂. After removal of the solvent *in vacuo*, recrystallization from CH₂Cl₂/methanol gave **S3** (1.5 g, 1.9 mmol, 95%).

S3: ¹H NMR (600 MHz, CDCl₃, 25 °C): δ = 9.79 (s, 1H, *meso*), 9.10 (d, *J* = 4.6 Hz, 2H, β), 8.79 (d, *J* = 4.2 Hz, 2H, β), 8.72 (d, *J* = 4.6 Hz, 2H, β), 8.63 (d, *J* = 5.0 Hz, 2H, β), 7.91 (d, *J* = 1.4 Hz, 2H, Ar-*o*), 7.72 (t, *J* = 1.6 Hz, 1H, Ar-*p*), 7.22 (s, 4H, Mes), 2.58 (s, 6H, Mes), 1.82 (s, 12H, Mes), and 1.47 (s, 18H, *tert*-butyl) ppm; ¹³C NMR (151 MHz, CDCl₃, 25 °C): δ = 148.95, 143.03, 142.97, 142.83, 142.65, 140.38, 139.22, 137.79, 137.57, 132.89, 132.47, 131.52, 130.93, 129.14, 127.89, 121.14, 120.57, 117.07, 104.25, 35.16, 31.84, 21.56, and 21.53 ppm; HR-APCI-TOF-MS: *m/z* = 790.3586. Calcd for C₅₂H₅₂N₄⁵⁸Ni: 790.3551 [M]⁺; UV/Vis (CH₂Cl₂): λ_{max} (ε [M⁻¹cm⁻¹]) = 408 (2.5 × 10⁵), and 521 (1.8 × 10⁴) nm.



Synthesis of S5: A Schlenk tube containing **S3** (633 mg, 0.80 mmol), (Bpin)₂ (1.02 g, 4.0 mmol), [Ir(cod)OMe]₂ (26 mg, 0.040 mol), and 4,4'-di-*tert*-butyl-2,2'-bipyridine (dtbpy) (20 mg, 0.080 mmol) was filled with argon, and then charged with dry mesitylene (4.0 mL) and dry MTBE (12 mL). After stirring at 70 °C for 12 h, the reaction mixture was passed through short silica gel column eluting with CH₂Cl₂. After removal of the solvent *in vacuo*, the product **S4** was obtained by recrystallization from CH₂Cl₂/methanol. Then, **S4** was dissolved in *N,N*-dimethylformamide (DMF) (80 mL) and toluene (40 mL). To the resulting solution, *N*-chlorosuccinimide (NCS) (322 mg, 2.4 mmol) and CuCl (238 mg, 2.4 mmol) were added. After stirring at 110 °C for 3 h, the reaction mixture was quenched with aqueous Na₂S₂O₃ solution, extracted with hexane, washed with water and brine, and dried over Na₂SO₄. After removal of the solvent *in vacuo*, the residue was separated by silica gel chromatography eluting with CH₂Cl₂/hexane. Recrystallization from CH₂Cl₂/methanol gave **S5** (565 mg, 0.66 mmol, 82%).

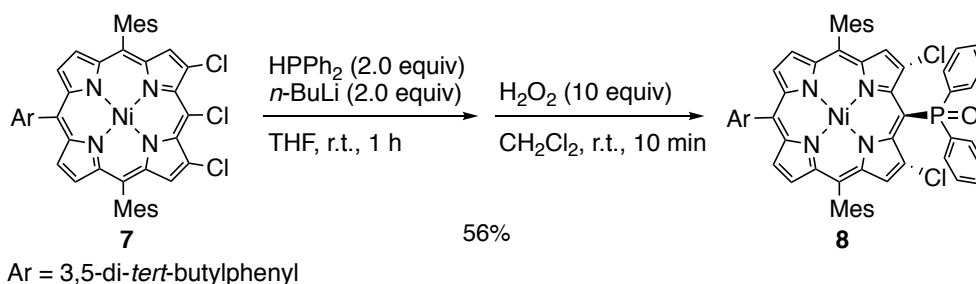
S5: ¹H NMR (600 MHz, CDCl₃, 25 °C): δ = 10.13 (s, 1H, *meso*), 8.74 (d, *J* = 4.6 Hz, 2H, β), 8.59 (d, *J* = 4.6 Hz, 2H, β), 8.56 (s, 2H, β), 7.88 (d, *J* = 1.8 Hz, 2H, Ar-*o*), 7.72 (s, 1H, Ar-*p*), 7.22 (s, 4H, Mes), 2.58 (s, 6H, Mes), 1.80 (s, 12H, Mes), and 1.47 (s, 18H, *tert*-butyl) ppm; ¹³C NMR (151 MHz, CDCl₃, 25 °C): δ = 149.14, 143.84, 143.02, 140.49, 139.94, 139.24, 139.10, 138.20, 136.82, 133.50, 133.14, 131.53, 129.06, 128.21, 128.06, 121.54, 121.39, 117.58, 98.25, 35.18, 31.82, 21.56, and 21.52 ppm; HR-APCI-TOF-MS: *m/z* = 858.2764. Calcd for C₅₂H₅₀N₄³⁵Cl₂⁵⁸Ni: 858.2771 [M]⁺; UV/Vis (CH₂Cl₂): λ_{max} (ε [M⁻¹cm⁻¹]) = 412 (2.5 × 10⁵) and 526 (1.5 × 10⁴) nm.



Synthesis of 7: To a flask containing **S5** (516 mg, 0.60 mmol) dissolved in CHCl₃ (30 mL), a suspension of PhICl₂ (180 mg, 0.66 mmol) in 30 mL of CHCl₃ was added. After stirring at room temperature for 20 min, the reaction mixture was passed through short silica gel column eluting with CH₂Cl₂. Recrystallization from CH₂Cl₂/methanol gave **7** (493 mg, 0.55 mmol, 92%).

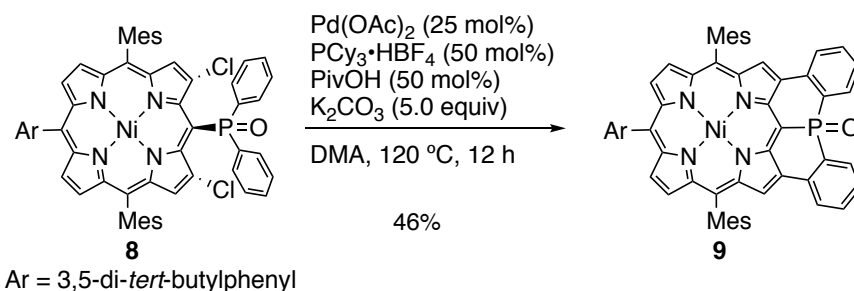
7: ¹H NMR (600 MHz, CDCl₃, 25 °C): δ = 8.62 (d, *J* = 4.6 Hz, 2H, β), 8.49 (s, 2H, β), 8.44 (d, *J* = 5.0 Hz, 2H, β), 7.78 (d, *J* = 1.8 Hz, 2H, Ar-*o*), 7.69 (s, 1H, Ar-*p*), 7.18 (s, 4H, Mes), 2.55 (s, 6H, Mes), 1.83 (s, 12H, Mes), and 1.44 (s, 18H, *tert*-butyl) ppm; ¹³C NMR (151 MHz, CDCl₃, 25 °C): δ = 149.39, 144.02, 142.11, 139.02, 138.99, 138.30, 137.74, 136.16, 134.78, 134.16, 133.23, 132.25, 132.50, 128.76, 128.09, 121.53, 120.40, 117.17, 110.48, 35.16,

31.78, 21.50, and 21.44 ppm; HR-APCI-TOF-MS: $m/z = 892.2376$. Calcd for $C_{52}H_{49}N_4^{35}Cl_3^{58}Ni$: 892.2382 [M]⁻; UV/Vis (CH_2Cl_2): λ_{max} (ϵ [$M^{-1}cm^{-1}$]) = 425 (1.9×10^5) and 543 (1.5×10^4) nm.



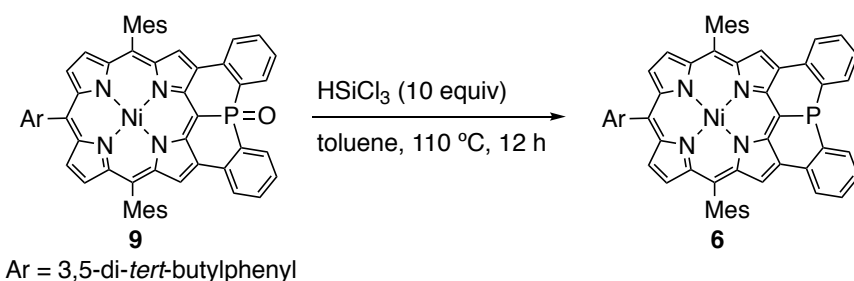
Synthesis of 8: To a Schlenk tube containing diphenylphosphine ($HPPH_2$, 103 μ L, 0.60 mmol) and dry THF (3.0 mL), n -BuLi (1.6 M in hexane, 0.37 mL, 0.60 mmol) was slowly added at 0 °C under argon atmosphere. After the solution was stirred at room temperature for 20 min, the resulting solution was transferred to a Schlenk tube containing 3,5,7-trichloroporphyrin **7** (269 mg, 0.30 mmol) and dry THF (15 mL) at room temperature under argon atmosphere. After stirring at room temperature for 1 h, the reaction mixture was quenched by aqueous NH_4Cl solution, extracted with CH_2Cl_2 , and dried over Na_2SO_4 . After removal of the solvent *in vacuo*, the residue was dissolved in CH_2Cl_2 (30 mL). To the CH_2Cl_2 solution, H_2O_2 (30% in water, 0.3 mL, 3 mmol) was added. After stirring at room temperature for 10 min, the reaction mixture was quenched by aqueous $Na_2S_2O_3$ solution, extracted with CH_2Cl_2 , and dried over Na_2SO_4 . After removal of the solvent *in vacuo*, the residue was separated by silica gel chromatography eluting with $AcOEt/CH_2Cl_2$. Recrystallization from CH_2Cl_2 /methanol gave **8** (177 mg, 167 μ mol, 56%).

8: 1H NMR (600 MHz, $CDCl_3$, -30 °C): δ = 8.60 (d, J = 4.6 Hz, 2H, β), 8.31 (s, 1H, Ar-*o*), 8.29 (d, J = 5.0 Hz, 2H, β), 8.02 (s, 2H, β), 7.70 (s, 1H, Ar-*p*), 7.44 (s, 1H, Ar-*o*), 7.22 (s, 2H, Mes), 7.02 (t, J = 7.3 Hz, 2H, Ph), 6.99 (s, 2H, Mes), 6.75 (broad, 4H, Ph), 6.49 (broad, 4H, Ph), 2.48 (s, 6H, Mes), 2.16 (s, 6H, Mes), 1.54 (s, 9H, *tert*-butyl), 1.37 (s, 9H, *tert*-butyl), and 1.29 (s, 6H, Mes) ppm; ^{13}C NMR (151 MHz, $CDCl_3$, 25 °C): δ = 149.54, 145.72, 145.67, 143.92, 142.85, 139.49, 139.34, 138.77, 138.35, 138.05 (d, J = 5.8 Hz), 135.74, 135.52, 134.37, 133.05, 130.99, 130.84 (d, J = 8.7 Hz), 129.98, 128.04 (d, J = 14.5 Hz), 127.16 (d, J = 11.6 Hz), 125.68, 121.86, 119.82, 94.53 (d, J = 110 Hz), 35.21, 31.80, 21.44, 21.23, and 21.11 ppm; ^{31}P NMR (243 MHz, $CDCl_3$, 25 °C): δ = 12.90 ppm; HR-APCI-TOF-MS: $m/z = 1058.3152$. Calcd for $C_{64}H_{59}ON_4^{35}Cl_2P^{58}Ni$: 1058.3163 [M]⁻; UV/Vis (CH_2Cl_2): λ_{max} (ϵ [$M^{-1}cm^{-1}$]) = 447 (1.8×10^5), 594 (9.1×10^3), and 625 (1.5×10^4) nm.



Synthesis of 9: A Schlenk tube containing **8** (127 mg, 0.12 mmol), Pd(OAc)₂ (6.7 mg, 0.030 mmol), PCy₃·HBF₄ (22 mg, 0.060 mmol), PivOH (6.0 mg, 0.060 mmol), and K₂CO₃ (84 mg, 0.60 mmol) was filled with argon, and then charged with dry DMA (12 mL). After stirring at 120 °C for 12 h, the reaction mixture was quenched with water, extracted with hexane/CH₂Cl₂, washed with water twice and brine, and dried over Na₂SO₄. After removal of the solvent *in vacuo*, the residue was separated by silica gel chromatography eluting with AcOEt/CH₂Cl₂. Recrystallization from CH₂Cl₂/methanol gave **9** (54 mg, 55 μmol, 46%).

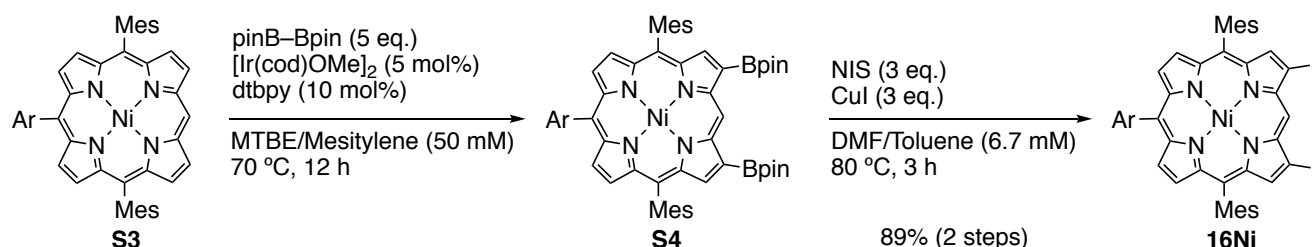
9: ¹H NMR (600 MHz, CDCl₃, -30 °C): δ = 8.68 (s, 2H, β), 8.56 (dd, *J* = 7.8 and 11.0 Hz, 2H, P-Ph), 8.50 (d, *J* = 5.0 Hz, 2H, β), 8.28 (d, *J* = 4.4 Hz, 2H, β), 8.24 (dd, *J* = 7.8 and 4.6 Hz, 2H, P-Ph), 8.19 (s, 1H, Ar-*o*), 7.67 (s, 1H, Ar-*p*), 7.65 (t, *J* = 7.8 Hz, 2H, P-Ph), 7.56 (t, *J* = 7.3 Hz, 2H, P-Ph), 7.44 (s, 1H, Ar-*o*), 7.32 (s, 2H, Mes), 7.08 (s, 2H, Mes), 2.56 (s, 6H, Mes), 2.31 (s, 6H, Mes), 1.51 (s, 9H, *tert*-butyl), 1.39 (s, 6H, Mes), and 1.37 (s, 9H, *tert*-butyl) ppm; ¹³C NMR (151 MHz, CDCl₃, 25 °C): δ = 149.19 (broad), 145.08, 143.93, 142.08, 140.81 (d, *J* = 7.2 Hz), 139.54, 139.12, 138.74 (d, *J* = 8.6 Hz), 138.52, 138.23, 136.08, 135.63 (d, *J* = 7.2 Hz), 134.00, 132.50, 132.05, 131.03, 128.84 (d, *J* = 10.1 Hz), 128.46, 128.23, 127.92, 127.66, 126.97 (d, *J* = 8.5 Hz), 125.24, 121.60, 120.61, 96.36 (d, *J* = 107 Hz), 35.16, 31.78, 21.88, 21.54, and 21.27 ppm; ³¹P NMR (243 MHz, CDCl₃, 25 °C): δ = 0.88 ppm; HR-APCI-TOF-MS: *m/z* = 986.3623. Calcd for C₆₄H₅₇ON₄P⁵⁸Ni: 986.3629 [M]⁻; UV/Vis (CH₂Cl₂): λ_{max} (ε [M⁻¹cm⁻¹]) = 455 (1.4 × 10⁵), 594 (9.8 × 10³), and 643 (1.4 × 10⁴) nm.



Synthesis of 9: A Schlenk tube containing **9** (30 mg, 30 μmol) was filled with argon, and then charged with dry toluene (1.5 mL) and HSiCl₃ (0.20 M in toluene, 1.5 mL, 30 μmol). After stirring at 110 °C for 12 h, the reaction mixture was quenched by aqueous NaHCO₃ solution, extracted with CH₂Cl₂, and dried over Na₂SO₄. After removal

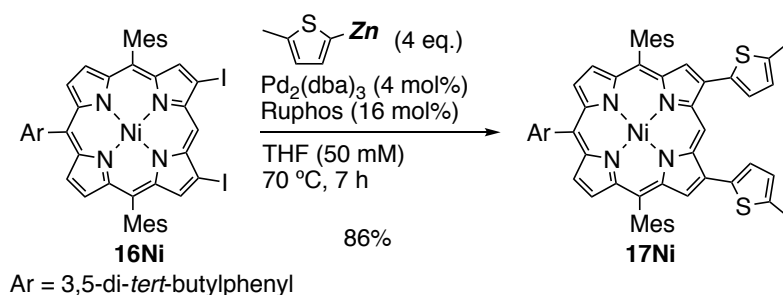
of the solvent *in vacuo*, the residue was separated by silica gel chromatography eluting with CH₂Cl₂/hexane. Recrystallization from CH₂Cl₂/methanol gave **6** (18 mg, 19 μmol, 65%).

6: ¹H NMR (600 MHz, CDCl₃, -30 °C): δ = 9.03 (s, 2H, β), 8.69 (m, 4H, β(2H) and Ph(2H)), 8.61 (d, *J* = 7.4 Hz, 2H, Ph), 8.54 (d, *J* = 5.0 Hz, 2H, β), 8.39 (s, 1H, Ar-*o*), 7.72 (m, 4H, Ph), 7.67 (t, *J* = 1.8 Hz, 1H, Ar-*p*), 7.40 (s, 2H, Mes), 7.38 (s, 1H, Ar-*o*), 7.09 (s, 2H, Mes), 2.58 (s, 6H, Mes), 2.45 (s, 6H, Mes), 1.55 (s, 9H, *tert*-butyl), 1.35 (s, 9H, *tert*-butyl), and 1.28 (s, 6H, Mes) ppm; ¹³C NMR (151 MHz, CDCl₃, 25 °C): δ = 149.13, 144.04, 142.52, 140.90, 140.13, 140.01, 139.28 (broad), 137.88, 137.13, 136.33, 134.16, 132.95, 131.73, 130.63, 129.04, 128.86, 128.05, 127.61, 126.64, 122.47, 121.12, 118.68, 117.35, 113.75, 35.17, 31.83, and 21.59 ppm; ³¹P NMR (243 MHz, CDCl₃, 25 °C): δ = -20 ppm (broad); HR-APCI-TOF-MS: *m/z* = 970.3671. Calcd for C₆₄H₅₇N₄P⁵⁸Ni: 970.3680 [M]⁻; UV/Vis (CH₂Cl₂): λ_{max} (ε [M⁻¹cm⁻¹]) = 456 (1.7 × 10⁵), 564 (1.8 × 10⁴), and 611 (7.8 × 10³) nm.



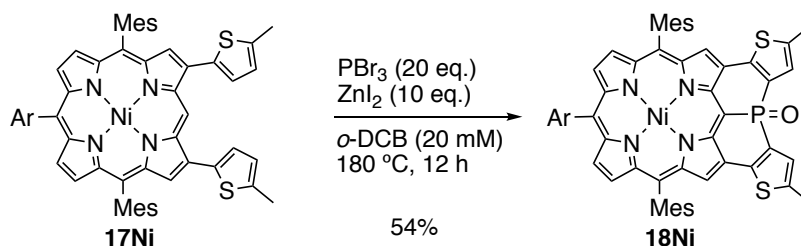
Synthesis of 16Ni: A Schlenk tube containing **S3** (791 mg, 1.0 mmol), (Bpin)₂ (1.27 g, 5.0 mmol), [Ir(cod)OMe]₂ (33 mg, 0.050 mmol), and dtbpy (27 mg, 0.10 mmol) was filled with argon, and then charged with dry mesitylene (5.0 mL) and dry MTBE (15 mL). After stirring at 70 °C for 12 h, the reaction mixture was passed through short silica gel column eluting with CH₂Cl₂. After removal of the solvent *in vacuo*, the borylated porphyrin **S4** was obtained by recrystallization from CH₂Cl₂/methanol. Then, **S4** was dissolved in DMF (100 mL) and toluene (50 mL). To the resulting solution, *N*-iodosuccinimide (NIS) (675 mg, 3.0 mmol) and CuI (570 mg, 3.0 mmol) were added. After stirring at 80 °C for 3 h, the reaction mixture was diluted with toluene (400 mL), washed with aqueous NH₄Cl solution, aqueous Na₂S₂O₃ solution, water, and brine, and dried over Na₂SO₄. After passed through short silica gel column eluting with toluene, the solvent was removed *in vacuo*. Recrystallization from CH₂Cl₂/methanol gave **16Ni** (930 mg, 0.89 mmol, 89%).

16Ni: ¹H NMR (600 MHz, CDCl₃, 25 °C): δ = 9.96 (s, 1H, *meso*), 8.92 (s, 2H, β), 8.73 (d, *J* = 5.0 Hz, 2H, β), 8.59 (d, *J* = 5.0 Hz, 2H, β), 7.87 (d, *J* = 1.8 Hz, 2H, Ar-*o*), 7.72 (t, *J* = 1.8 Hz, 1H, Ar-*p*), 7.23 (s, 4H, Mes), 2.59 (s, 6H, Mes), 1.80 (s, 12H, Mes), and 1.46 (s, 18H, *tert*-butyl) ppm; ¹³C NMR (151 MHz, CDCl₃, 25 °C): δ = 149.13, 143.98, 143.17, 142.86, 142.61, 139.86, 139.62, 139.13, 138.18, 136.73, 133.51, 131.80, 129.01, 128.04, 121.38, 121.28, 116.86, 106.10, 92.04, 35.17, 31.80, and 21.54 ppm; HR-APCI-TOF-MS: *m/z* = 1042.1502. Calcd for C₅₂H₅₀N₄I₂⁵⁸Ni: 1042.1473 [M]⁻; UV/Vis (CH₂Cl₂): λ_{max} (ε [M⁻¹cm⁻¹]) = 418 (2.3 × 10⁵), 529 (1.5 × 10⁴), and 559 nm (6.0 × 10³).



Synthesis of 17Ni: To a Schlenk tube containing 2-bromo-5-methylthiophene (0.20 mL, 1.76 mmol) and dry THF (8.0 mL), *n*-BuLi (1.6 M hexane solution, 1.00 mL, 1.6 mmol) was slowly added at $-80\text{ }^\circ\text{C}$ under argon atmosphere. After the reaction mixture was stirred at $-80\text{ }^\circ\text{C}$ for 1 h, $\text{ZnCl}_2\cdot\text{tmeda}$ (445 mg, 1.76 mmol) was added and further stirred for 1 h at room temperature. To the resulting thienylzinc solution, **16Ni** (417 mg, 0.40 mmol), $\text{Pd}_2(\text{dba})_3$ (15 mg, 0.016 mmol), and Ruphos (30 mg, 0.064 mmol) were added. After stirred at $70\text{ }^\circ\text{C}$ for 7 h, the reaction mixture was quenched with aqueous NH_4Cl solution, extracted with CH_2Cl_2 , and dried over Na_2SO_4 . After removal of the solvent *in vacuo*, the residue was separated by silica gel chromatography eluting with CH_2Cl_2 /hexane. Recrystallization from CH_2Cl_2 /methanol gave **17Ni** (339 mg, 0.34 mmol, 86%).

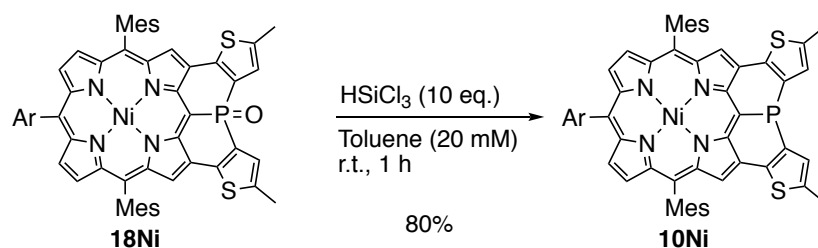
17Ni: ^1H NMR (600 MHz, CDCl_3 , $25\text{ }^\circ\text{C}$): δ = 10.55 (s, 1H, *meso*), 8.73 (d, J = 4.6 Hz, 2H, β), 8.64 (s, 2H, β), 8.56 (d, J = 4.6 Hz, 2H, β), 7.90 (d, J = 1.4 Hz, 2H, Ar-*o*), 7.71 (s, 1H, Ar-*p*), 7.61 (d, J = 3.2 Hz, 2H, thienyl), 7.21 (s, 4H, Mes), 7.04 (d, J = 2.3 Hz, 2H, thienyl), 2.69 (s, 6H, thienyl), 2.58 (s, 6H, Mes), 1.84 (s, 12H, Mes), and 1.47 (s, 18H, *tert*-butyl) ppm; ^{13}C NMR (151 MHz, CDCl_3 , $25\text{ }^\circ\text{C}$): δ = 149.03, 143.35, 142.90, 141.67, 141.24, 140.75, 140.14, 139.18, 139.10, 137.84, 137.26, 135.89, 133.08, 131.14, 129.06, 128.32, 127.96, 127.94, 126.86, 121.18, 120.42, 117.09, 103.31, 35.16, 31.83, 21.58, and 15.72 ppm; HR-APCI-TOF-MS: m/z = 982.3625. Calcd for $\text{C}_{62}\text{H}_{60}\text{N}_4^{58}\text{NiS}_2$: 982.3607 [M] $^+$; UV/Vis (CH_2Cl_2): λ_{max} (ϵ [$\text{M}^{-1}\text{cm}^{-1}$]) = 426 (1.9×10^5), 537 (2.0×10^4), and 569 (1.2×10^4) nm.



Synthesis of 18Ni: A Schlenk tube containing **17Ni** (197 mg, 0.20 mmol) and ZnI_2 (636 mg, 2.0 mmol) was filled with argon, and then charged with dry *o*-DCB (10 mL) and PBr_3 (0.40 mL, 4.0 mmol). After stirring at $180\text{ }^\circ\text{C}$ for 12 h, the reaction mixture was quenched by aqueous NaHCO_3 solution, extracted with CH_2Cl_2 , washed with water, and dried over Na_2SO_4 . After removal of CH_2Cl_2 *in vacuo*, H_2O_2 (30% in water, 0.4 mL, 4 mmol) was added to the resulting *o*-DCB solution. After stirring at room temperature for 10 min, the reaction mixture was quenched by aqueous $\text{Na}_2\text{S}_2\text{O}_3$ solution, extracted with CH_2Cl_2 , and dried over Na_2SO_4 . After removal of the solvent *in vacuo*, the

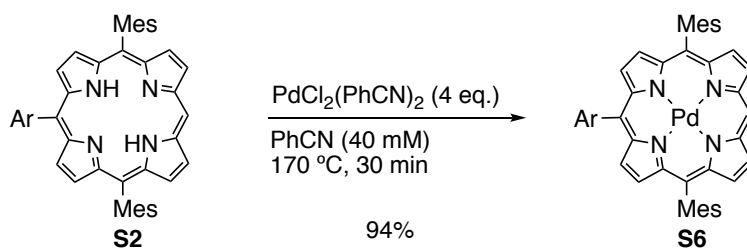
residue was separated by silica gel chromatography eluting with AcOEt/CH₂Cl₂. Recrystallization from CHCl₃/MeCN gave **18Ni** (110 mg, 107 μmol, 54%).

18Ni: ¹H NMR (600 MHz, CDCl₃, 25 °C): δ = 8.32 (d, *J* = 4.6 Hz, 2H, β), 8.12-8.08 (broad, 1H, Ar-*o*), 8.08 (d, *J* = 4.6 Hz, 2H, β), 8.02 (s, 2H, β), 7.67 (s, 1H, Ar-*p*), 7.46-7.42 (broad, 1H, Ar-*o*), 7.29 (s, 4H, Mes), 7.05 (s, 2H, thienyl), 2.61 (s, 6H, thienyl), 2.55 (s, 6H, Mes), 2.26 (s, 6H, Mes), 1.52-1.48 (broad, 9H, *tert*-butyl), 1.46 (s, 6H, Mes), and 1.40-1.36 (broad, 9H, *tert*-butyl) ppm; ¹³C NMR (151 MHz, CDCl₃, 25 °C): δ = 149.6-149.2 (broad), 145.46, 143.76, 142.79, 142.68, 142.37, 142.33, 139.40, 138.87, 138.37, 138.18, 135.73, 135.56 (d, *J* = 8.6 Hz), 133.76, 130.44, 128.20, 127.87, 127.77 (d, *J* = 114 Hz), 126.42, 126.33, 125.75 (d, *J* = 15.0 Hz), 121.62, 120.80, 96.74 (d, *J* = 113 Hz), 35.15, 31.76, 21.75, 21.50, 21.20, and 15.46 ppm; ³¹P NMR (243 MHz, CDCl₃, 25 °C): δ = -3.71 ppm HR-APCI-TOF-MS: *m/z* = 1026.3047. Calcd for C₆₂H₅₇N₄⁵⁸NiS₂PO: 1026.3059 [M]⁻; UV/Vis (CH₂Cl₂): λ_{max} (ε [M⁻¹cm⁻¹]) = 470 (1.0 × 10⁵), 647 (8.7 × 10³), and 706 (1.1 × 10⁴) nm.



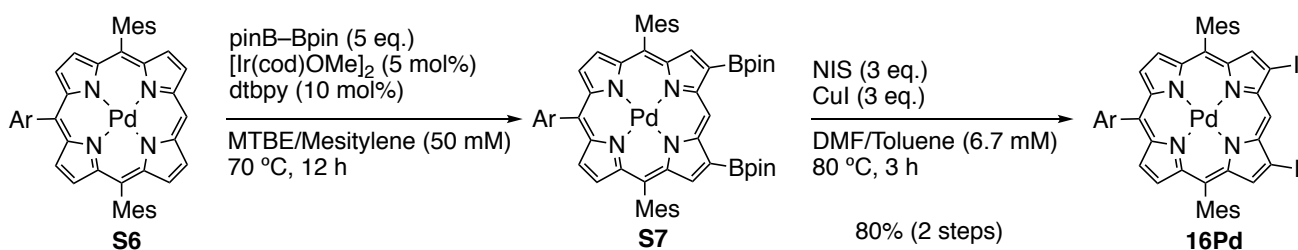
Synthesis of 10Ni: A Schlenk tube containing **18Ni** (10 mg, 10 μmol) was filled with argon, and then charged with and HSiCl₃ (0.2 M toluene solution, 0.50 mL, 0.10 mmol). After stirring at room temperature for 1 h, the reaction mixture was quenched by aqueous NaHCO₃ solution, extracted with CH₂Cl₂ and dried over Na₂SO₄. After removal of the solvent *in vacuo*, the residue was separated by silica gel chromatography eluting with CH₂Cl₂. Recrystallization from CH₂Cl₂/MeCN gave **10Ni** (8.0 mg, 8.0 μmol, 80%).

10Ni: ¹H NMR (600 MHz, CDCl₃, -40 °C): δ = 8.71 (d, *J* = 4.6 Hz, 2H, β), 8.59 (s, 2H, β), 8.53 (d, *J* = 4.6 Hz, 2H, β), 8.41 (s, 1H, Ar-*o*), 7.66 (t, *J* = 2.1 Hz, 1H, Ar-*p*), 7.60 (s, 2H, thienyl), 7.42 (s, 2H, Mes), 7.36 (s, 1H, Ar-*o*), 7.09 (s, 2H, Mes), 2.78 (s, 6H, thienyl), 2.60 (s, 6H, Mes), 2.49 (s, 6H, Mes), 1.55 (s, 9H, *tert*-butyl), 1.33 (s, 9H, *tert*-butyl), and 1.21 (s, 6H, Mes) ppm; ³¹P NMR (243 MHz, CDCl₃, 25 °C): δ = -15.4 ppm (broad); UV/Vis (CH₂Cl₂): λ_{max} (ε [M⁻¹cm⁻¹]) = 457 (9.4 × 10⁴) and 574 (1.9 × 10⁴) nm.



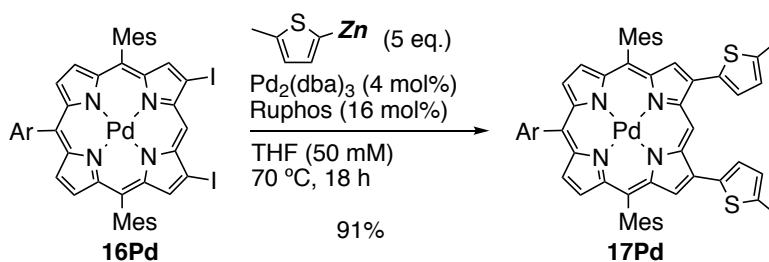
Synthesis of S6: A flask containing **S2** (735 mg, 1.0 mmol), $\text{PdCl}_2(\text{PhCN})_2$ (1.54 g, 4.0 mmol), and PhCN (25 mL, 40 mM) was warmed to 170 °C and stirred for 30 min. After the reaction mixture was cooled to room temperature, addition of MeOH (60 mL) gave red precipitation. Then, the resulting precipitate was filtered, washed with MeOH, and recrystallized from $\text{CHCl}_3/\text{MeOH}$ to obtain pure red solids of **S6** (788 mg, 0.94 mmol, 94%).

S6: ^1H NMR (600 MHz, CDCl_3 , 25 °C): δ = 10.13 (s, 1H, *meso*), 9.20 (d, J = 4.6 Hz, 2H, β), 8.83 (d, J = 5.0 Hz, 2H, β), 8.79 (d, J = 4.6 Hz, 2H, β), 8.68 (d, J = 5.0 Hz, 2H, β), 8.05 (d, J = 1.8 Hz, 2H, *Ar-o*), 7.77 (t, J = 1.8 Hz, 1H, *Ar-p*), 7.28 (s, 4H, Mes), 2.63 (s, 6H, Mes), 1.82 (s, 12H, Mes), and 1.51 (s, 18H, *tert*-butyl) ppm; ^{13}C NMR (151 MHz, CDCl_3 , 25 °C): δ = 148.87, 141.52, 141.44, 141.34, 141.17, 140.95, 139.40, 138.12, 137.86, 131.96, 131.47, 130.41, 129.73, 129.68, 127.93, 123.05, 121.15, 119.39, 106.12, 35.22, 31.90, 21.71, and 21.63 ppm; HR-APCI-TOF-MS: m/z = 836.3256. Calcd for $\text{C}_{52}\text{H}_{52}\text{N}_4^{104}\text{Pd}$: 836.3227 [M] $^-$; UV/Vis (CH_2Cl_2): λ_{max} (ϵ [$\text{M}^{-1}\text{cm}^{-1}$]) = 408 (2.1×10^5), 517 (1.8×10^4), and 549 (3.2×10^3) nm.



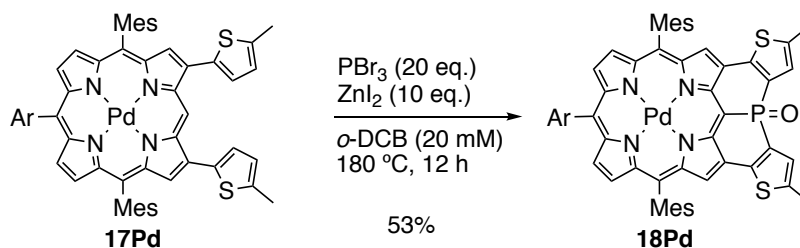
Synthesis of 16Pd: A Schlenk tube containing **S6** (671 mg, 0.80 mmol), $(\text{Bpin})_2$ (1.01 g, 4.0 mmol), $[\text{Ir}(\text{cod})\text{OMe}]_2$ (26 mg, 0.040 mmol), and dtbpy (22 mg, 0.080 mmol) was filled with argon, and then charged with dry mesitylene (4.0 mL) and dry MTBE (12 mL). After stirring at 70 °C for 12 h, the reaction mixture was passed through short silica gel column eluting with CH_2Cl_2 . After removal of the solvent *in vacuo*, the product **S7** was obtained by recrystallization from $\text{CH}_2\text{Cl}_2/\text{methanol}$. Then, **S7** was dissolved in DMF (80 mL) and toluene (40 mL). To the resulting solution, NIS (540 mg, 2.4 mmol) and Cul (456 mg, 2.4 mmol) were added. After stirring at 80 °C for 3 h, the reaction mixture was diluted with toluene (400 mL), washed with aqueous NH_4Cl solution, aqueous $\text{Na}_2\text{S}_2\text{O}_3$ solution, water, and brine, and dried over Na_2SO_4 . After passed through short silica gel column eluting with toluene, the solvent was removed *in vacuo*. Recrystallization from $\text{CHCl}_3/\text{methanol}$ gave **16Pd** (695 mg, 0.64 mmol, 80%).

16Pd: ^1H NMR (600 MHz, CDCl_3 , 25 °C): δ = 10.28 (s, 1H, *meso*), 9.00 (s, 2H, β), 8.78 (d, J = 5.0 Hz, 2H, β), 8.65 (d, J = 5.0 Hz, 2H, β), 8.01 (d, J = 1.8 Hz, 2H, Ar-*o*), 7.77 (t, J = 1.8 Hz, 1H, Ar-*p*), 7.28 (s, 4H, Mes), 2.63 (s, 6H, Mes), 1.81 (s, 12H, Mes), and 1.50 (s, 18H, *tert*-butyl) ppm; ^{13}C NMR was not obtained due to the poor solubility; HR-APCI-TOF-MS: m/z = 1088.1160. Calcd for $\text{C}_{52}\text{H}_{50}\text{N}_4\text{I}_2^{104}\text{Pd}$: 1088.1160 $[\text{M}]^-$; UV/Vis (CH_2Cl_2): λ_{max} (ϵ [$\text{M}^{-1}\text{cm}^{-1}$]) = 416 (2.1×10^5), 525 (2.2×10^4), and 552 nm (5.2×10^4).



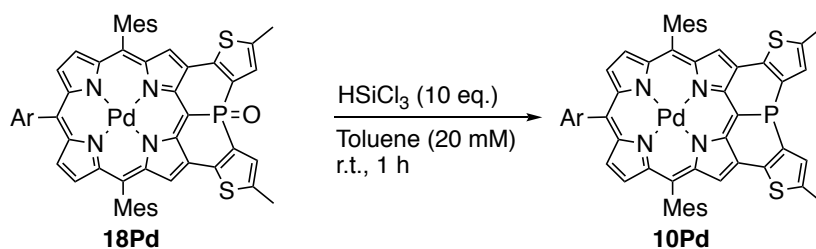
Synthesis of 17Pd: To a Schlenk tube containing 2-bromo-5-methylthiophene (0.31 mL, 2.8 mmol) and dry THF (10 mL), *n*-BuLi (1.6 M hexane solution, 1.60 mL, 2.5 mmol) was slowly added at -80 °C under argon atmosphere. After the reaction mixture was stirred at -80 °C for 1 h, $\text{ZnCl}_2 \cdot \text{tmeda}$ (696 mg, 2.8 mmol) was added and further stirred for 1 h at room temperature. To the resulting thienylzinc solution, **16Pd** (546 mg, 0.50 mmol), $\text{Pd}_2(\text{dba})_3$ (18 mg, 0.020 mmol), and Ruphos (37 mg, 0.080 mmol) were added. After stirred at 70 °C for 18 h, the reaction mixture was quenched with aqueous NH_4Cl solution, extracted with CH_2Cl_2 , and dried over Na_2SO_4 . After removal of the solvent *in vacuo*, the residue was separated by silica gel chromatography eluting with CH_2Cl_2 /hexane. Recrystallization from CH_2Cl_2 /methanol gave **17Pd** (469 mg, 0.45 mmol, 91%).

17Pd: ^1H NMR (600 MHz, CDCl_3 , 25 °C): δ = 10.94 (s, 1H, *meso*), 8.78 (d, J = 4.6 Hz, 2H, β), 8.72 (s, 2H, β), 8.62 (d, J = 4.6 Hz, 2H, β), 8.04 (d, J = 1.4 Hz, 2H, Ar-*o*), 7.79 (d, J = 2.3 Hz, 2H, thienyl), 7.77 (s, 1H, Ar-*p*), 7.27 (s, 4H, Mes), 7.10 (d, J = 2.3 Hz, 2H, thienyl), 2.73 (s, 6H, thienyl), 2.62 (s, 6H, Mes), 1.85 (s, 12H, Mes), and 1.51 (s, 18H, *tert*-butyl) ppm; ^{13}C NMR (151 MHz, CDCl_3 , 25 °C): δ = 148.93, 141.91, 141.82, 141.64, 140.80, 139.93, 139.41, 139.35, 138.23, 137.95, 137.91, 135.88, 132.10, 129.80, 129.62, 128.21, 127.99, 127.22, 126.89, 122.97, 121.17, 119.57, 104.49, 35.22, 31.89, 21.75, 21.63, and 15.77 ppm; HR-APCI-TOF-MS: m/z = 1028.3264. Calcd for $\text{C}_{62}\text{H}_{60}\text{N}_4^{104}\text{PdS}_2$: 1028.3294 $[\text{M}]^-$; UV/Vis (CH_2Cl_2): λ_{max} (ϵ [$\text{M}^{-1}\text{cm}^{-1}$]) = 424 (1.6×10^5), 533 (2.5×10^4), and 566 (1.2×10^4) nm.



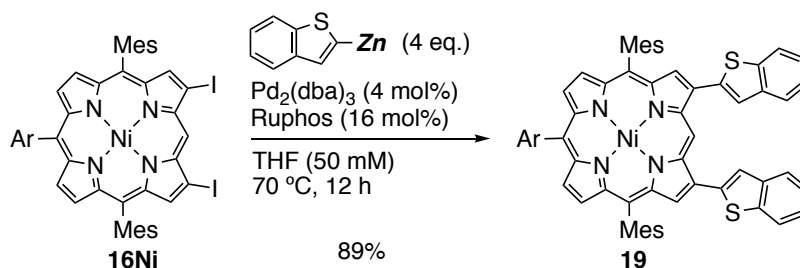
Synthesis of 18Pd: A Schlenk tube containing **17Pd** (206 mg, 0.20 mmol) and ZnI_2 (636 mg, 2.0 mmol) was filled with argon, and then charged with dry $o\text{-DCB}$ (10 mL) and PBr_3 (0.40 mL, 4.0 mmol). After stirring at $180\text{ }^\circ\text{C}$ for 12 h, the reaction mixture was quenched by aqueous NaHCO_3 solution, extracted with CH_2Cl_2 , washed with water, and dried over Na_2SO_4 . After removal of the solvent *in vacuo*, the residue was separated by silica gel chromatography eluting with $\text{AcOEt}/\text{CH}_2\text{Cl}_2$. Recrystallization from CH_2Cl_2 /methanol gave **18Pd** (114 mg, 106 μmol , 53%).

18Pd: ^1H NMR (600 MHz, CDCl_3 , $25\text{ }^\circ\text{C}$): δ = 8.40 (d, J = 4.6 Hz, 2H, β), 8.19 (d, J = 4.6 Hz, 2H, β), 8.13 (s, 2H, β), 8.03 (s, 1H, Ar), 7.76 (s, 1H, Ar), 7.73 (s, 1H, Ar), 7.38 (s, 2H, thienyl), 7.30 (s, 2H, Mes), 7.16 (s, 2H, Mes), 2.65 (s, 6H, thienyl), 2.59 (s, 6H, Mes), 2.11 (s, 6H, Mes), 1.63 (s, 6H, Mes), 1.50 (s, 9H, *tert*-butyl), and 1.45 (s, 9H, *tert*-butyl) ppm; ^{13}C NMR (151 MHz, CDCl_3 , $25\text{ }^\circ\text{C}$): δ = 149.23 (d, J = 24.6 Hz), 143.86, 143.34 (d, J = 11.6 Hz), 142.72 (d, J = 17.3 Hz), 142.14, 141.77 (d, J = 8.7 Hz), 141.47, 139.64, 139.50, 138.54, 138.25, 136.50, 133.59 (d, J = 8.7 Hz), 132.85, 129.28, 128.94, 128.80, 128.53, 128.21, 127.93, 125.82 (d, J = 13.0 Hz), 124.92, 123.00, 121.58, 100.50 (d, J = 108 Hz), 35.17, 31.80, 31.77, 21.85, 21.55, 21.45, and 15.46 ppm; ^{31}P NMR (243 MHz, CDCl_3 , $25\text{ }^\circ\text{C}$): δ = -1.84 ppm; HR-APCI-TOF-MS: m/z = 1073.2713. Calcd for $\text{C}_{62}\text{H}_{57}\text{N}_4^{104}\text{PdS}_2\text{PO}$: 1073.2758 [M] $^-$; UV/Vis (CH_2Cl_2): λ_{max} (ϵ [$\text{M}^{-1}\text{cm}^{-1}$]) = 388 (4.4×10^4), 468 (1.2×10^5), 633 (9.0×10^3), and 687 (1.1×10^4) nm.



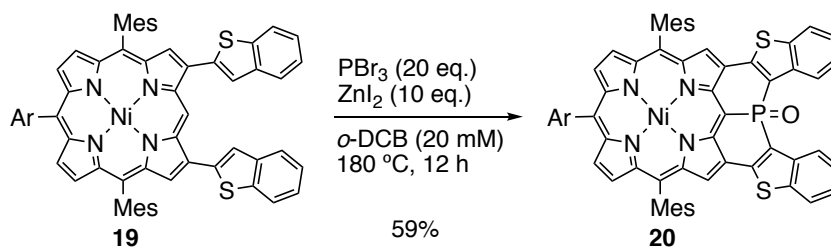
Synthesis of 10Pd: A Schlenk tube containing **18Pd** (11 mg, 10 μmol) was filled with argon, and then charged with HSiCl_3 (0.20 M toluene solution, 0.50 mL, 0.10 mmol). After stirring at room temperature for 1 h, the reaction mixture was dried *in vacuo*. Then, the crude mixture was sequentially passed through short alumina column and silica gel column eluting with thoroughly degassed CH_2Cl_2 under argon atmosphere. Removal of the solvent *in vacuo* gave analytically pure amorphous of **10Pd**. Because **10Pd** was quite sensitive to air, all spectroscopic measurements were conducted under argon atmosphere.

10Pd: ^1H NMR (600 MHz, CD_2Cl_2 , 25 °C): δ = 8.80 (d, J = 2.8 Hz, 2H, β), 8.78 (d, J = 5.0 Hz, 2H, β), 8.62 (d, J = 5.0 Hz, 2H, β), 8.05 (s, 2H, Ar-*o*), 7.82 (t, J = 1.9 Hz, 1H, Ar-*p*), 7.80 (s, 2H, thienyl), 7.34 (s, 4H, Mes), 2.87 (s, 6H, thienyl), 2.66 (s, 6H, Mes), 1.87 (s, 12H, Mes), and 1.51 (s, 18H, *tert*-butyl) ppm; ^{31}P NMR (243 MHz, CDCl_3 , 25 °C): δ = -8.32 ppm; UV/Vis (CH_2Cl_2): λ_{max} (ϵ [$\text{M}^{-1}\text{cm}^{-1}$]) = 459 (8.4×10^4), 483 (1.3×10^5), 573 (2.3×10^4), and 618 (8.1×10^3) nm



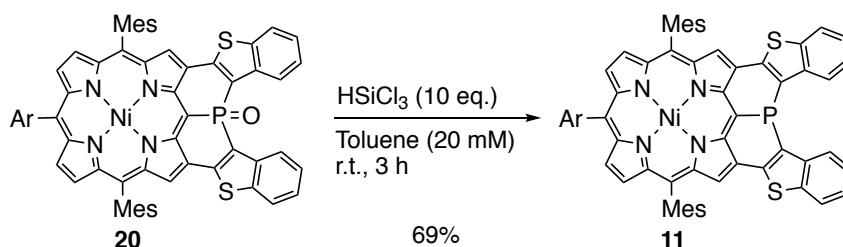
Synthesis of 19: To a Schlenk tube containing 2-bromobenzothiophene (469 mg, 2.2 mmol) and dry THF (10 mL), *n*-BuLi (1.6 M hexane solution, 1.25 mL, 2.0 mmol) was slowly added at -80 °C under argon atmosphere. After the reaction mixture was stirred at -80 °C for 1 h, $\text{ZnCl}_2 \cdot \text{tmeda}$ (557 mg, 2.2 mmol) was added and further stirred for 1 h at room temperature. To the resulting arylzinc solution, **16Ni** (522 mg, 0.50 mmol), $\text{Pd}_2(\text{dba})_3$ (18 mg, 0.020 mmol), and Ruphos (37 mg, 0.080 mmol) were added. After stirred at 70 °C for 12 h, the reaction mixture was quenched with aqueous NH_4Cl solution, extracted with CH_2Cl_2 , and dried over Na_2SO_4 . After removal of the solvent *in vacuo*, the residue was separated by silica gel chromatography eluting with CH_2Cl_2 /hexane. Recrystallization from CH_2Cl_2 /methanol gave **19** (472 mg, 0.25 mmol, 89%).

19: ^1H NMR (600 MHz, CDCl_3 , 25 °C): δ = 10.82 (s, 1H, *meso*), 8.83 (s, 2H, β), 8.74 (d, J = 5.0 Hz, 2H, β), 8.59 (d, J = 5.0 Hz, 2H, β), 8.11 (s, 2H, benzothiophene), 7.97 (d, J = 7.2 Hz, 2H, benzothiophene), 7.94 (d, J = 7.2 Hz, 2H, benzothiophene), 7.90 (d, J = 1.8 Hz, 2H, Ar-*o*), 7.73 (t, J = 1.8 Hz, 1H, Ar-*p*), 7.46 (d, J = 7.2 Hz, 2H, benzothiophene), 7.43 (d, J = 7.2 Hz, 2H, benzothiophene), 7.24 (s, 4H, Mes), 2.60 (s, 6H, Mes), 1.87 (s, 12H, Mes), and 1.48 (s, 18H, *tert*-butyl) ppm; ^{13}C NMR (151 MHz, CDCl_3 , 25 °C): δ = 149.15, 143.78, 143.20, 141.31, 141.05, 140.90, 140.70, 140.03, 139.19, 138.62, 138.10, 138.04, 137.05, 133.40, 131.60, 129.82, 129.04, 128.08, 124.81, 124.72, 124.63, 124.46, 123.99, 122.34, 121.33, 120.75, 117.65, 103.31, 35.19, 31.85, and 21.60 ppm; HR-APCI-TOF-MS: m/z = 1054.3619. Calcd for $\text{C}_{68}\text{H}_{60}\text{N}_4^{58}\text{NiS}_2$: 1054.3607 [M] $^-$; UV/Vis (CH_2Cl_2): λ_{max} (ϵ [$\text{M}^{-1}\text{cm}^{-1}$]) = 430 (2.0×10^5), 538 (2.2×10^4), and 572 (1.3×10^4) nm.



Synthesis of 20: A Schlenk tube containing **19** (211 mg, 0.20 mmol) and ZnI_2 (636 mg, 2.0 mmol) was filled with argon, and then charged with dry $o\text{-DCB}$ (10 mL) and PBr_3 (0.40 mL, 4.0 mmol). After stirring at $180\text{ }^\circ\text{C}$ for 12 h, the reaction mixture was quenched by aqueous NaHCO_3 solution, extracted with CH_2Cl_2 , washed with water, and dried over Na_2SO_4 . After removal of CH_2Cl_2 *in vacuo*, H_2O_2 (30% in water, 0.4 mL, 4 mmol) was added to the resulting $o\text{-DCB}$ solution. After stirring at room temperature for 10 min, the reaction mixture was quenched by aqueous $\text{Na}_2\text{S}_2\text{O}_3$ solution, extracted with CH_2Cl_2 , and dried over Na_2SO_4 . After removal of the solvent *in vacuo*, the residue was separated by silica gel chromatography eluting with $\text{AcOEt}/\text{CH}_2\text{Cl}_2$. Recrystallization from CH_2Cl_2 /methanol gave **20** (130 mg, 0.12 mmol, 59%).

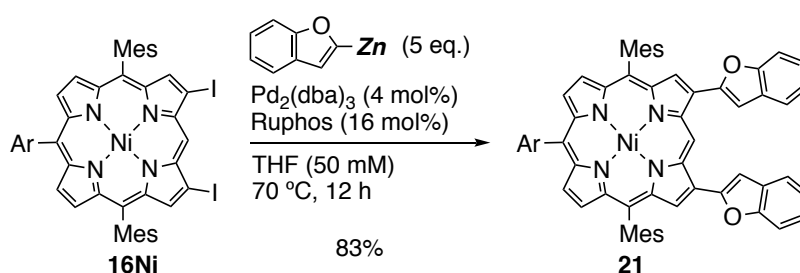
20: ^1H NMR (600 MHz, CDCl_3 , $-30\text{ }^\circ\text{C}$): δ = 8.35 (d, J = 4.6 Hz, 2H, β), 8.32 (m, 2H, benzo), 8.28 (s, 2H, β), 8.12 (d, J = 4.6 Hz, 2H, β), 7.93 (m, 2H, benzo), 8.11 (s, 1H, Ar-*o*), 7.65 (t, J = 1.8 Hz, 1H, Ar-*p*), 7.45-7.41 (m, 4H, benzo), 7.40 (s, 1H, Ar-*o*), 7.33 (s, 2H, Mes), 7.07 (s, 2H, Mes), 2.56 (s, 6H, Mes), 2.37 (s, 6H, Mes), 1.49 (s, 9H, *tert*-butyl), 1.41 (s, 6H, Mes), and 1.34 (s, 9H, *tert*-butyl) ppm; ^{13}C NMR (151 MHz, CDCl_3 , $25\text{ }^\circ\text{C}$): δ = 149.6-149.2, 146.43 (d, J = 11.5 Hz), 145.75, 144.23, 142.43, 142.08 (d, J = 8.6 Hz), 140.02 (d, J = 14.3 Hz), 139.68 (d, J = 13.0 Hz), 139.33, 138.67, 138.45 (d, J = 5.7 Hz), 135.60 (d, J = 8.8 Hz), 135.43, 134.04, 130.95, 128.99, 128.31, 128.00, 126.63, 126.03, 125.93, 125.84, 125.35, 125.12, 122.58, 121.77, 121.63, 98.21 (d, J = 111 Hz), 35.16, 31.76, 21.92, 21.52, and 21.21 ppm; ^{31}P NMR (243 MHz, CDCl_3 , $25\text{ }^\circ\text{C}$): δ = -0.37 ppm; HR-APCI-TOF-MS: m/z = 1098.3048. Calcd for $\text{C}_{68}\text{H}_{57}\text{N}_4^{58}\text{NiOPS}_2$: 1098.3059 [M] $^-$; UV/Vis (CH_2Cl_2): λ_{max} (ϵ [$\text{M}^{-1}\text{cm}^{-1}$]) = 476 (1.1×10^5), 665 (7.9×10^3), and 723 (8.4×10^3) nm.



Synthesis of 11: A Schlenk tube containing **20** (22 mg, 20 μmol) was filled with argon, and then charged with HSiCl_3 (0.20 M toluene solution, 1.0 mL, 0.20 mmol). After stirring at room temperature for 3 h, the reaction mixture was quenched by aqueous NaHCO_3 solution, extracted with CH_2Cl_2 , washed with brine, and dried over Na_2SO_4 .

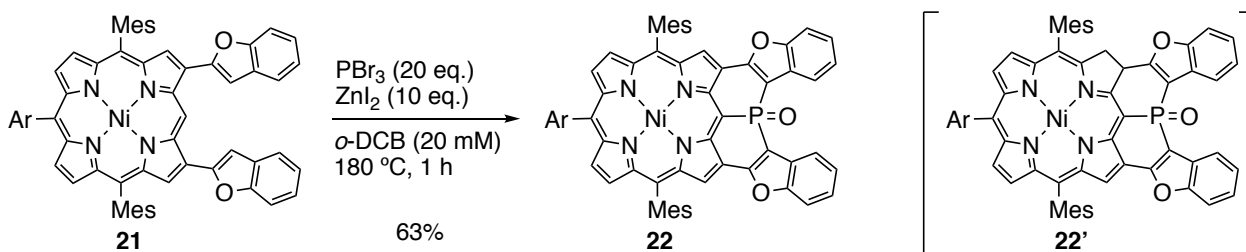
After removal of the solvent *in vacuo*, the residue was separated by silica gel chromatography eluting with CH₂Cl₂/hexane. Recrystallization from CHCl₃/MeCN gave **11** (15 mg, 14 μmol, 69%).

11: ¹H NMR (600 MHz, CD₂Cl₂, 25 °C): δ = 8.90 (d, *J* = 3.2 Hz, 2H, β), 8.71 (d, *J* = 5.0 Hz, 2H, β), 8.55 (d, *J* = 5.0 Hz, 2H, β), 8.47 (d, *J* = 7.3 Hz, 2H, benzo), 8.14 (d, *J* = 7.8 Hz, 2H, benzo), 7.92-7.85 (broad, 2H, Ar-*o*), 7.76 (s, 1H, Ar-*p*), 7.59-7.52 (m, 4H, benzo), 7.30 (s, 4H, Mes), 2.63 (s, 6H, Mes), 1.94-1.82 (broad, 12H, Mes), and 1.48 (s, 18H, *tert*-butyl) ppm; ³¹P NMR (243 MHz, CDCl₃, 25 °C): δ = -17.05 ppm; UV/Vis (CH₂Cl₂): λ_{max} (ε [M⁻¹cm⁻¹]) = 473 (1.1 × 10⁵), 581 (2.0 × 10⁴), and 632 (7.6 × 10³) nm.



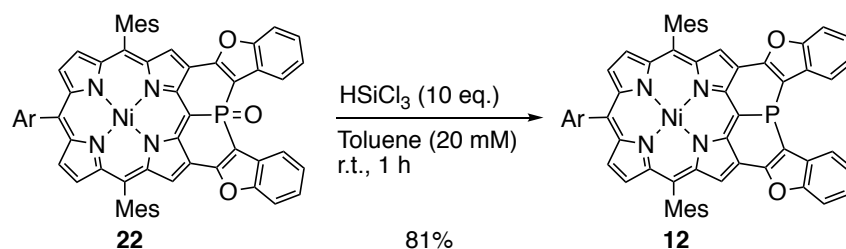
Synthesis of 21: To a Schlenk tube containing benzofuran (0.18 mL, 1.7 mmol) and dry THF (6.0 mL), *n*-BuLi (1.6 M hexane solution, 0.94 mL, 1.5 mmol) was slowly added at -40 °C under argon atmosphere. After the reaction mixture was stirred at room temperature for 1 h, ZnCl₂·tmeda (417 mg, 1.7 mmol) was added and further stirred for 1 h at room temperature. To the resulting arylzinc solution, **16Ni** (313 mg, 0.30 mmol), Pd₂(dba)₃ (11 mg, 0.012 mmol), and Ruphos (22 mg, 0.048 mmol) were added. After stirred at 70 °C for 12 h, the reaction mixture was quenched with aqueous NH₄Cl solution, extracted with CH₂Cl₂, washed with brine, and dried over Na₂SO₄. After removal of the solvent *in vacuo*, the residue was separated by silica gel chromatography eluting with CH₂Cl₂/hexane. Recrystallization from CH₂Cl₂/methanol gave **21** (255 mg, 0.25 mmol, 83%).

21: ¹H NMR (600 MHz, CDCl₃, 25 °C): δ = 11.31 (s, 1H, *meso*), 9.00 (s, 2H, β), 8.72 (d, *J* = 5.0 Hz, 2H, β), 8.58 (d, *J* = 5.0 Hz, 2H, β), 7.89 (d, *J* = 1.9 Hz, 2H, Ar-*o*), 7.82 (d, *J* = 7.8 Hz, benzofuran, 2H), 7.78 (m, 4H, benzofuran), 7.72 (t, *J* = 1.9 Hz, 1H, Ar-*p*), 7.46 (t, *J* = 7.4 Hz, 2H, benzofuran), 7.40 (t, *J* = 7.4 Hz, 2H, benzofuran), 7.26 (s, 4H, Mes), 2.62 (s, 6H, Mes), 1.88 (s, 12H, Mes), and 1.48 (s, 18H, *tert*-butyl) ppm; ¹³C NMR (151 MHz, CDCl₃, 25 °C): δ = 155.63, 153.21, 149.15, 143.99, 143.27, 141.58, 140.03, 139.98, 139.23, 138.05, 137.11, 134.28, 133.34, 131.60, 129.74, 129.03, 128.34, 128.08, 124.94, 123.47, 121.39, 121.32, 120.70, 117.90, 111.52, 106.13, 103.67, 35.18, 31.83, and 21.62 ppm; HR-APCI-TOF-MS: *m/z* = 1022.4044. Calcd for C₆₈H₆₀N₄⁵⁸NiO₂: 1022.4064 [M]⁺; UV/Vis (CH₂Cl₂): λ_{max} (ε [M⁻¹cm⁻¹]) = 435 (1.6 × 10⁵), 545 (2.1 × 10⁴), and 580 (1.4 × 10⁴) nm.



Synthesis of 22: A Schlenk tube containing **21** (123 mg, 0.12 mmol) and ZnI_2 (382 mg, 1.2 mmol) was filled with argon, and then charged with dry *o*-DCB (6.0 mL) and PBr_3 (0.24 mL, 2.4 mmol). After stirring at 180 °C for 1 h, the reaction mixture was quenched by aqueous NaHCO_3 solution, extracted with CH_2Cl_2 , washed with brine, and dried over Na_2SO_4 . After removal of CH_2Cl_2 *in vacuo*, H_2O_2 (30% in water, 0.4 mL, 4 mmol) was added to the resulting *o*-DCB solution. After stirring at room temperature for 10 min, the reaction mixture was quenched by aqueous $\text{Na}_2\text{S}_2\text{O}_3$ solution, extracted with CH_2Cl_2 , and dried over Na_2SO_4 . After removal of the solvent *in vacuo*, the residue which includes **22** and its reduced form **22'** (proposed structure) were separated by silica gel chromatography eluting with $\text{AcOEt}/\text{CH}_2\text{Cl}_2/\text{hexane}$. Then, the obtained **22'** (30 mg, 0.028 mmol) was dissolved in CHCl_3 (10 mL), oxidized to **22** with DDQ (7.0 mg, 0.031 mmol) at 50 °C for 30 min, and separated by silica gel chromatography eluting with $\text{AcOEt}/\text{CH}_2\text{Cl}_2/\text{hexane}$. Recrystallization from $\text{CH}_2\text{Cl}_2/\text{methanol}$ gave **22** (81 mg, 0.076 mmol, 63%).

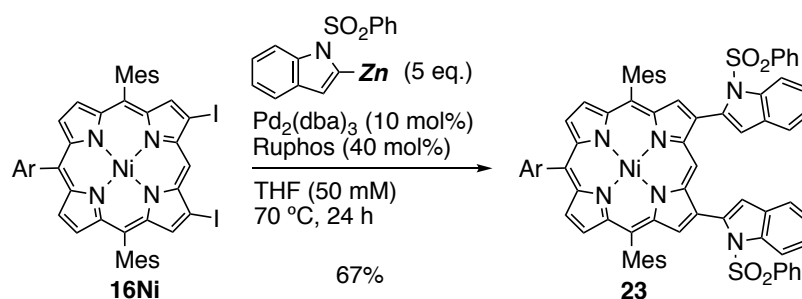
22: ^1H NMR (600 MHz, CDCl_3 , -30 °C): δ = 8.37 (s, 2H, β), 8.33 (d, J = 5.0 Hz, 2H, β), 8.31 (d, J = 7.8 Hz, 2H, benzo), 8.10 (d, J = 5.0 Hz, 2H, β), 8.09 (s, 1H, Ar-*o*), 7.65 (t, J = 1.8 Hz, 1H, Ar-*p*), 7.62 (d, J = 7.8 Hz, 2H, benzo), 7.50 (t, J = 7.2 Hz, 2H, benzo), 7.45 (t, J = 7.2 Hz, 2H, benzo), 7.41 (s, 1H, Ar-*o*), 7.30 (s, 2H, Mes), 7.04 (s, 2H, Mes), 2.54 (s, 6H, Mes), 2.33 (s, 6H, Mes), 1.49 (s, 9H, *tert*-butyl), 1.44 (s, 6H, Mes), and 1.35 (s, 9H, *tert*-butyl) ppm; ^{13}C NMR (151 MHz, CDCl_3 , 25 °C): δ = 157.76 (d, J = 8.8 Hz), 155.84 (d, J = 13.0 Hz), 149.8-149.3 (broad), 145.92, 144.35, 142.55, 142.47, 139.33, 138.49, 138.43, 138.29, 135.36, 134.18, 131.37 (d, J = 4.3 Hz), 130.95, 128.58, 128.29, 127.99, 127.27, 126.93 (d, J = 7.2 Hz), 126.24, 124.71, 122.29, 121.82, 111.92, 107.91, 107.05, 96.99 (d, J = 116 Hz), 35.17, 31.75, 21.82, 21.49, and 21.19 ppm; ^{31}P NMR (243 MHz, CDCl_3 , 25 °C): δ = 2.45 ppm; HR-APCI-TOF-MS: m/z = 1066.3482. Calcd for $\text{C}_{68}\text{H}_{57}\text{N}_4^{58}\text{NiO}_3\text{P}$: 1066.3516 [M] $^-$; UV/Vis (CH_2Cl_2): λ_{max} (ϵ [$\text{M}^{-1}\text{cm}^{-1}$]) = 473 (1.1×10^5), 671 (7.7×10^3), and 732 (8.6×10^3) nm.



Synthesis of 12: A Schlenk tube containing **22** (21 mg, 20 μmol) was filled with argon, and then charged with and HSiCl_3 (0.20 M toluene solution, 1.0 mL, 0.20 mmol). After stirring at room temperature for 1 h, the reaction mixture

was quenched by aqueous NaHCO₃ solution, extracted with CH₂Cl₂, washed with brine, and dried over Na₂SO₄. After removal of the solvent *in vacuo*, the residue was separated by silica gel chromatography eluting with CH₂Cl₂/hexane. Recrystallization from CH₂Cl₂/MeCN gave **12** (17 mg, 16 μmol, 81%).

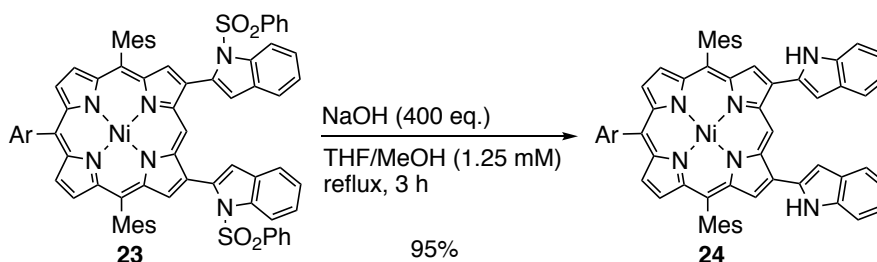
12: ¹H NMR (600 MHz, CDCl₃, -40 °C): δ = 9.07 (d, *J* = 3.2 Hz, 2H, β), 8.75 (d, *J* = 5.0 Hz, 2H, β), 8.61 (d, *J* = 4.6 Hz, 2H, β), 8.52 (d, *J* = 7.8 Hz, 2H, benzo), 8.43 (s, 1H, Ar-*o*), 7.84 (d, *J* = 7.8 Hz, 2H, benzo), 7.68 (s, 1H, Ar-*p*), 7.63 (d, *J* = 7.8 Hz, 2H, benzo), 7.58 (d, *J* = 7.8 Hz, 2H, benzo), 7.43 (s, 2H, Mes), 7.35 (s, 1H, Ar-*o*), 7.08 (s, 2H, Mes), 2.60 (s, 6H, Mes), 2.52 (s, 6H, Mes), 1.56 (s, 9H, *tert*-butyl), 1.34 (s, 9H, *tert*-butyl), and 1.23 (s, 6H, Mes); ³¹P NMR (243 MHz, CDCl₃, 25 °C): δ = -25.38 ppm; UV/Vis (CH₂Cl₂): λ_{max} (ε [M⁻¹cm⁻¹]) = 468 (1.0 × 10⁵), 580 (2.0 × 10⁴), and 628 (8.1 × 10³) nm.



Synthesis of 23: To a Schlenk tube containing 1-phenylsulfonyl-indole (424 mg, 1.7 mmol) and dry THF (6.0 mL), *n*-BuLi (1.6 M hexane solution, 0.94 mL, 1.5 mmol) was slowly added at -80 °C under argon atmosphere. After the reaction mixture was stirred at -80 °C for 1 h, ZnCl₂·tmeda (417 mg, 1.7 mmol) was added and further stirred for 1 h at room temperature. To the resulting solution, **16Ni** (313 mg, 0.30 mmol), Pd₂(dba)₃ (27 mg, 0.030 mmol), and Ruphos (56 mg, 0.12 mmol) were added. After stirred at 70 °C for 24 h, the reaction mixture was quenched with aqueous NH₄Cl solution, extracted with CH₂Cl₂, washed with brine, and dried over Na₂SO₄. After removal of the solvent *in vacuo*, the residue was separated by silica gel chromatography eluting with CH₂Cl₂/hexane. Recrystallization from CH₂Cl₂/methanol gave **23** (262 mg, 0.20 mmol, 67%).

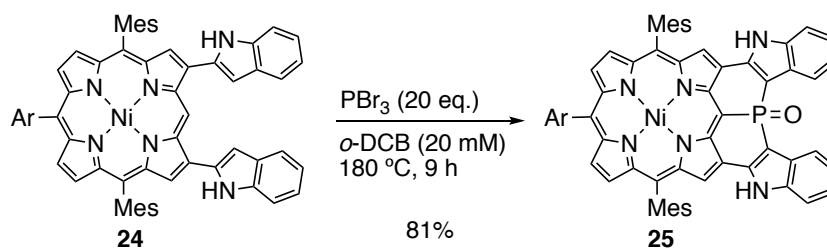
23: ¹H NMR (600 MHz, CDCl₃, 25 °C): δ = 9.67 (s, 1H, *meso*), 8.82 (s, 2H, β), 8.78 (d, *J* = 5.0 Hz, 2H, β), 8.65 (d, *J* = 4.6 Hz, 2H, β), 8.35 (d, *J* = 7.8 Hz, 2H, indole), 7.93 (d, *J* = 1.8 Hz, 2H, Ar-*o*), 7.74 (s, 1H, Ar-*p*), 7.60 (d, *J* = 7.2 Hz, 2H, indole), 7.41 (t, *J* = 7.2 Hz, 2H, indole), 7.36 (t, *J* = 7.2 Hz, 2H, indole), 7.22 (d, *J* = 7.2 Hz, 4H, Ph), 7.09 (s, 2H, indole), 7.02 (t, *J* = 7.2 Hz, 2H, Ph), 6.79 (t, *J* = 7.2 Hz, 4H, Ph), 2.60 (s, 6H, Mes), 1.93 (s, 12H, Mes), and 1.49 (s, 18H, *tert*-butyl) ppm; ¹³C NMR (151 MHz, CDCl₃, 25 °C): δ = 149.08, 143.78, 143.24, 142.45, 141.14, 140.24, 139.25, 139.07, 137.97, 137.50, 137.29, 135.80, 135.18, 133.42, 133.10, 132.66, 131.35, 131.32, 129.13, 128.40, 128.01, 126.66, 125.28, 124.75, 121.25, 121.11, 120.69, 118.22, 117.92, 116.98, 103.89, 35.19, 31.86, and 21.60

ppm; HR-APCI-TOF-MS: $m/z = 1300.4197$. Calcd for $C_{80}H_{70}N_6^{58}NiO_4S_2$: 1300.4248 $[M]^-$; UV/Vis (CH_2Cl_2): λ_{max} (ϵ [$M^{-1}cm^{-1}$]) = 424 (2.2×10^5), 533 (2.2×10^4), and 566 (1.1×10^4) nm.



Synthesis of 24: To a flask containing **23** (260 mg, 0.20 mmol) dissolved in THF (80 mL), MeOH (80 mL) and NaOH (3.2 g, 80 mmol) were added and the resulting reaction mixture was stirred for 3 h at reflux. Then, the reaction mixture was quenched with aqueous NH_4Cl solution, extracted with AcOEt, washed with brine, and dried over Na_2SO_4 . After removal of the solvent *in vacuo*, recrystallization from CH_2Cl_2 /methanol gave **24** (195 mg, 0.19 mmol, 95%).

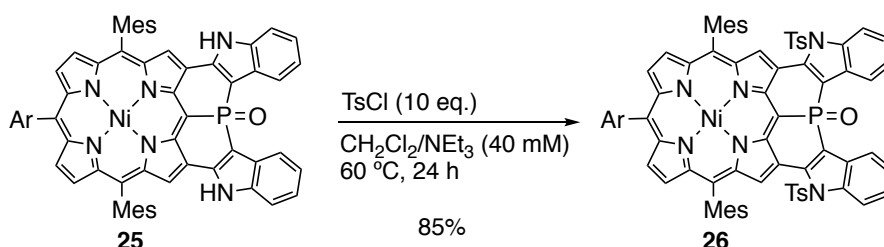
24: 1H NMR (600 MHz, $CDCl_3$, 25 °C): $\delta = 10.87$ (s, 1H, *meso*), 8.86 (s, 2H, NH), 8.76 (s, 2H, β), 8.74 (d, $J = 5.0$ Hz, 2H, β), 8.59 (d, $J = 5.0$ Hz, 2H, β), 7.90 (d, $J = 1.8$ Hz, 2H, Ar-*o*), 7.83 (d, $J = 7.8$ Hz, 2H, indole), 7.73 (t, $J = 1.8$ Hz, 1H, Ar-*p*), 7.55 (d, $J = 7.8$ Hz, 2H, indole), 7.48 (s, 2H, indole), 7.32 (t, $J = 7.2$ Hz, 2H, indole), 7.26 (s, 4H, Mes), 7.23 (t, $J = 7.2$ Hz, 2H, indole), 2.61 (s, 6H, Mes), 1.87 (s, 12H, Mes), and 1.48 (s, 18H, *tert*-butyl) ppm; ^{13}C NMR (151 MHz, $CDCl_3$, 25 °C): $\delta = 149.08$, 143.78, 143.24, 142.45, 141.14, 140.24, 139.25, 139.07, 137.97, 137.50, 137.29, 135.80, 135.18, 133.42, 133.10, 132.66, 131.35, 131.32, 129.13, 128.40, 128.01, 126.66, 125.28, 124.75, 121.25, 121.11, 120.69, 118.22, 117.92, 116.98, 103.89, 35.19, 31.86, and 21.60 ppm; HR-APCI-TOF-MS: $m/z = 1020.4356$. Calcd for $C_{68}H_{62}N_6^{58}Ni$: 1020.4384 $[M]^-$; UV/Vis (CH_2Cl_2): λ_{max} (ϵ [$M^{-1}cm^{-1}$]) = 431 (1.4×10^5), 541 (2.1×10^4), and 578 (1.5×10^4) nm.



Synthesis of 25: A Schlenk tube containing **24** (184 mg, 0.18 mmol) was filled with argon, and then charged with dry *o*-DCB (9.0 mL) and PBr_3 (0.36 mL, 3.6 mmol). After stirring at 180 °C for 9 h, the reaction mixture was quenched by aqueous $NaHCO_3$ solution, extracted with CH_2Cl_2 , washed with brine, and dried over Na_2SO_4 . After

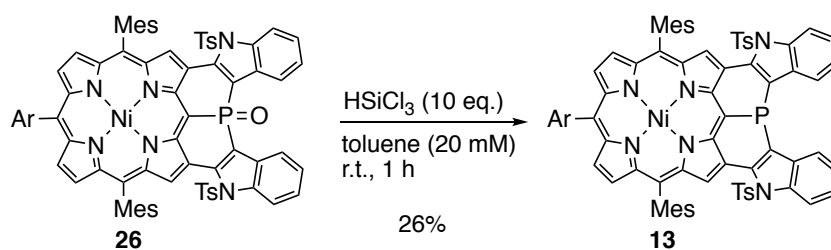
removal of the solvent *in vacuo*, the residue was separated by silica gel chromatography eluting with AcOEt/CH₂Cl₂. Recrystallization from CHCl₃/methanol gave **25** (155 mg, 0.15 mmol, 81%).

25: ¹H NMR (600 MHz, CDCl₃, 25 °C): δ = 8.85 (s, 2H, NH), 8.37 (d, *J* = 7.2 Hz, 2H, indole), 8.35 (d, *J* = 4.6 Hz, 2H, β), 8.15 (s, 2H, β), 8.12 (d, *J* = 4.6 Hz, 2H, β), 8.16-8.11 (broad, 1H, Ar-*o*), 7.68 (s, 1H, Ar-*p*), 7.46-7.41 (broad, 1H, Ar-*o*), 7.40 (d, *J* = 7.2 Hz, 2H, indole), 7.31 (s, 2H, Mes), 7.31-7.26 (m, 4H, indole), 7.06 (s, 2H, Mes), 2.55 (s, 6H, Mes), 2.33 (s, 6H, Mes), 1.53-1.47 (broad, 9H, *tert*-butyl), 1.47 (s, 6H, Mes), and 1.42-1.36 (broad, 9H, *tert*-butyl) ppm. ¹³C NMR was not obtained due to the poor solubility. ³¹P NMR (243 MHz, CDCl₃, 25 °C): δ = 0.73 ppm; HR-APCI-TOF-MS: *m/z* = 1064.3809. Calcd for C₆₈H₅₉N₆⁵⁸NiOP: 1064.3836 [M]⁻; UV/Vis (CH₂Cl₂): λ_{max} (ε [M⁻¹cm⁻¹]) = 432 (7.3 × 10⁴), 472 (8.8 × 10⁴), 663 (6.7 × 10³), and 723 (6.1 × 10³) nm.



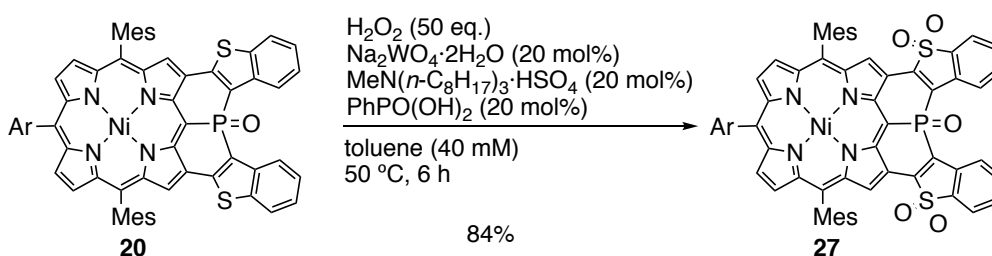
Synthesis of 26: A Schlenk tube containing **25** (64 mg, 0.060 mmol) and TsCl (115 mg, 0.60 mmol) was filled with argon, and then charged with dry CH₂Cl₂ (1.5 mL) and NEt₃ (0.15 mL). After stirring at 60 °C for 24 h, the reaction mixture was quenched by water, extracted with CH₂Cl₂, washed with brine, and dried over Na₂SO₄. After removal of the solvent *in vacuo*, the residue was separated by silica gel chromatography eluting with AcOEt/CH₂Cl₂. Recrystallization from CH₂Cl₂/methanol gave **26** (70 mg, 0.051 mmol, 85%).

26: ¹H NMR (600 MHz, CDCl₃, -30 °C): δ = 8.74 (s, 2H, β), 8.30 (d, *J* = 8.4 Hz, 2H, benzo), 8.27 (d, *J* = 4.6 Hz, 2H, β), 8.05 (s, 1H, Ar-*o*), 8.03 (d, *J* = 5.0 Hz, 2H, β), 7.75 (d, *J* = 7.8 Hz, 2H, benzo), 7.64 (s, 1H, Ar-*p*), 7.46-7.42 (m, 6H, benzo (2H) and *N*-Ts 4H), 7.39 (s, 1H, Ar-*o*), 7.30-7.26 (m, 4H, benzo (2H) and Mes (2H)), 7.08 (s, 2H, Mes), 7.02 (d, *J* = 8.2 Hz, 4H, *N*-Ts), 2.58 (s, 6H, Mes), 2.21 (s, 6H, *N*-Ts), 2.20 (s, 6H, Mes), 1.47 (s, 9H, *tert*-butyl), 1.41 (s, 6H, Mes), and 1.35 (s, 9H, *tert*-butyl) ppm; ¹³C NMR (151 MHz, CDCl₃, 25 °C): δ = 149.6-149.3 (broad), 145.77, 145.03, 144.22, 143.66 (d, *J* = 10.1 Hz), 141.97, 141.76 (d, *J* = 15.9 Hz), 140.59 (d, *J* = 11.6 Hz), 139.23, 138.54, 138.29, 138.18, 135.62, 135.21, 134.72, 133.95, 131.29 (d, *J* = 5.1 Hz), 130.74, 129.90, 129.37 (d, *J* = 8.7 Hz), 128.28, 127.95, 127.20, 126.61, 126.51, 125.18, 122.52, 122.41, 121.79, 117.03, 116.53, 115.70, 94.42 (d, *J* = 115 Hz), 35.16, 31.75, 21.76, 21.65, 21.60, and 21.21 ppm; ³¹P NMR (243 MHz, CDCl₃, 25 °C): δ = -2.91 ppm; HR-APCI-TOF-MS: *m/z* = 1064.3766. Calcd for C₆₈H₅₉N₆⁵⁸NiOP: 1064.3836 [M-2(Ts)+2H]⁻; UV/Vis (CH₂Cl₂): λ_{max} (ε [M⁻¹cm⁻¹]) = 479 (1.0 × 10⁵), 683 (7.1 × 10³), and 746 (7.1 × 10³) nm.



Synthesis of 13: A Schlenk tube containing **26** (27 mg, 20 μ mol) was filled with argon, and then charged with HSiCl_3 (0.20 M toluene solution, 1.0 mL, 0.20 mmol). After stirring at room temperature for 1 h, the reaction mixture was quenched by aqueous NaHCO_3 solution, extracted with CH_2Cl_2 , washed with brine, and dried over Na_2SO_4 . After removal of the solvent *in vacuo*, the residue was separated by silica gel chromatography eluting with CH_2Cl_2 /hexane. Recrystallization from CH_2Cl_2 /methanol gave **13** (7.0 mg, 5.2 μ mol, 26%).

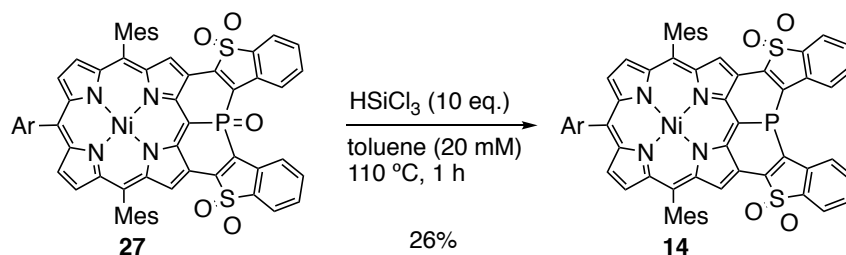
13: ^1H NMR (600 MHz, CD_2Cl_2 , -40°C): δ = 9.48 (d, J = 3.2 Hz, 2H, β), 8.72 (d, J = 4.6 Hz, 2H, β), 8.56 (d, J = 5.0 Hz, 2H, β), 8.49 (d, J = 8.3 Hz, 2H, indole), 8.42 (s, 1H, Ar-*o*), 7.67 (s, 3H, Ar-*p* (1H) and indole(2H)), 7.51 (t, J = 7.6 Hz, 2H, indole), 7.45 (s, 2H, Mes), 7.39-7.33 (m, 6H, indole (2H) and *N*-Ts (4H)), 7.30 (s, 1H, Ar-*o*), 7.11 (s, 2H, Mes), 6.84 (d, J = 8.3 Hz, 4H, *N*-Ts), 2.63 (s, 6H, Mes), 2.50 (s, 6H, Mes), 2.07 (s, 6H, *N*-Ts), 1.55 (s, 9H, *tert*-butyl), 1.35 (s, 9H, *tert*-butyl), and 1.20 (s, 6H, Mes) ppm; ^{31}P NMR (243 MHz, CDCl_3 , 25°C): δ = -32.73 ppm; UV/Vis (CH_2Cl_2): λ_{max} (ϵ [$\text{M}^{-1}\text{cm}^{-1}$]) = 472 (9.7×10^4), 583 (1.8×10^4), and 631 (7.9×10^3) nm.



Synthesis of 27: A Schlenk tube containing **20** (132 mg, 0.12 mmol), $\text{Na}_2\text{WO}_4 \cdot 2\text{H}_2\text{O}$ (7.9 mg, 0.024 mmol), $\text{MeN}(n\text{-C}_8\text{H}_{17})_3 \cdot \text{HSO}_4$ (11.2 mg, 0.024 mmol), and $\text{PhPO}(\text{OH})_2$ (3.8 mg, 0.024 mmol) was filled with argon, and then charged with dry toluene (3.0 mL) and H_2O_2 (30% in water, 0.60 mL, 6.0 mmol). After stirring at 50°C for 6 h, the reaction mixture was quenched by aqueous $\text{Na}_2\text{S}_2\text{O}_3$ solution, extracted with CH_2Cl_2 , and dried over Na_2SO_4 . After removal of the solvent *in vacuo*, the residue was separated by silica gel chromatography eluting with $\text{AcOEt}/\text{CH}_2\text{Cl}_2$. Recrystallization from CH_2Cl_2 /MeOH gave **27** (118 mg, 0.101 mmol, 84%).

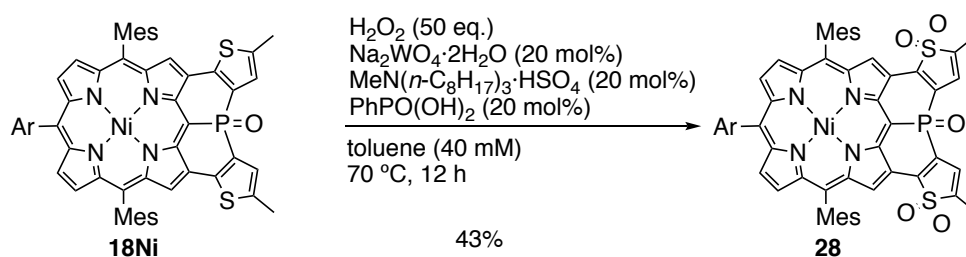
27: ^1H NMR (600 MHz, CDCl_3 , -30°C): δ = 8.45 (s, 2H, β), 8.20 (d, J = 4.6 Hz, 2H, β), 8.00 (broad, 3H, Ar-*o* (1H) and benzo (2H)), 7.97 (d, J = 5.0 Hz, 2H, β), 7.91 (m, 2H, benzo), 7.69 (m, 4H, benzo), 7.65 (s, 1H, Ar-*p*), 7.35 (s, 1H, Ar-*o*), 7.26 (s, 2H, Mes), 7.02 (s, 2H, Mes), 2.51 (s, 6H, Mes), 2.32 (s, 6H, Mes), 1.47 (s, 9H, *tert*-butyl), 1.46 (s, 6H, Mes), and 1.35 (s, 9H, *tert*-butyl) ppm; ^{13}C NMR (151 MHz, CDCl_3 , 25°C): δ = 149.9-149.7 (broad), 147.32,

145.48, 144.97 (d, $J = 5.8$ Hz), 143.07 (d, $J = 7.2$ Hz), 142.87, 138.91 (d, $J = 7.2$ Hz), 138.05, 137.82, 135.72 (d, $J = 5.8$ Hz), 134.73, 134.04, 133.90, 131.82, 130.53, 130.16 (d, $J = 7.2$ Hz), 129.71, 128.61, 128.33, 128.2-127.8 (broad), 127.51 (d, $J = 10.1$ Hz), 126.51, 125.78, 125.17, 124.47, 122.75, 122.26, 93.68 (d, $J = 119$ Hz), 35.17, 31.71, 21.82, 21.48 and, 21.21 ppm; ^{31}P NMR (243 MHz, CDCl_3 , 25 °C): $\delta = 1.00$ ppm; HR-APCI-TOF-MS: $m/z = 1162.2836$. Calcd for $\text{C}_{68}\text{H}_{57}\text{N}_4^{58}\text{NiO}_5\text{PS}_2$: 1162.2856 $[\text{M}]^-$; UV/Vis (CH_2Cl_2): λ_{max} (ϵ [$\text{M}^{-1}\text{cm}^{-1}$]) = 377 (5.2×10^4), 504 (1.0×10^5), 600 (6.0×10^3), 682 (5.9×10^3), 753 (6.9×10^3), and 823 (7.0×10^3) nm.



Synthesis of 14: A Schlenk tube containing **27** (12 mg, 0.010 mmol) was filled with argon, and then charged with HSiCl_3 (0.20 M toluene solution, 0.50 mL, 0.10 mmol). After stirring at 110 °C for 1 h, the reaction mixture was quenched by aqueous NaHCO_3 solution, extracted with CH_2Cl_2 , and dried over Na_2SO_4 . After removal of the solvent *in vacuo*, recrystallization from CH_2Cl_2 /hexane gave **14** (3.0 mg, 2.6 μmol , 26%).

14: ^1H NMR (600 MHz, CD_2Cl_2 , 25 °C): $\delta = 9.20$ (d, $J = 5.0$ Hz, 2H, β), 8.76 (d, $J = 5.0$ Hz, 2H, β), 8.61 (d, $J = 5.0$ Hz, 2H, β), 8.09 (d, $J = 7.3$ Hz, 2H, benzo), 7.99 (d, $J = 7.3$ Hz, 2H, benzo), 7.88 (s, 2H, Ar-*o*), 7.79 (m, 3H, Ar-*p* (1H) and benzo (2H)), 7.73 (t, $J = 7.3$ Hz, 2H, benzo), 7.32 (s, 4H, Mes), 2.63 (s, 6H, Mes), 1.87 (s, 12H, Mes), and 1.48 (s, 18H, *tert*-butyl) ppm; ^{31}P NMR (243 MHz, CDCl_3 , 25 °C): $\delta = -20.93$ ppm; UV/Vis (CH_2Cl_2): λ_{max} (ϵ [$\text{M}^{-1}\text{cm}^{-1}$]) = 385 (4.9×10^4), 429 (5.0×10^4), 498 (6.4×10^4), 594 (1.7×10^4), and 647 (7.6×10^3) nm.



Synthesis of 28: A Schlenk tube containing **18Ni** (62 mg, 0.060 mmol), $\text{Na}_2\text{WO}_4 \cdot 2\text{H}_2\text{O}$ (4.0 mg, 0.012 mmol), $\text{MeN}(n\text{-C}_8\text{H}_{17})_3 \cdot \text{HSO}_4$ (5.6 mg, 0.012 mmol), and PhPO(OH)_2 (1.9 mg, 0.012 mmol) was filled with argon, and then charged with dry toluene (1.5 mL) and H_2O_2 (30% in water, 0.30 mL, 3.0 mmol). After stirring at 70 °C for 12 h, the reaction mixture was quenched by aqueous $\text{Na}_2\text{S}_2\text{O}_3$ solution, extracted with CH_2Cl_2 , and dried over Na_2SO_4 . After

removal of the solvent *in vacuo*, the residue was separated by silica gel chromatography eluting with AcOEt/CH₂Cl₂. Recrystallization from CH₂Cl₂/hexane gave **28** (28 mg, 0.026 mmol, 43%).

28: ¹H NMR (600 MHz, CDCl₃, 25 °C): δ = 8.16 (s, 2H, β), 8.10 (d, *J* = 5.0 Hz, 2H, β), 7.98-7.92 (broad, 1H, Ar-*o*), 7.87 (d, *J* = 4.6 Hz, 2H, β), 7.67 (s, 1H, Ar-*p*), 7.41-7.34 (broad, 1H, Ar-*o*), 7.22 (s, 2H, Mes), 7.01 (s, 2H, Mes), 6.85 (m, 2H, thiophene 1,1-dioxide), 2.50 (s, 6H, Mes), 2.35 (s, 6H, thiophene 1,1-dioxide), 2.23 (s, 6H, Mes), 1.54 (s, 6H, Mes), and 1.50-1.35 (broad, 18H, *tert*-butyl) ppm; ¹³C NMR (151 MHz, CDCl₃, 25 °C): δ = 149.9-149.7 (broad), 147.48, 145.50, 143.90 (d, *J* = 8.7 Hz), 142.92, 142.05 (d, *J* = 7.6 Hz), 140.79 (d, *J* = 7.2 Hz), 138.86, 138.74, 137.89, 137.71, 134.58, 133.90, 133.53, 131.51, 130.23, 128.58, 128.29, 128.00 (d, *J* = 10.1 Hz), 127.8-127.5 (broad), 125.90, 122.26, 120.41 (d, *J* = 5.8 Hz), 119.57 (d, *J* = 110 Hz), 93.62 (d, *J* = 115 Hz), 35.16, 31.69, 22.78, 21.70, 21.44, 21.18, 14.25, and 9.99 ppm; ³¹P NMR (243 MHz, CDCl₃, 25 °C): δ = -1.52 ppm; HR-APCI-TOF-MS: *m/z* = 1090.2849. Calcd for C₆₂H₅₇N₄⁵⁸NiO₅PS₂: 1090.2856 [M]⁻; UV/Vis (CH₂Cl₂): λ_{max} (ε [M⁻¹cm⁻¹]) = 398 (5.1 × 10⁴), 506 (8.4 × 10⁴), 606 (5.1 × 10³), 695 (5.5 × 10³), 779 (6.0 × 10³), and 842 (5.7 × 10³) nm.



Synthesis of 15: A Schlenk tube containing **28** (11 mg, 0.010 mmol) was filled with argon, and then charged with HSiCl₃ (0.20 M toluene solution, 0.50 mL, 0.10 mmol). After stirring at 110 °C for 1 h, the reaction mixture was quenched by aqueous NaHCO₃ solution, extracted with CH₂Cl₂, and dried over Na₂SO₄. After removal of the solvent *in vacuo*, recrystallization from CH₂Cl₂/hexane gave **15** (3.0 mg, 2.8 μmol, 28%).

15: ¹H NMR (600 MHz, CD₂Cl₂, 25 °C): δ = 9.06 (d, *J* = 5.0 Hz, 2H, β), 8.78 (d, *J* = 5.0 Hz, 2H, β), 8.62 (d, *J* = 5.0 Hz, 2H, β), 7.88 (d, *J* = 1.9 Hz, 2H, Ar-*o*), 7.78 (d, *J* = 1.9 Hz, 1H, Ar-*p*), 7.32 (t, *J* = 2.3 Hz, 2H, thiophene 1,1-dioxide), 7.30 (s, 4H, Mes), 2.61 (s, 6H, Mes), 2.51 (d, *J* = 1.9 Hz, 6H, thiophene 1,1-dioxide), 1.83 (s, 12H, Mes), and 1.50 (s, 18H, *tert*-butyl) ppm; ³¹P NMR (243 MHz, CDCl₃, 25 °C): δ = -17.96 ppm; UV/Vis (CH₂Cl₂): λ_{max} (ε [M⁻¹cm⁻¹]) = 391 (4.7 × 10⁴), 440 (6.2 × 10⁴), 484 (5.4 × 10⁴), 588 (1.6 × 10⁴), and 638 (6.7 × 10³) nm.

3. NMR spectra

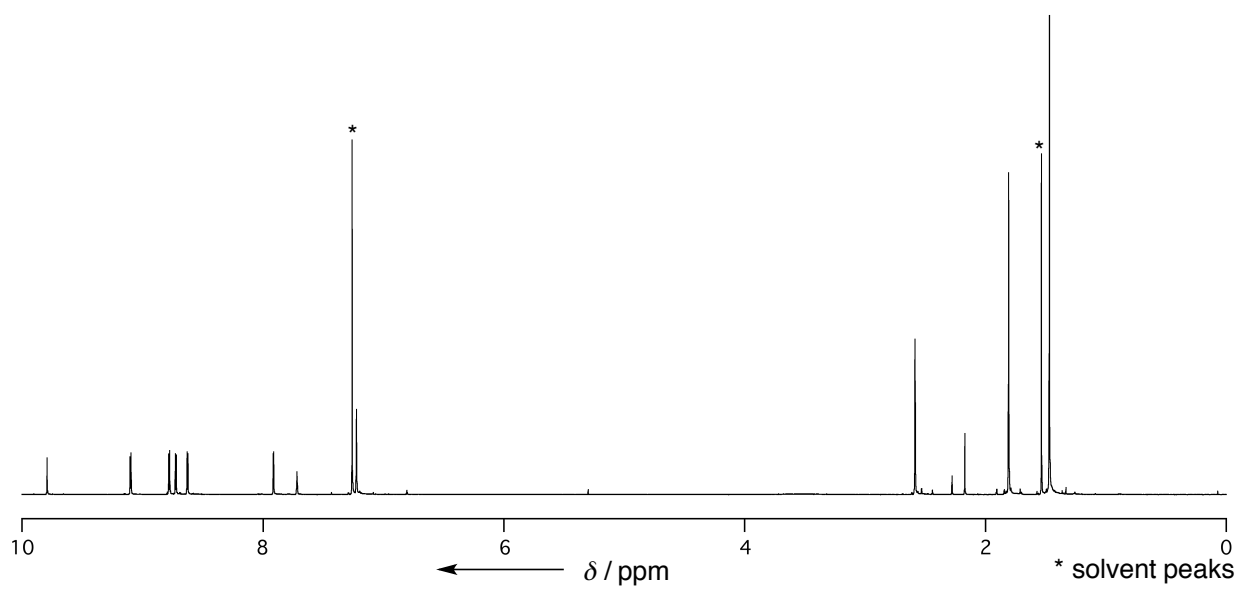


Figure S1. ¹H NMR spectrum of **S3** in CDCl₃ at 25 °C.

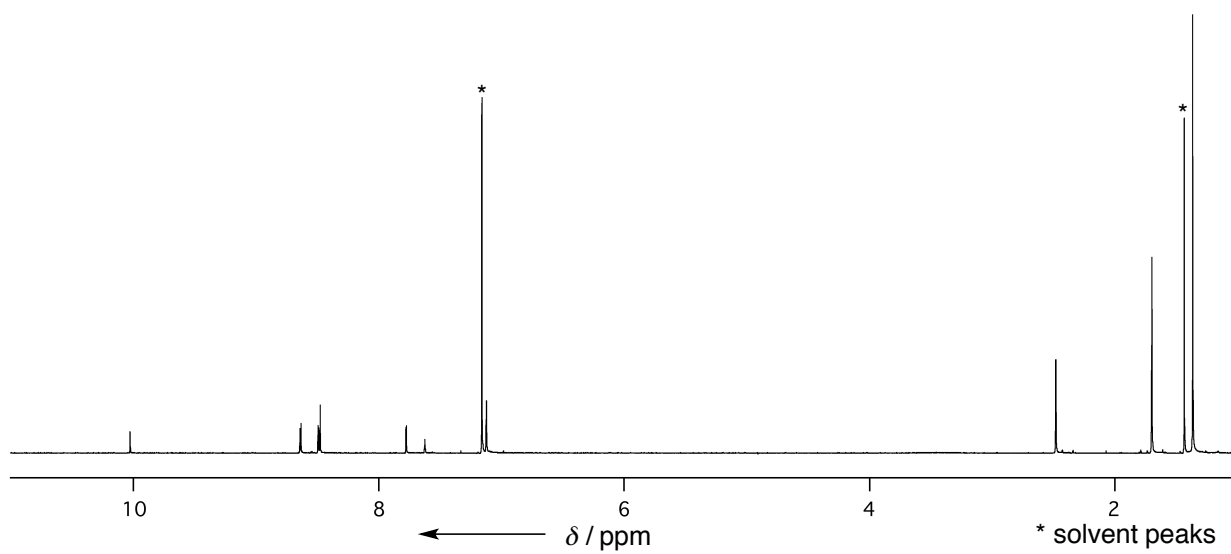


Figure S2. ¹H NMR spectrum of **S5** in CDCl₃ at 25 °C.

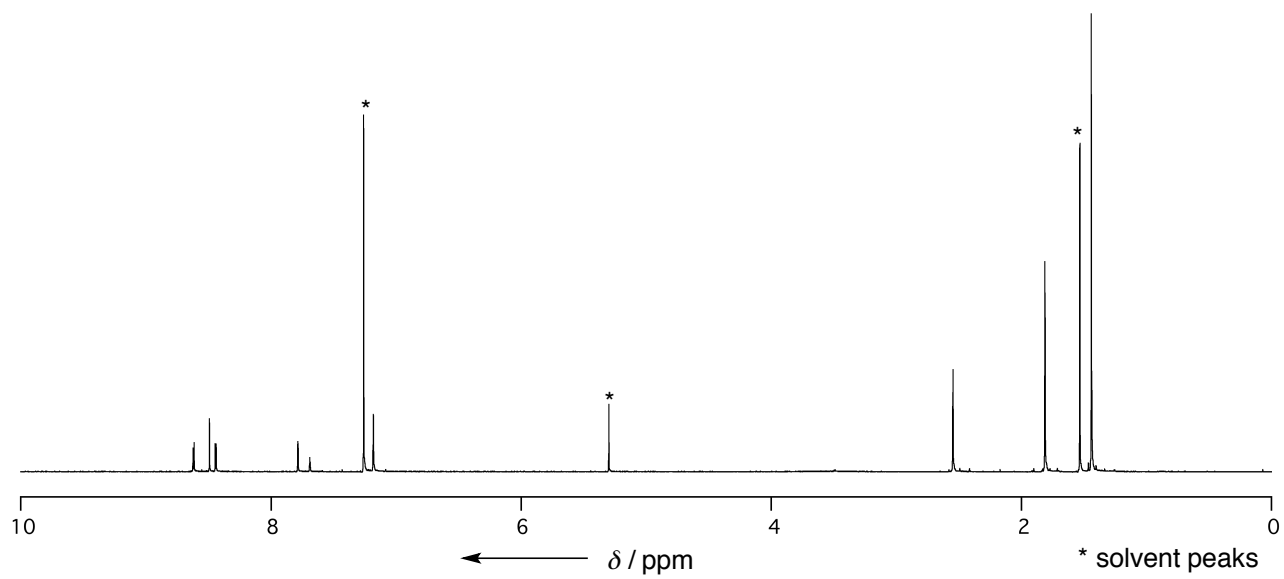


Figure S3. ¹H NMR spectrum of **7** in CDCl₃ at 25 °C.

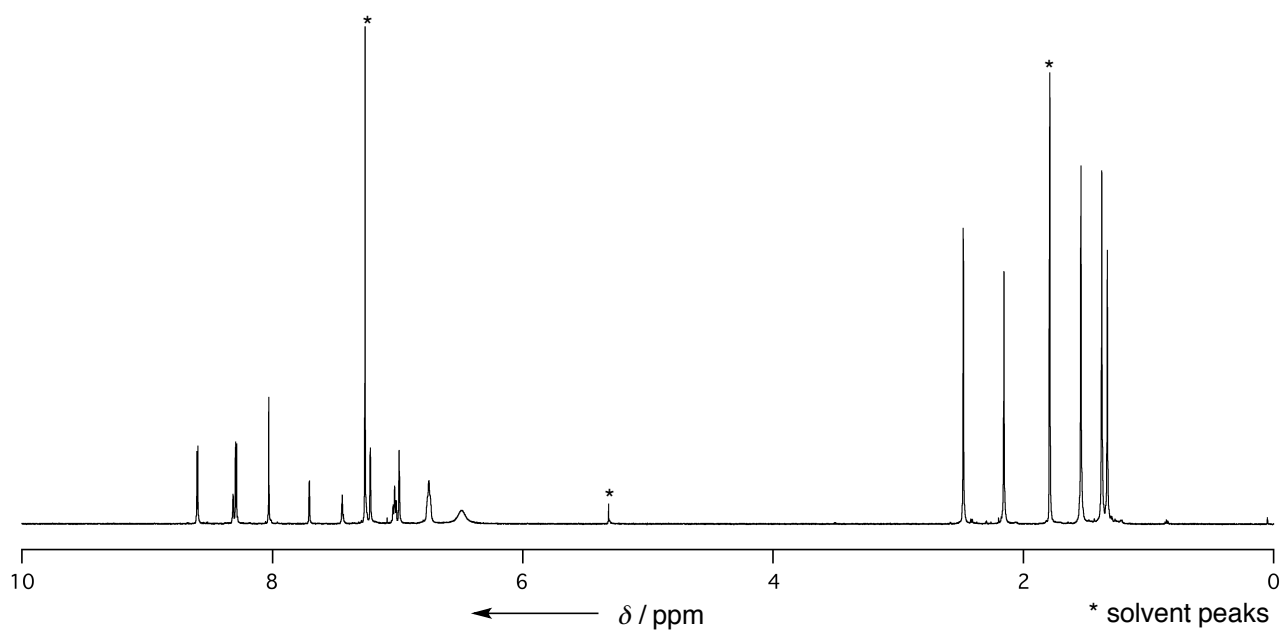


Figure S4. ¹H NMR spectrum of **8** in CDCl₃ at -30 °C.

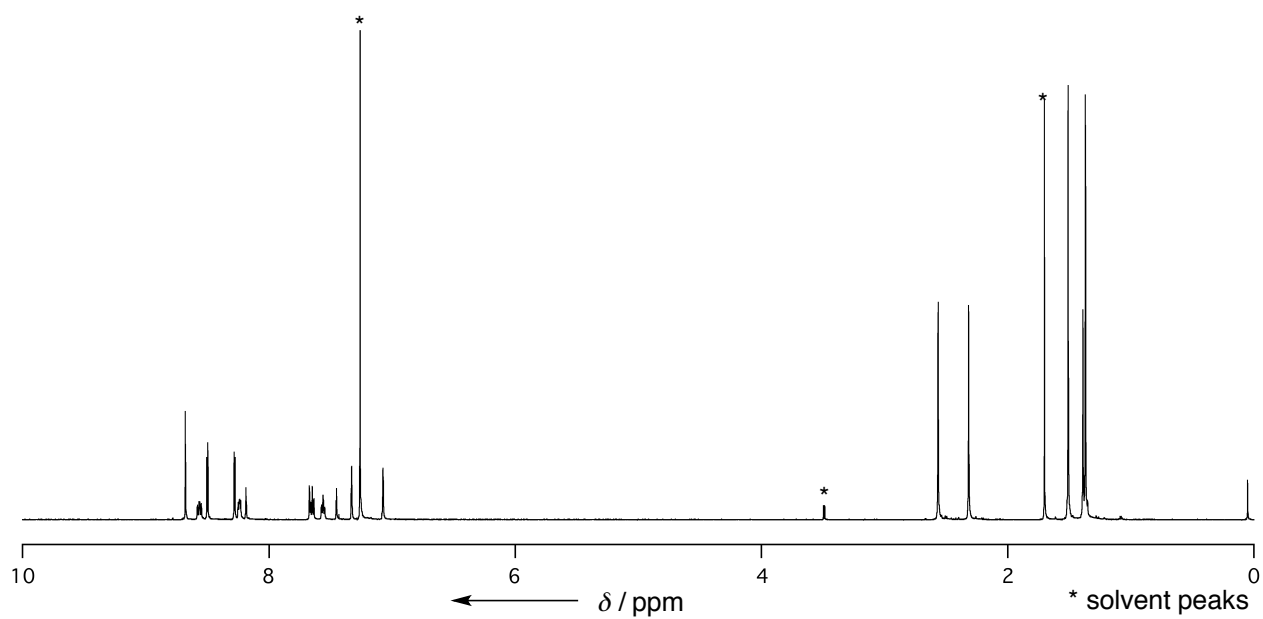


Figure S5. ¹H NMR spectrum of **9** in CDCl₃ at -30 °C.

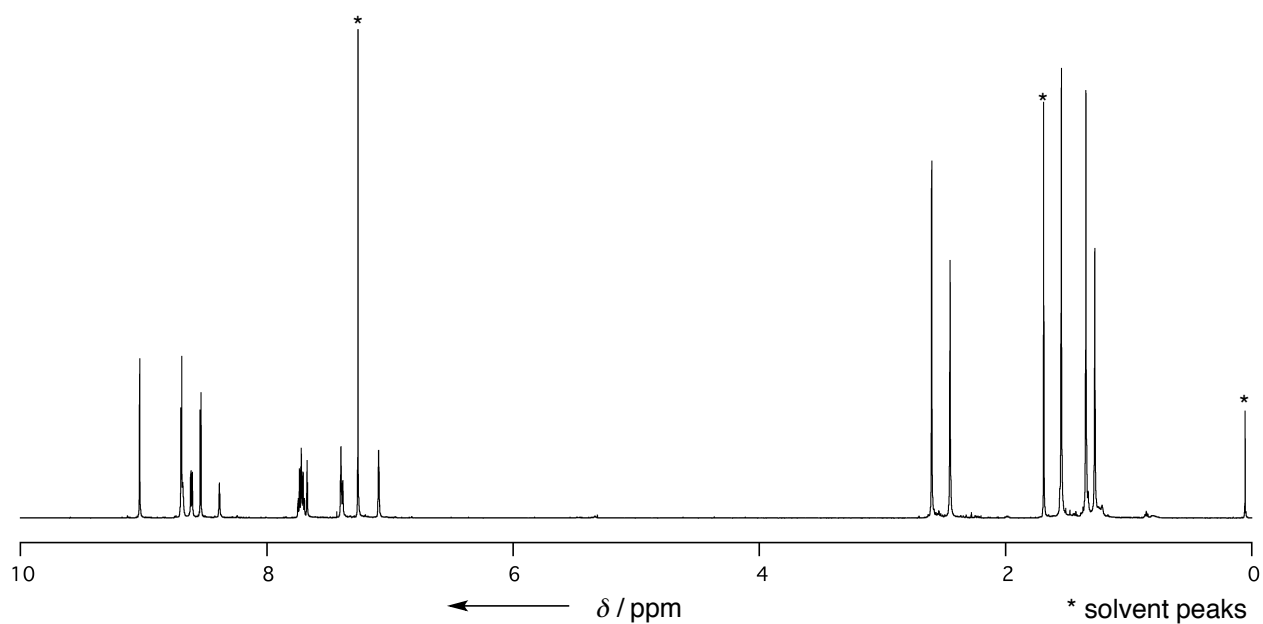


Figure S6. ¹H NMR spectrum of **6** in CDCl₃ at -30 °C.

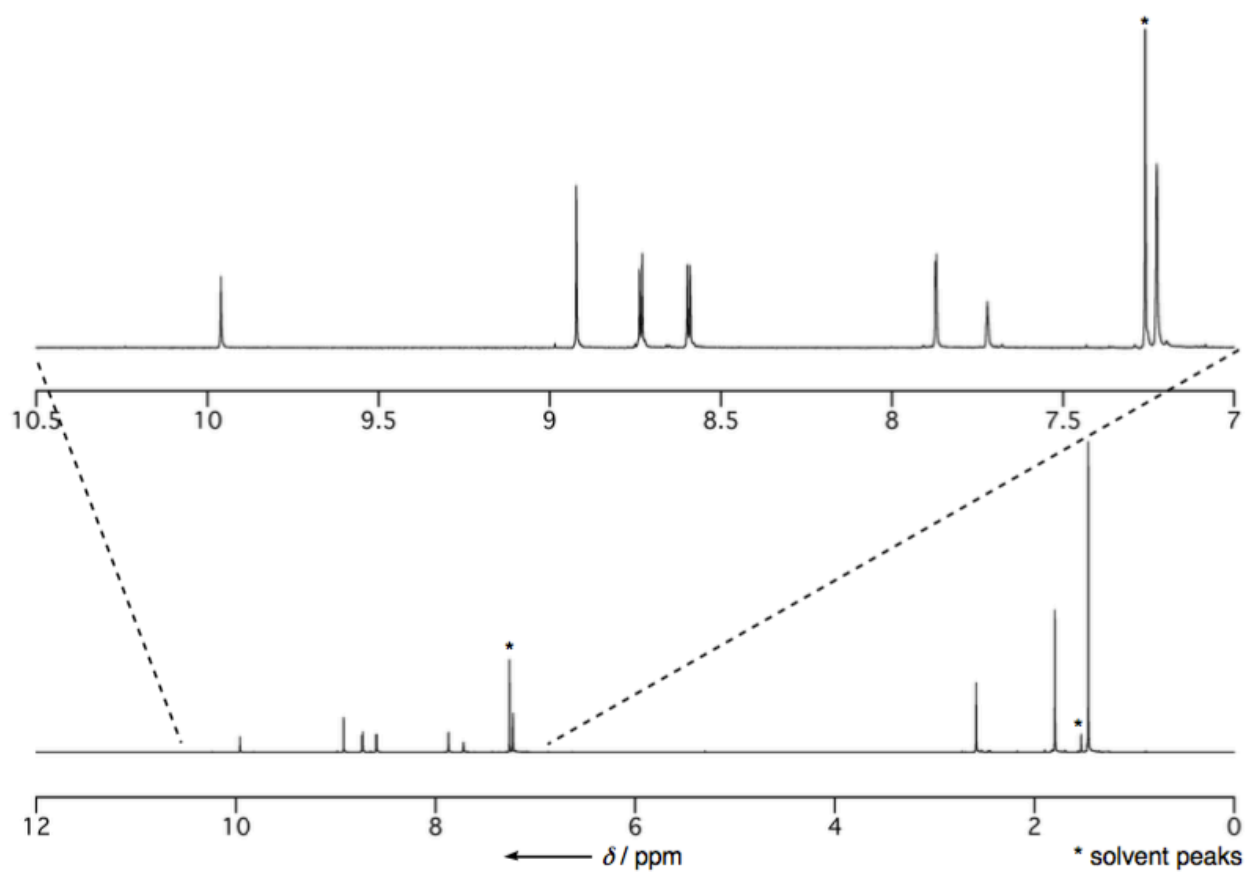


Figure S7. ^1H NMR spectrum of **16Ni** in CDCl_3 at 25°C .

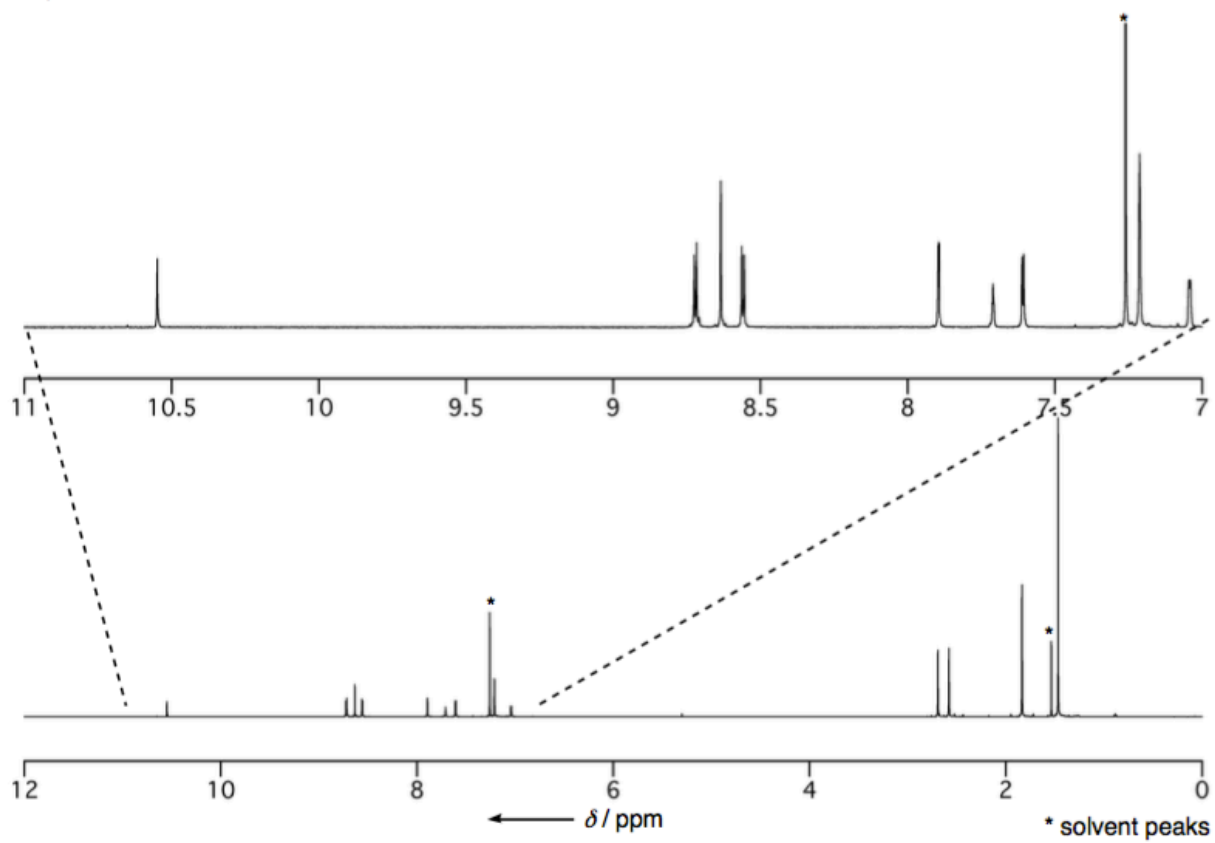


Figure S8. ^1H NMR spectrum of **17Ni** in CDCl_3 at 25°C .

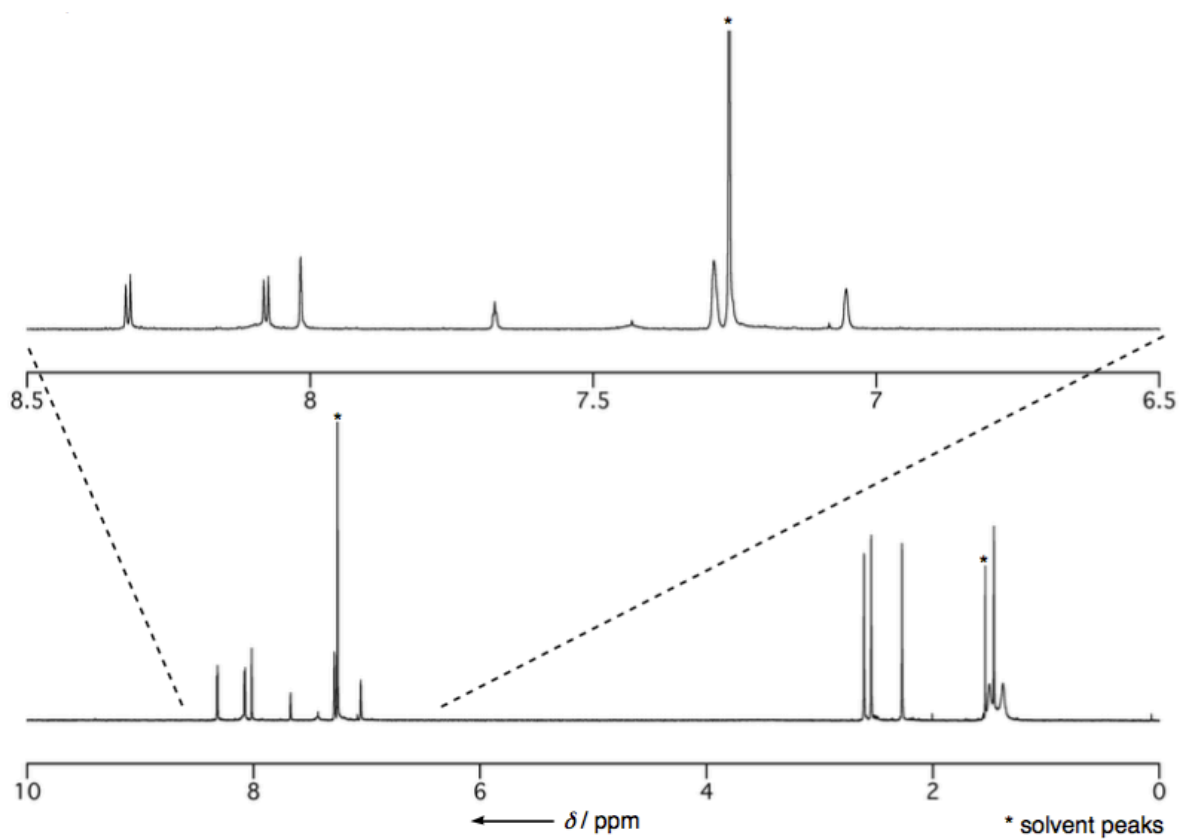


Figure S9. ^1H NMR spectrum of **18Ni** in CDCl_3 at $25\text{ }^\circ\text{C}$.

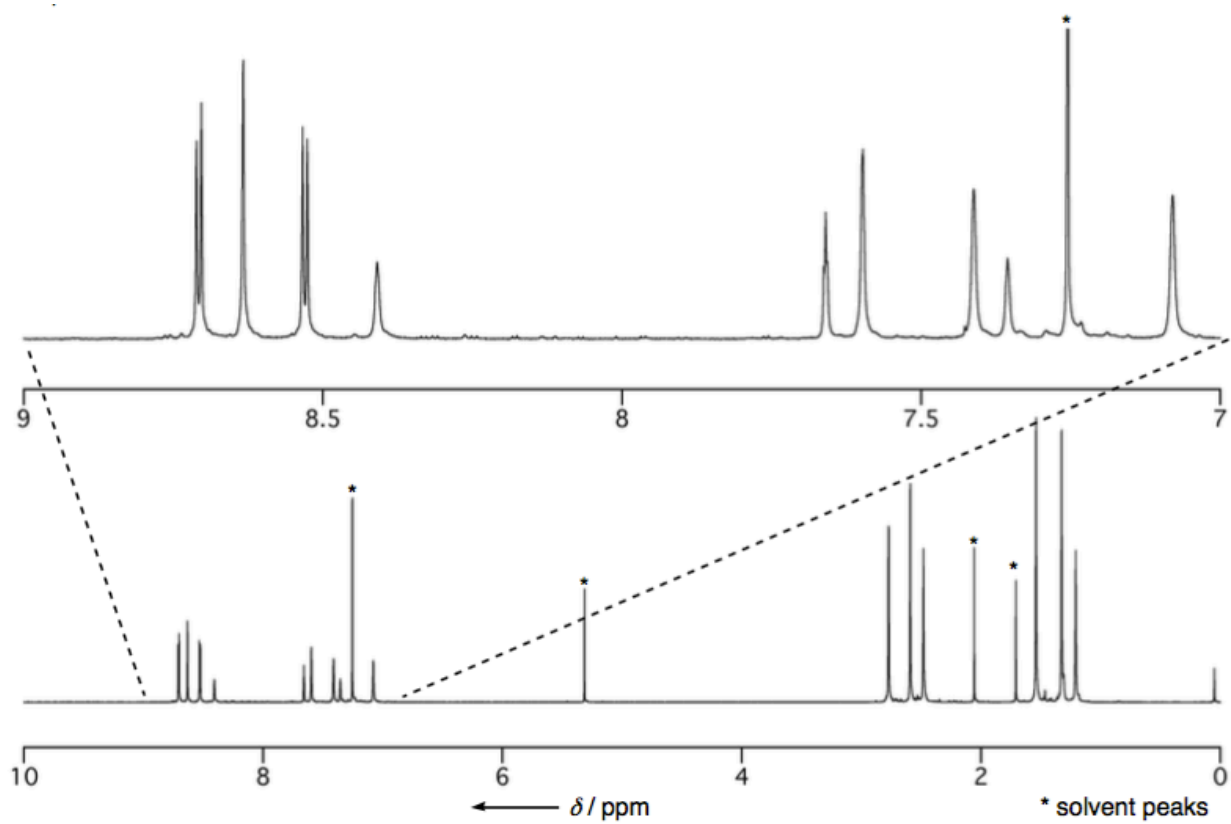


Figure S10. ^1H NMR spectrum of **10Ni** in CDCl_3 at $-40\text{ }^\circ\text{C}$.

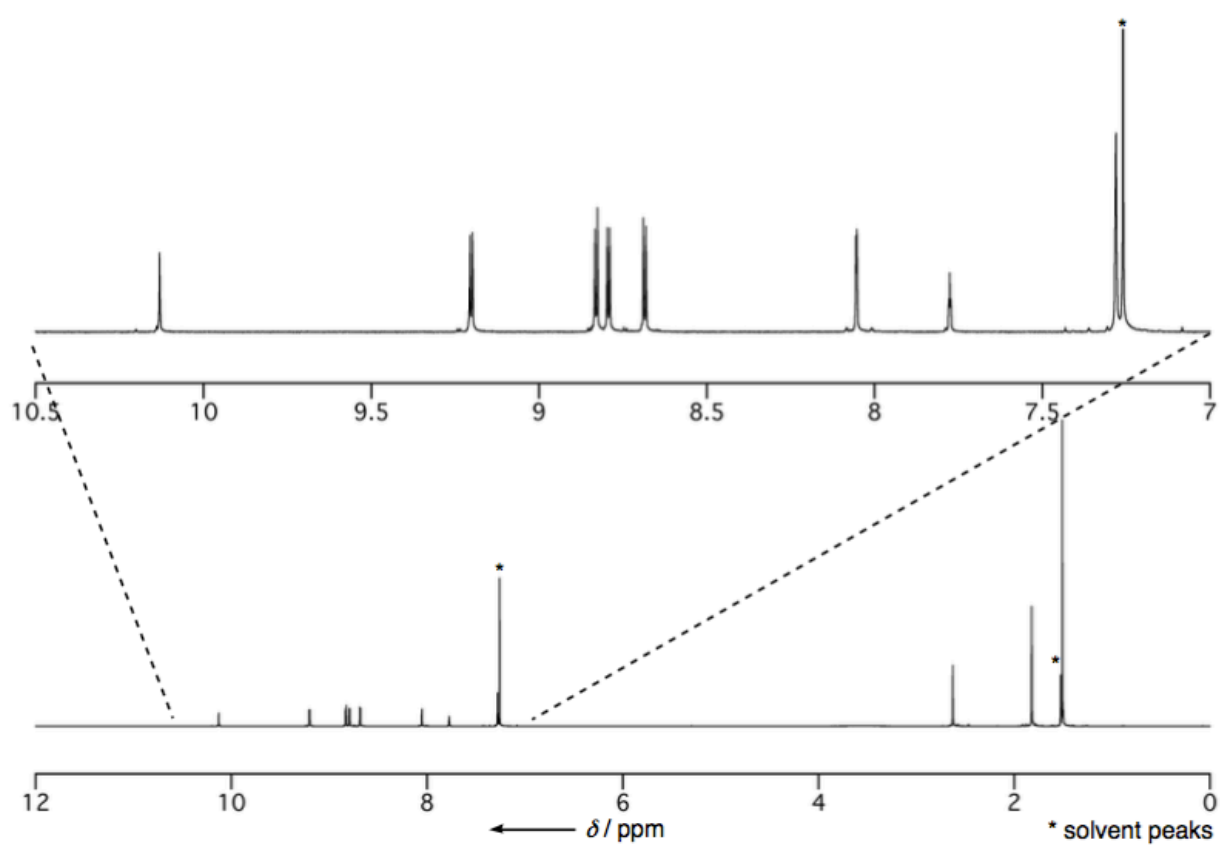


Figure S11. ¹H NMR spectrum of **S6** in CDCl₃ at 25 °C.

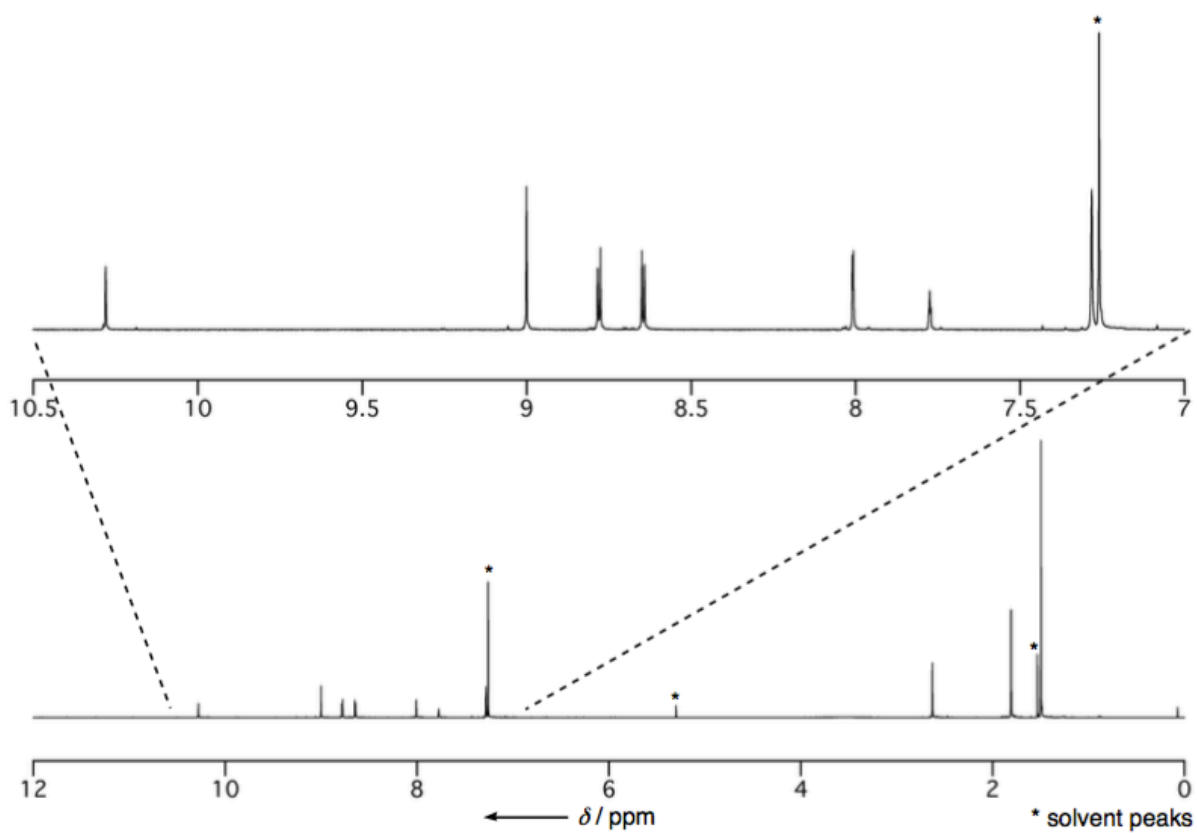


Figure S12. ¹H NMR spectrum of **16Pd** in CDCl₃ at 25 °C.

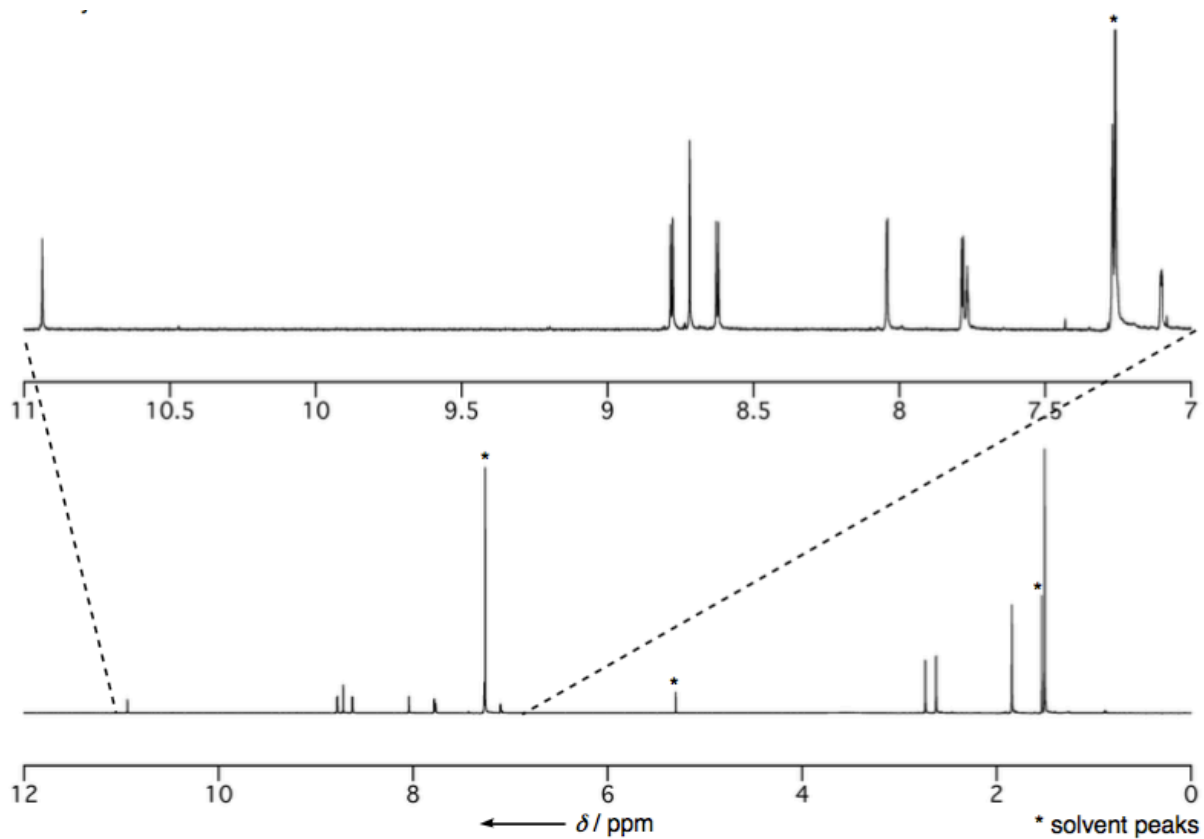


Figure S13. ^1H NMR spectrum of **17Pd** in CDCl_3 at $25\text{ }^\circ\text{C}$.

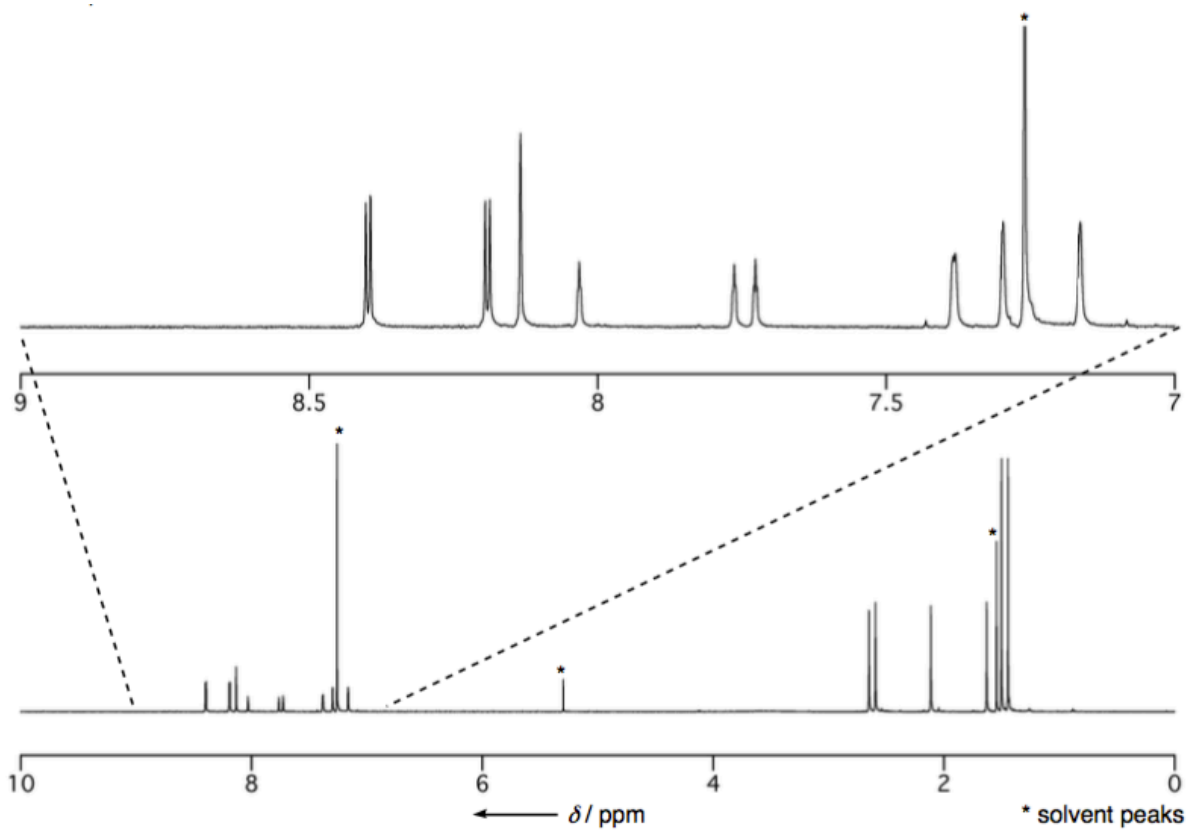


Figure S14. ^1H NMR spectrum of **18Pd** in CDCl_3 at $25\text{ }^\circ\text{C}$.

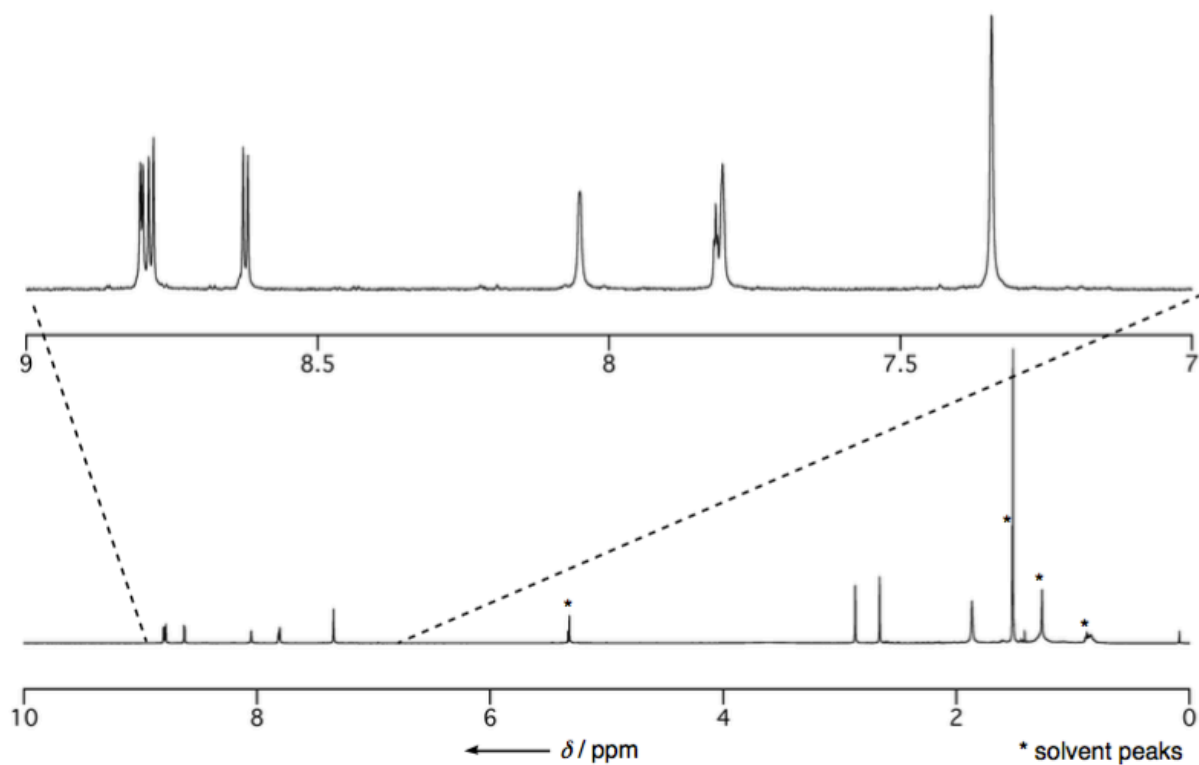


Figure S15. ^1H NMR spectrum of **10Pd** in CD_2Cl_2 at 25 $^\circ\text{C}$.

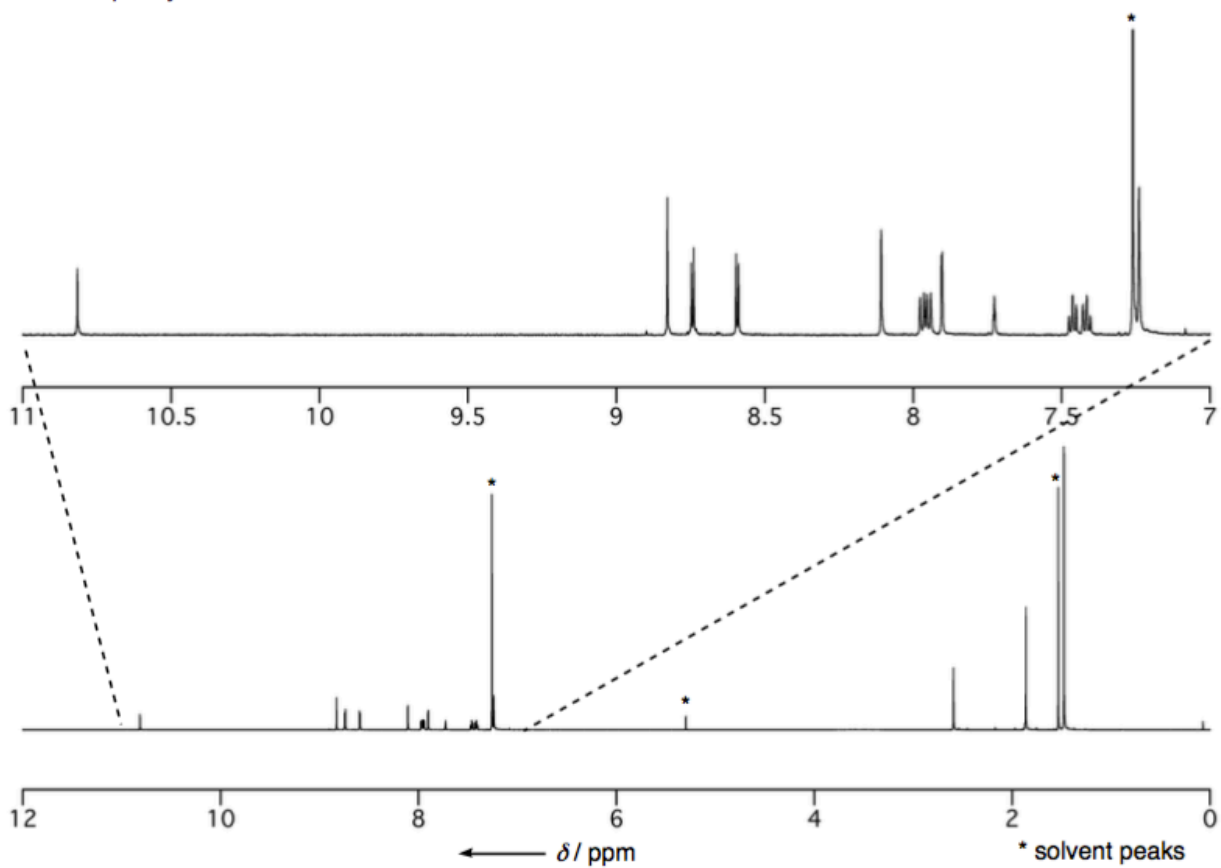


Figure S16. ^1H NMR spectrum of **19** in CDCl_3 at 25 $^\circ\text{C}$.

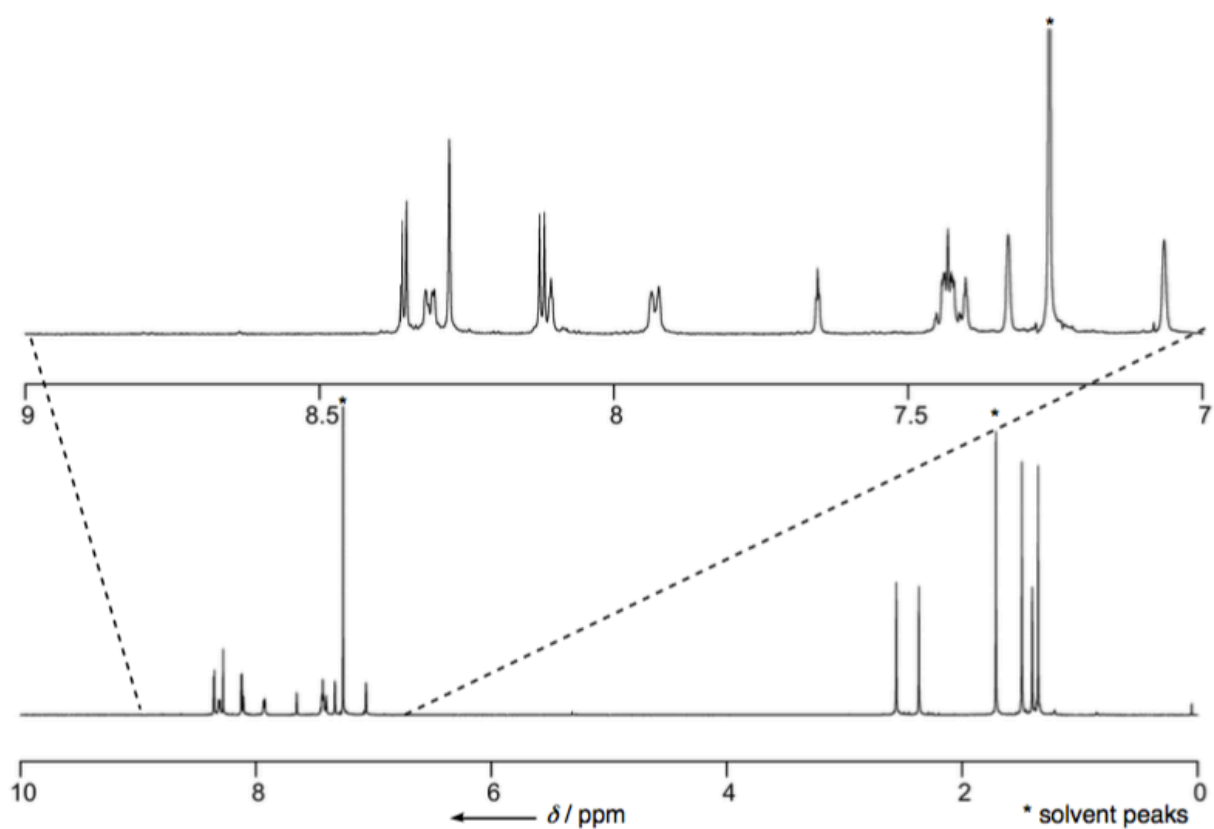


Figure S17. ^1H NMR spectrum of **20** in CDCl_3 at $-30\text{ }^\circ\text{C}$.

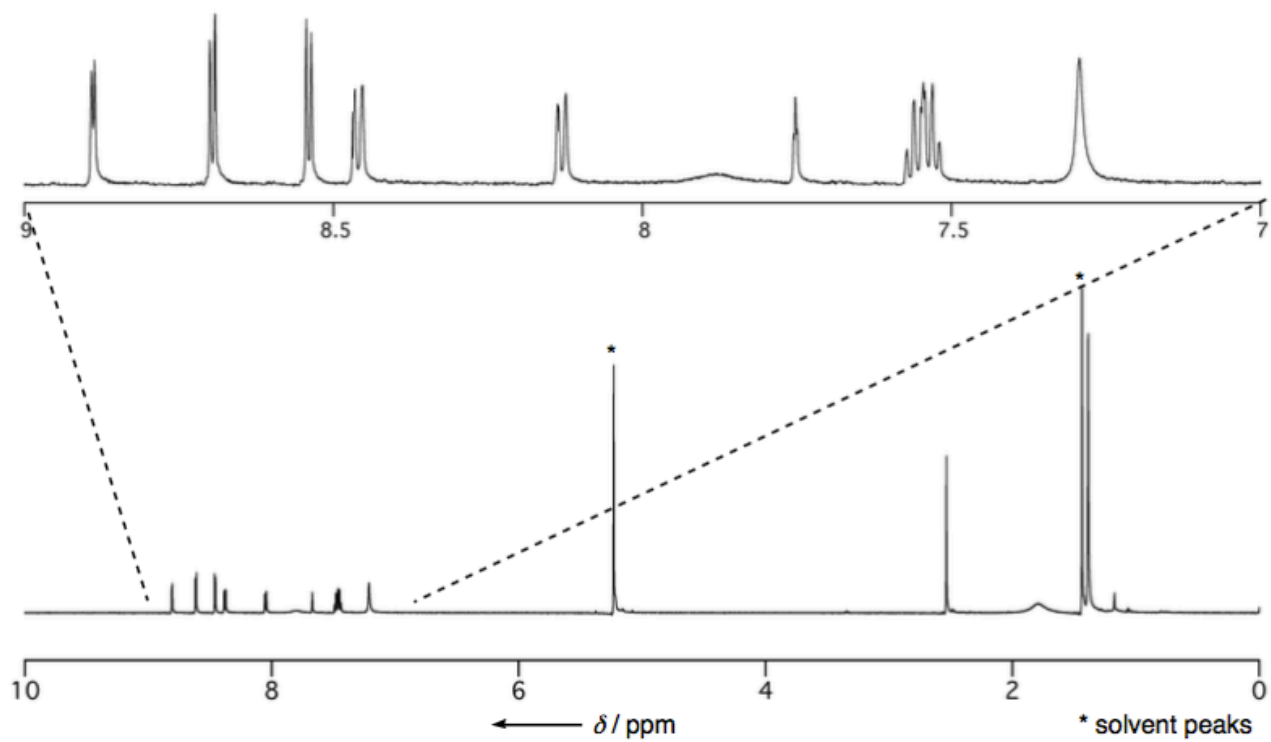


Figure S18. ^1H NMR spectrum of **11** in CD_2Cl_2 at $25\text{ }^\circ\text{C}$.

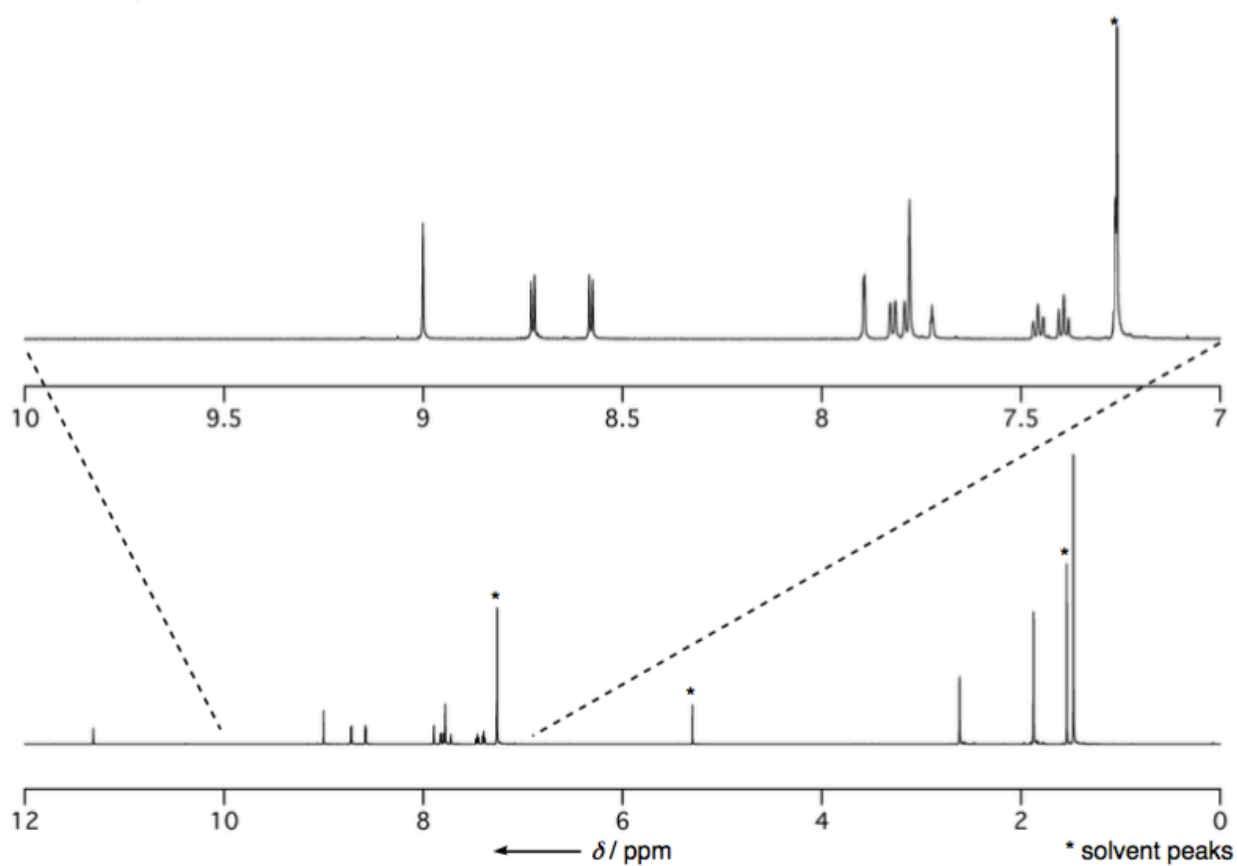


Figure S19. ^1H NMR spectrum of **21** in CDCl_3 at 25°C .

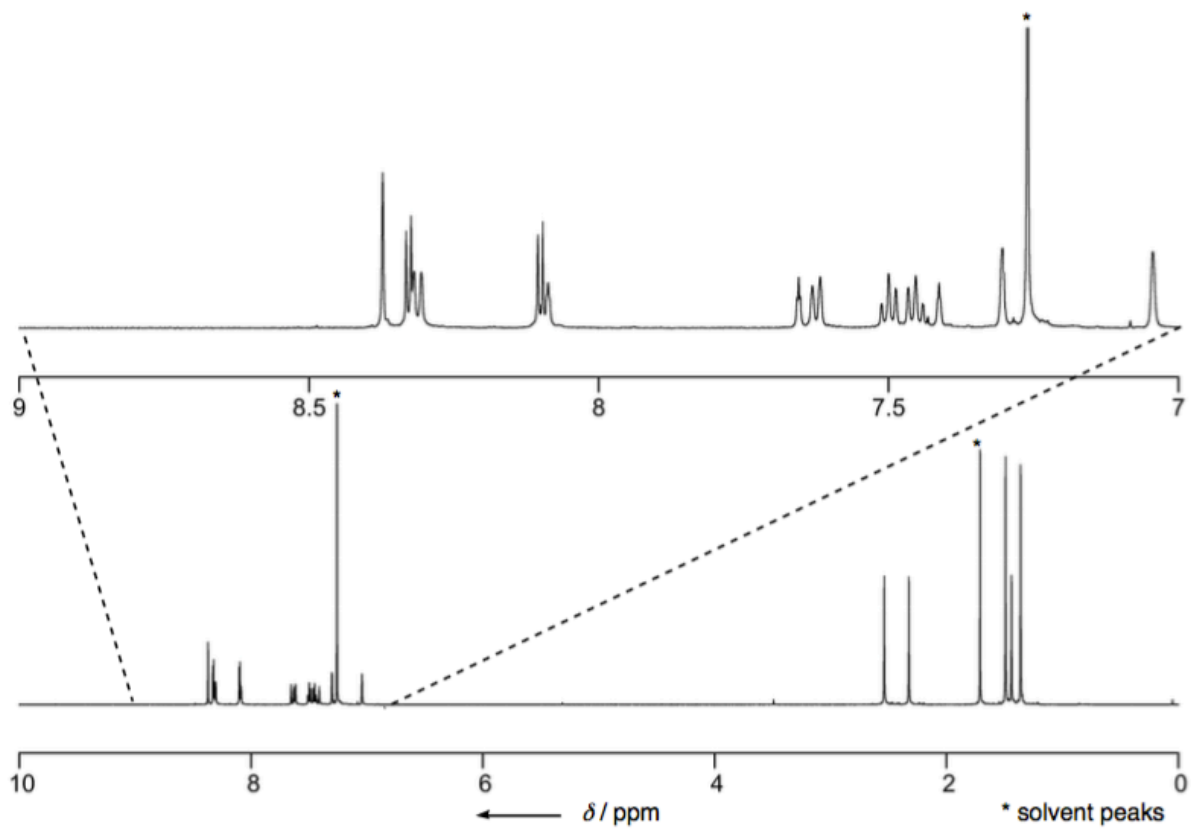


Figure S20. ^1H NMR spectrum of **22** in CDCl_3 at -30°C .

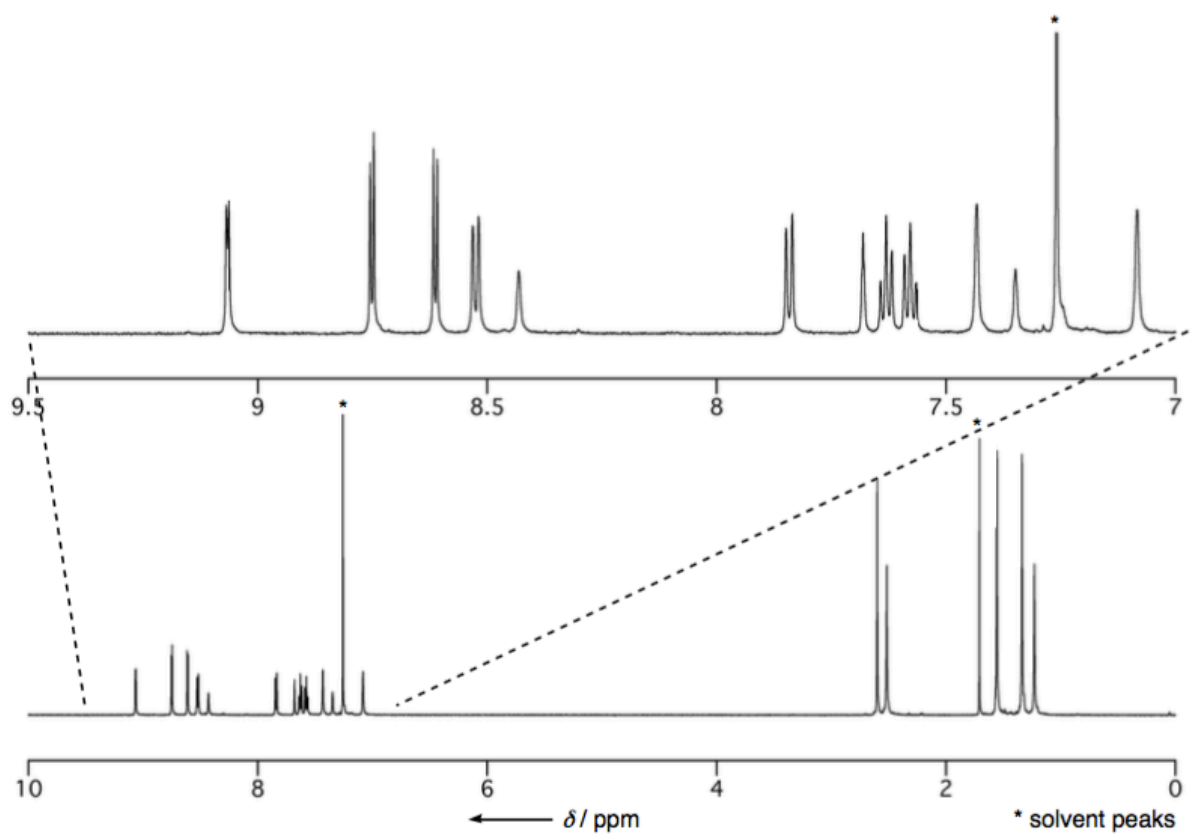


Figure S21. ^1H NMR spectrum of **12** in CDCl_3 at $-40\text{ }^\circ\text{C}$.

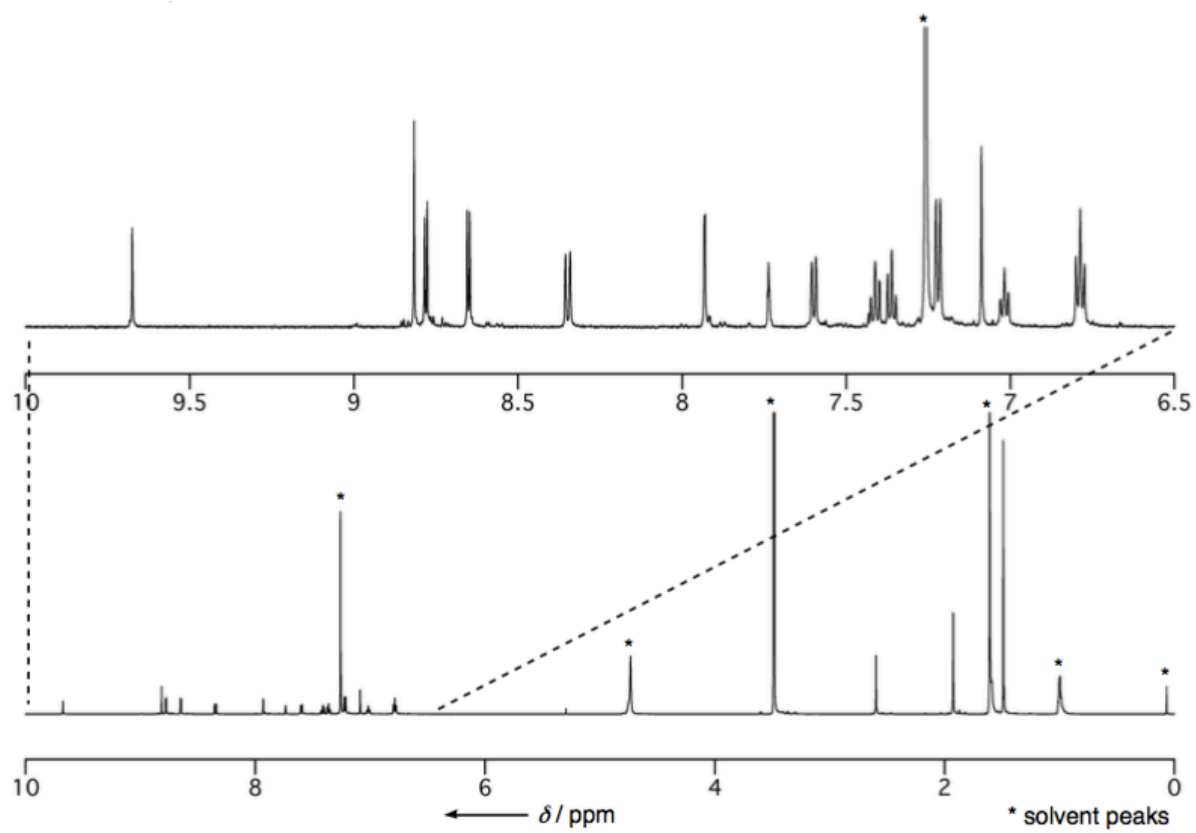


Figure S22. ^1H NMR spectrum of **23** in CDCl_3 at $25\text{ }^\circ\text{C}$.

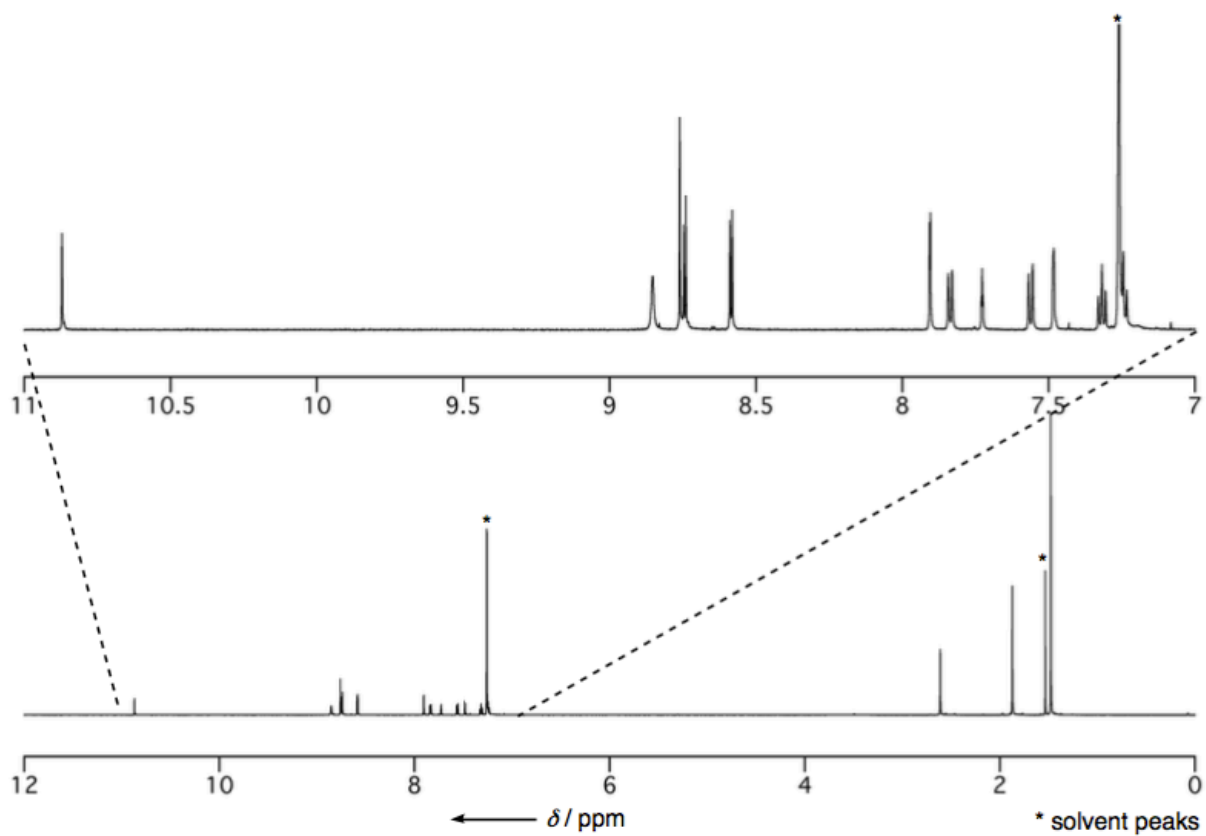


Figure S23. ¹H NMR spectrum of **24** in CDCl₃ at 25 °C.

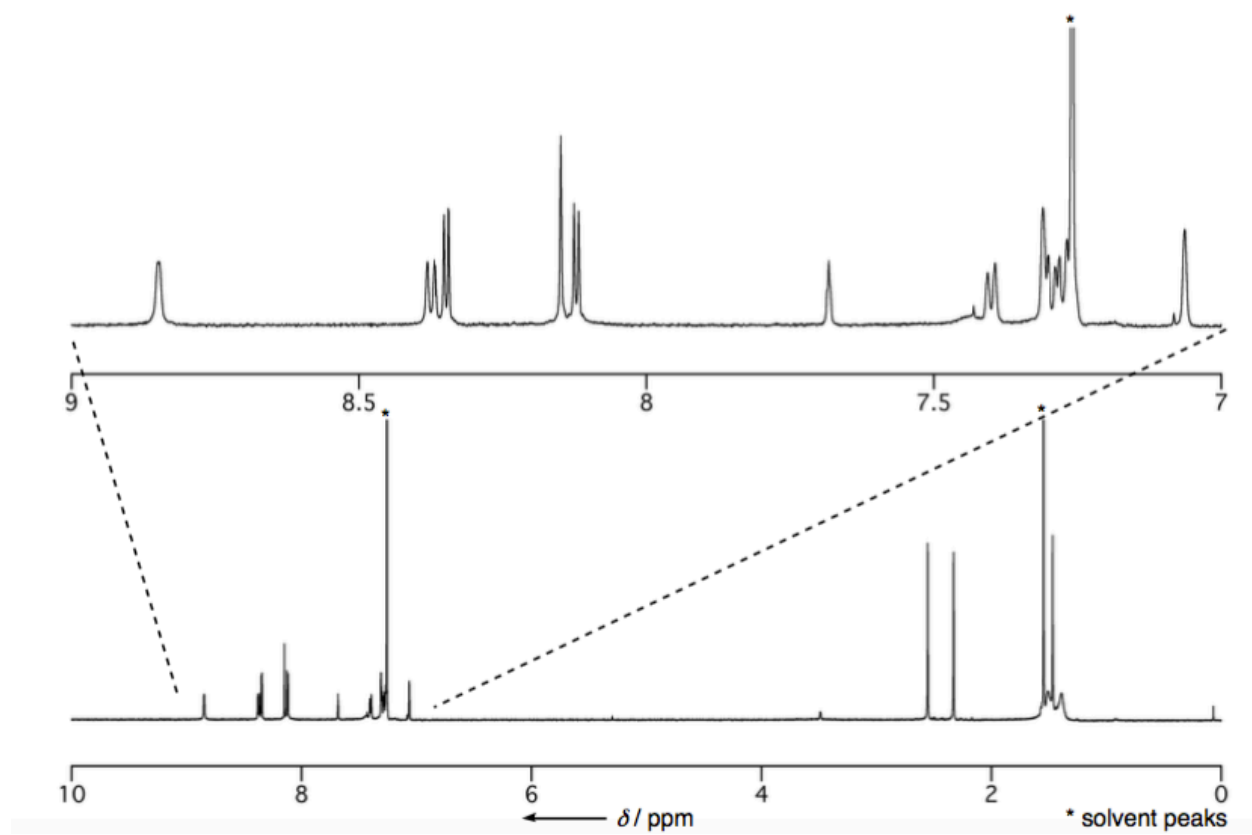


Figure S24. ¹H NMR spectrum of **25** in CDCl₃ at 25 °C.

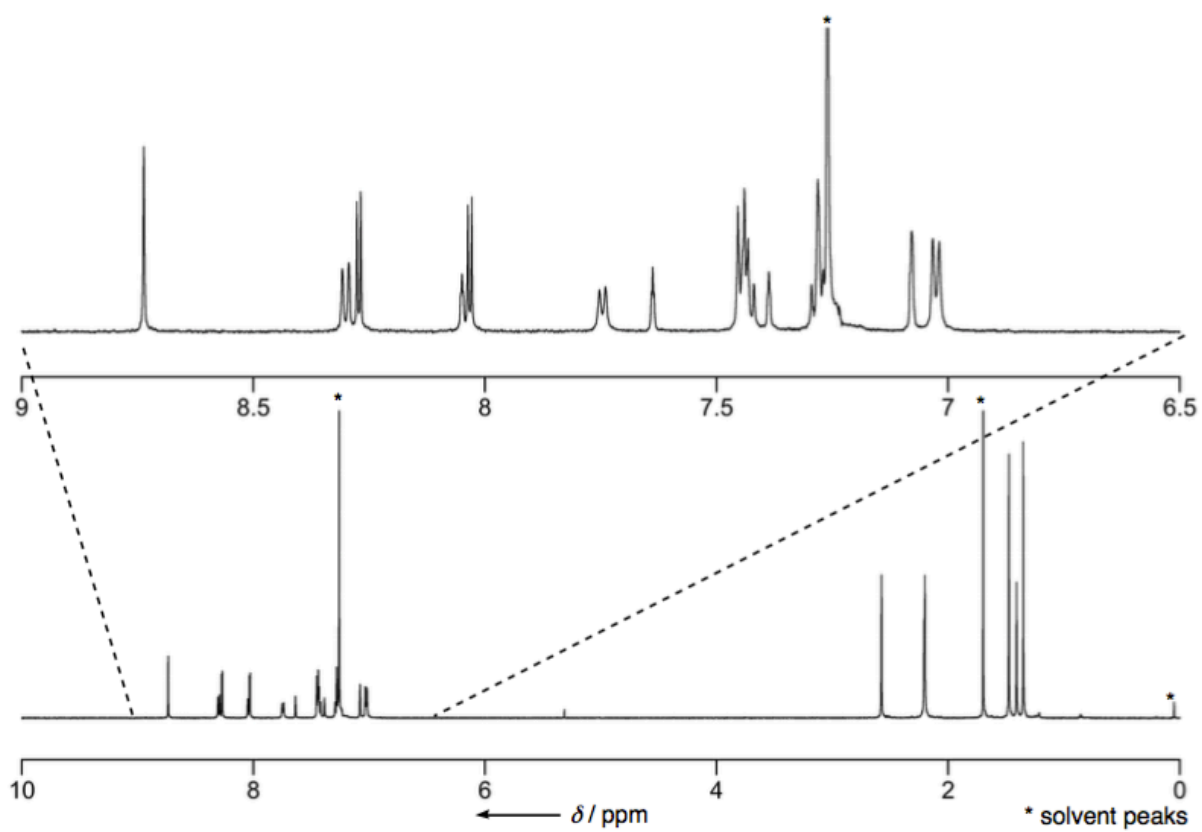


Figure S25. ^1H NMR spectrum of **26** in CDCl_3 at $-30\text{ }^\circ\text{C}$.

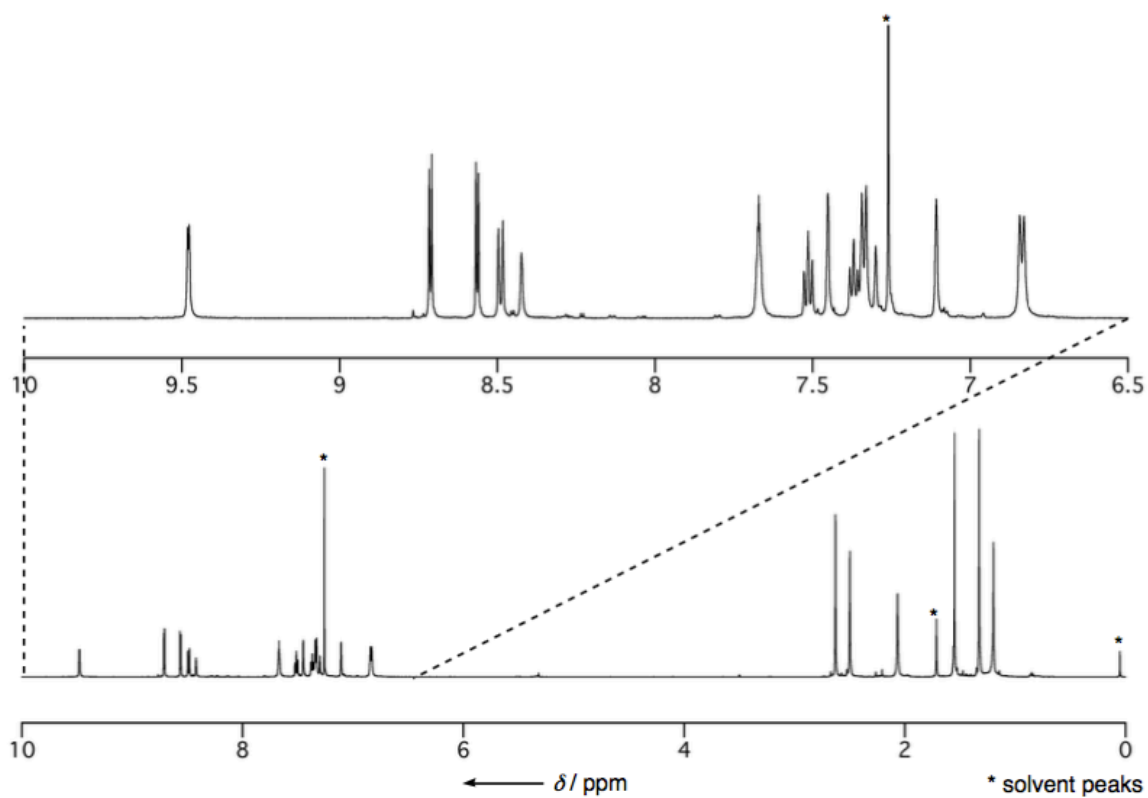


Figure S26. ^1H NMR spectrum of **13** in CDCl_3 at $-40\text{ }^\circ\text{C}$.

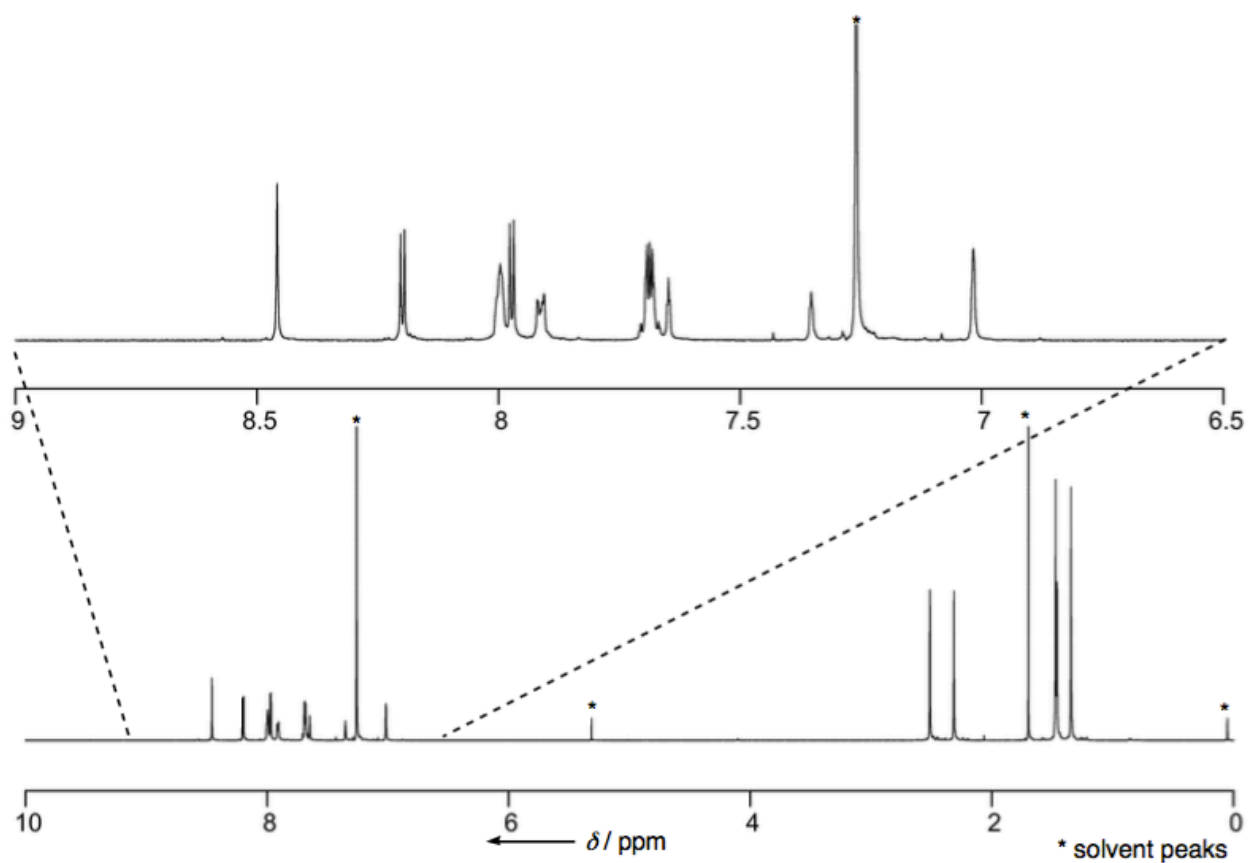


Figure S27. ^1H NMR spectrum of **27** in CDCl_3 at $-30\text{ }^\circ\text{C}$.

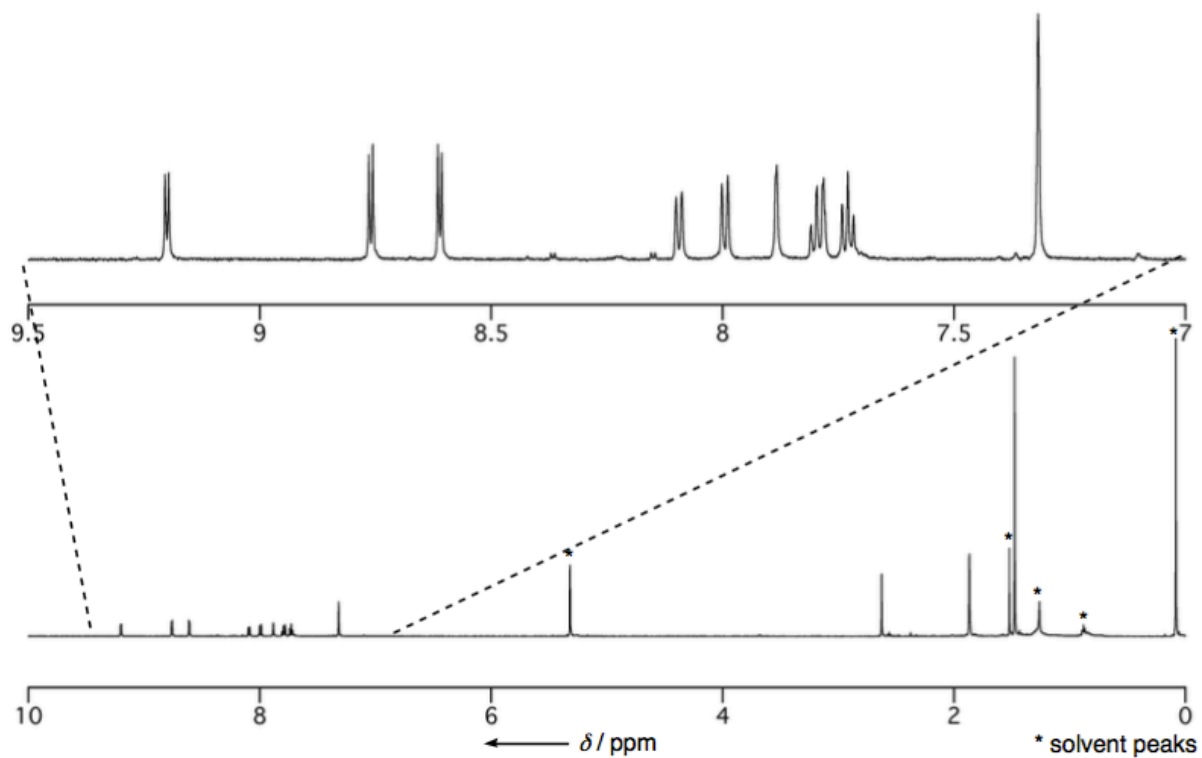


Figure S28. ^1H NMR spectrum of **14** in CD_2Cl_2 at $25\text{ }^\circ\text{C}$.

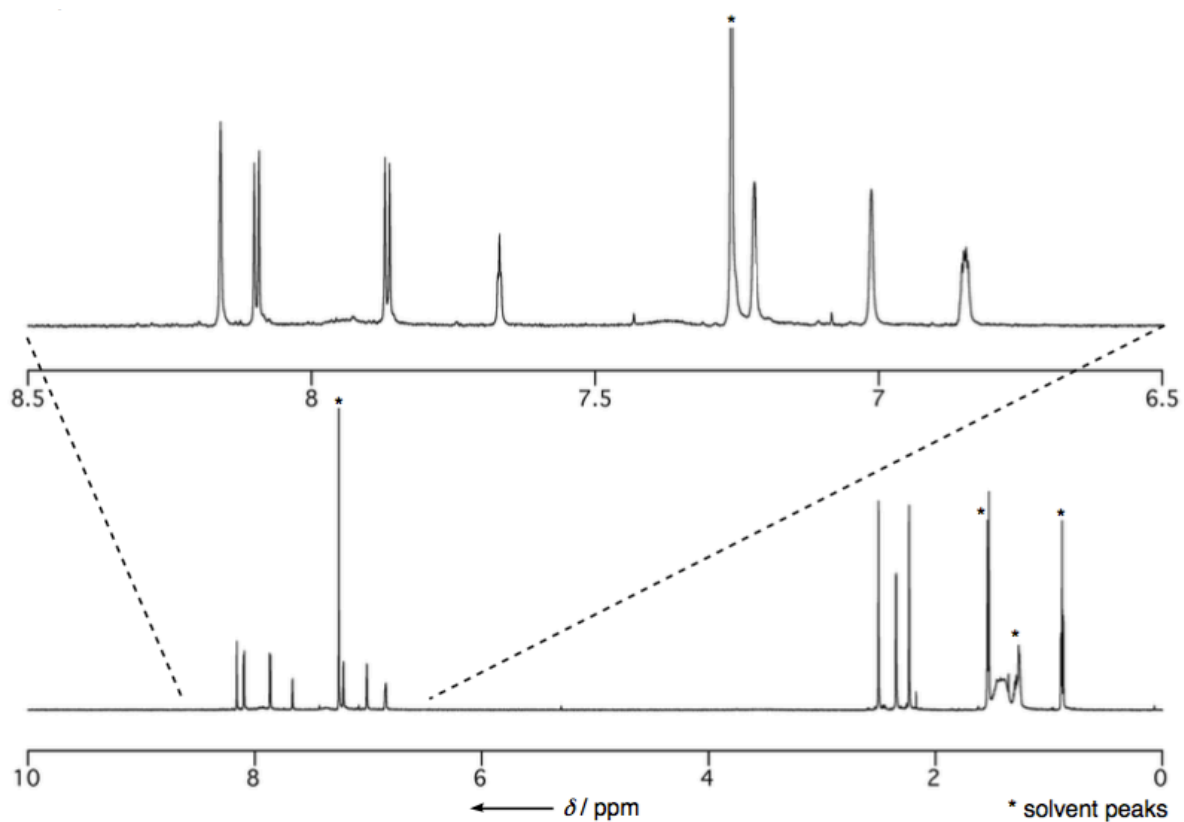


Figure S29. ^1H NMR spectrum of **28** in CDCl_3 at $25\text{ }^\circ\text{C}$.

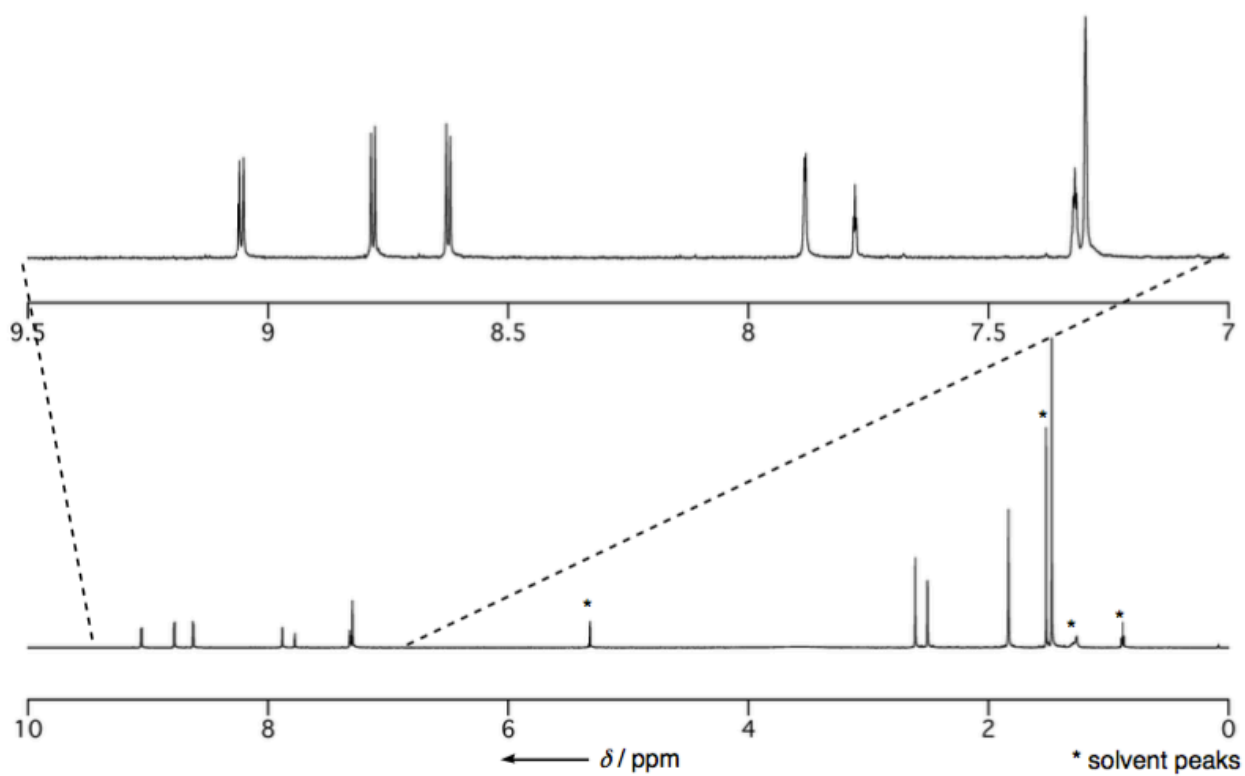


Figure S30. ^1H NMR spectrum of **15** in CD_2Cl_2 at $25\text{ }^\circ\text{C}$.

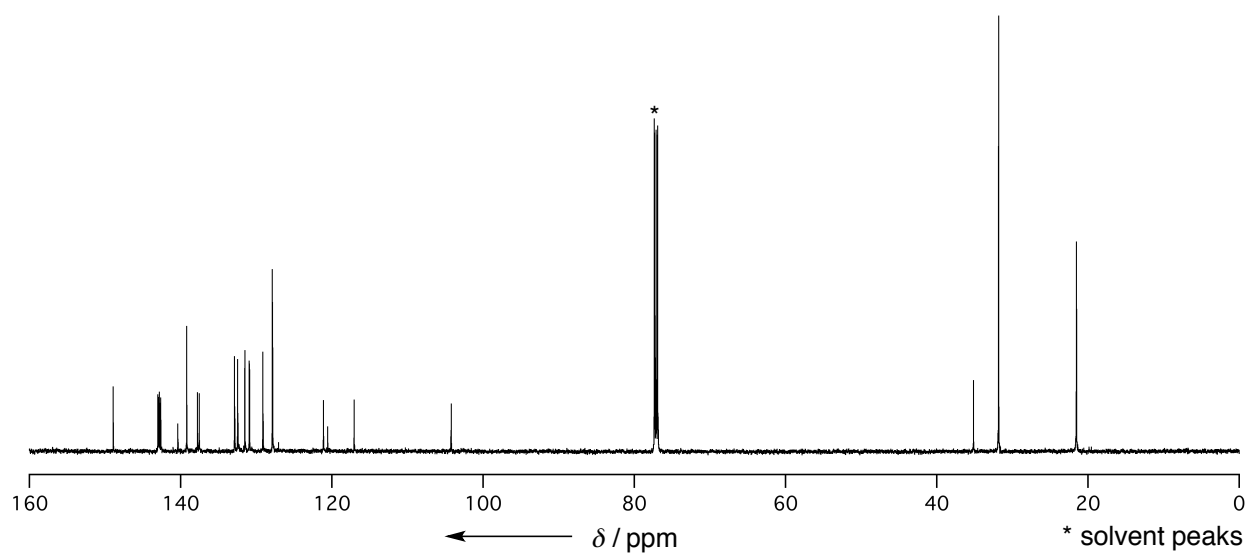


Figure S31. ^{13}C NMR spectrum of **S3** in CDCl_3 at $25\text{ }^\circ\text{C}$.

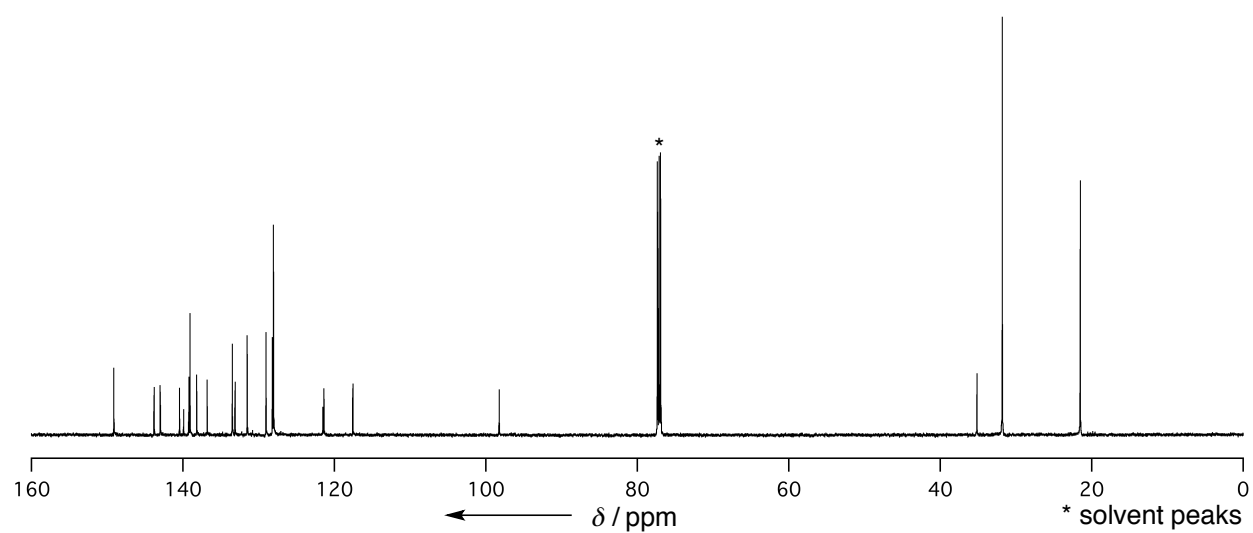


Figure S32. ^{13}C NMR spectrum of **S5** in CDCl_3 at $25\text{ }^\circ\text{C}$.

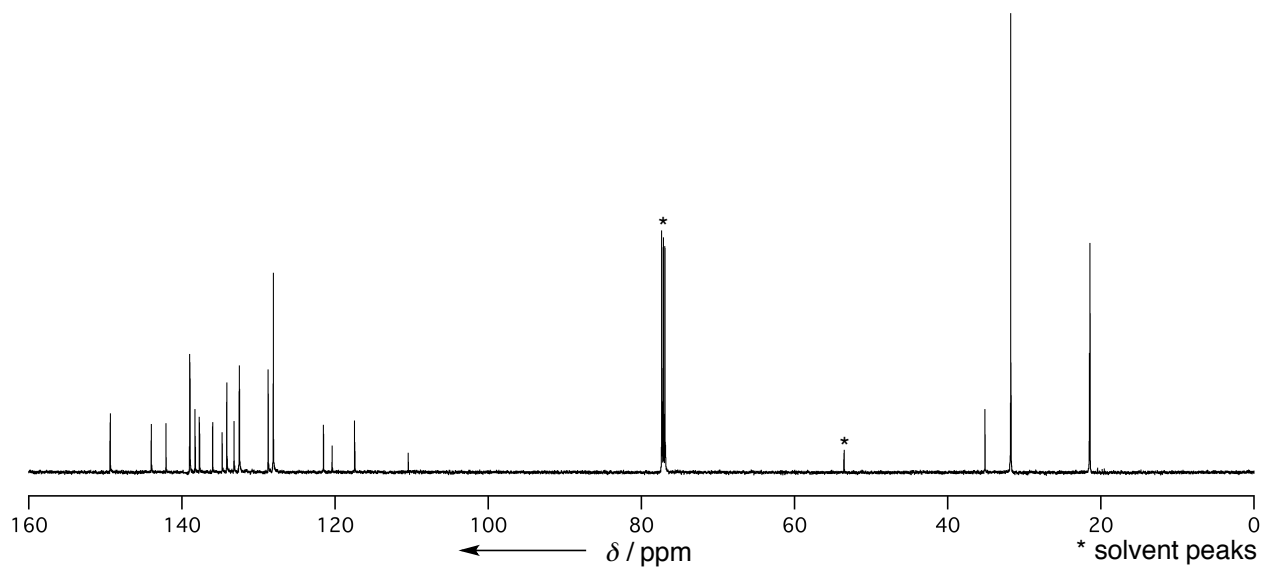


Figure S33. ^{13}C NMR spectrum of **7** in CDCl_3 at 25 °C.

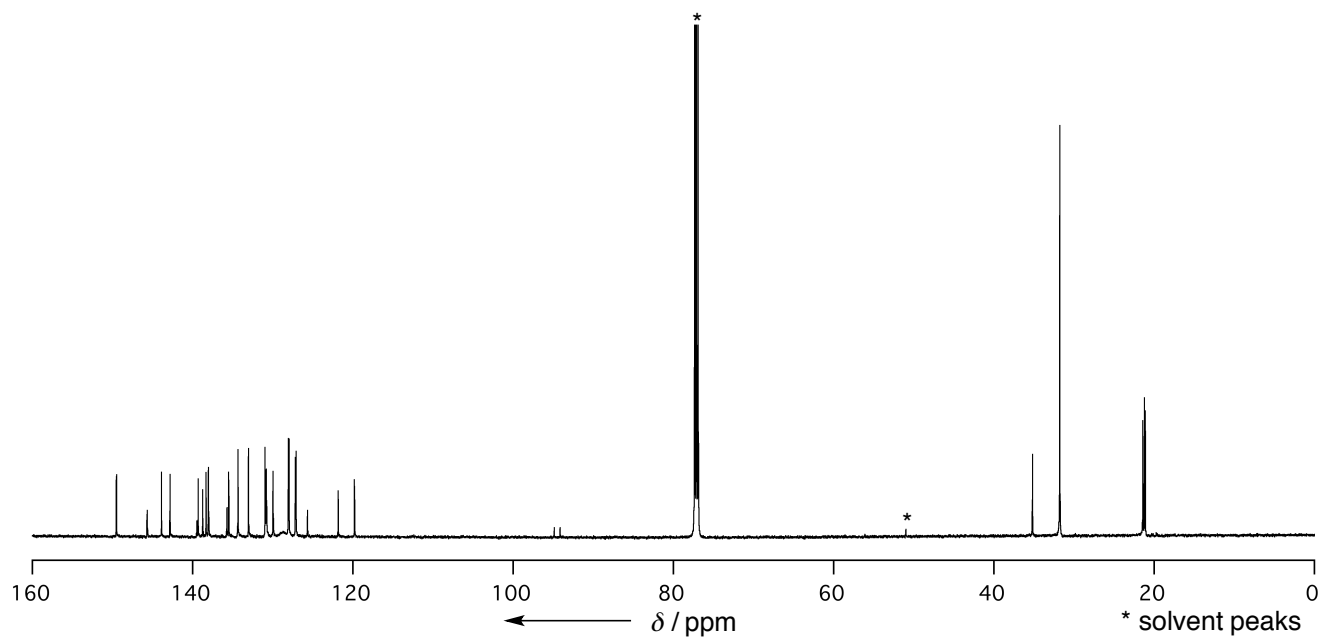


Figure S34. ^{13}C NMR spectrum of **8** in CDCl_3 at 25 °C.

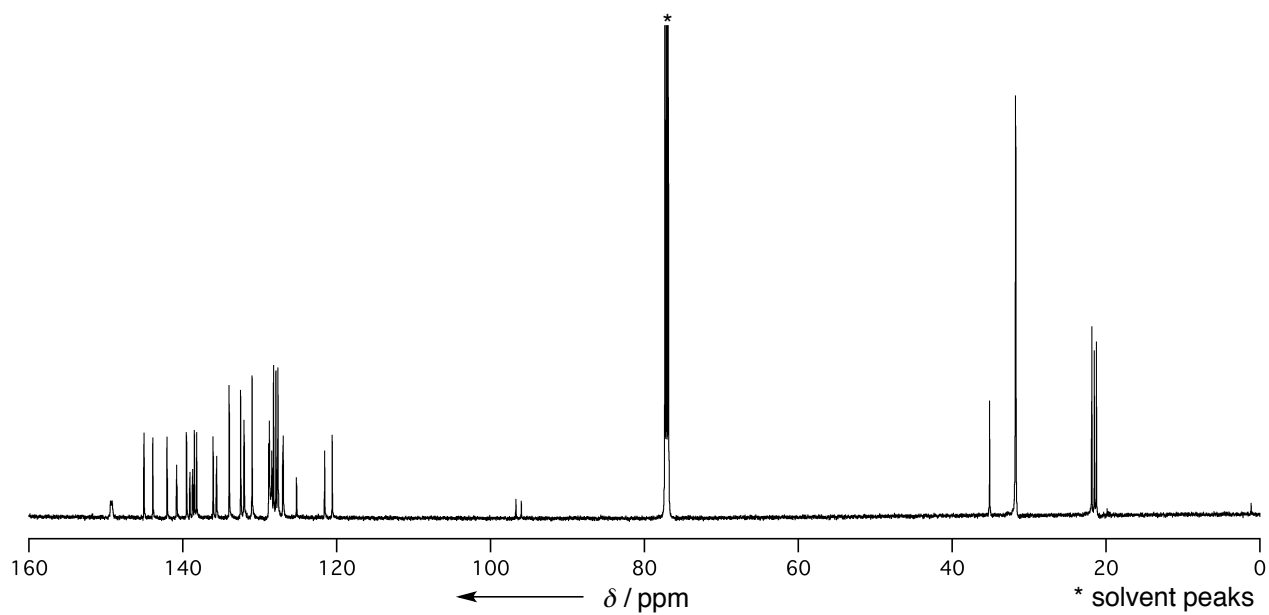


Figure S35. ^{13}C NMR spectrum of **9** in CDCl_3 at 25°C .

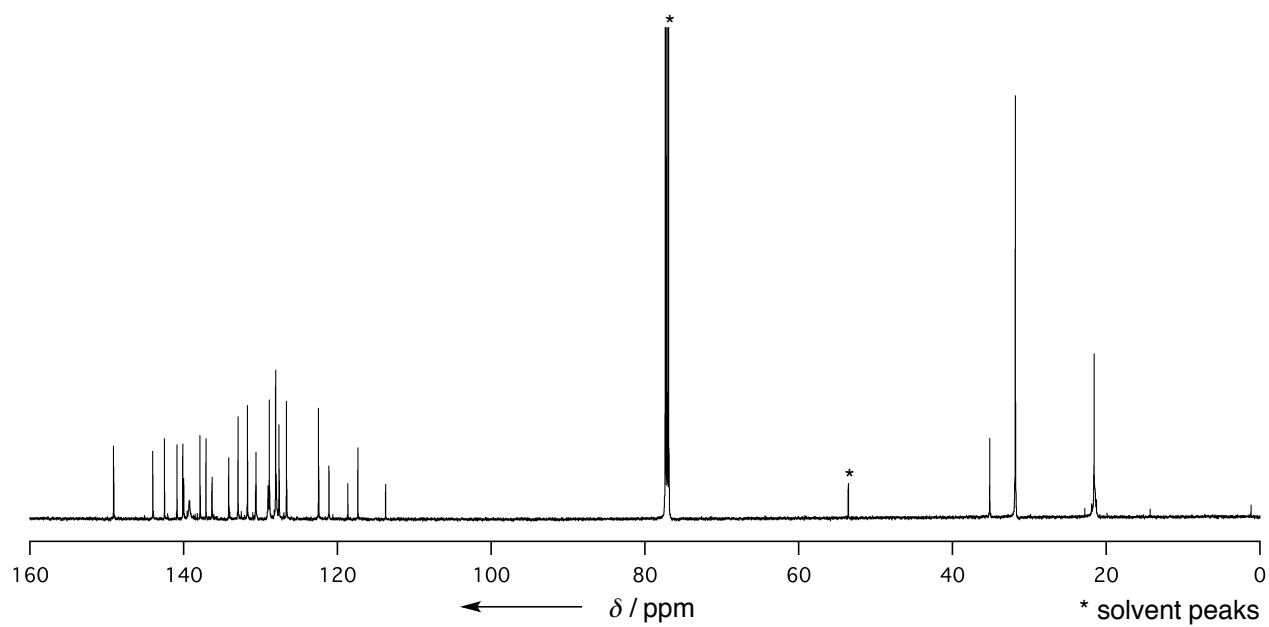


Figure S36. ^{13}C NMR spectrum of **6** in CDCl_3 at 25°C .

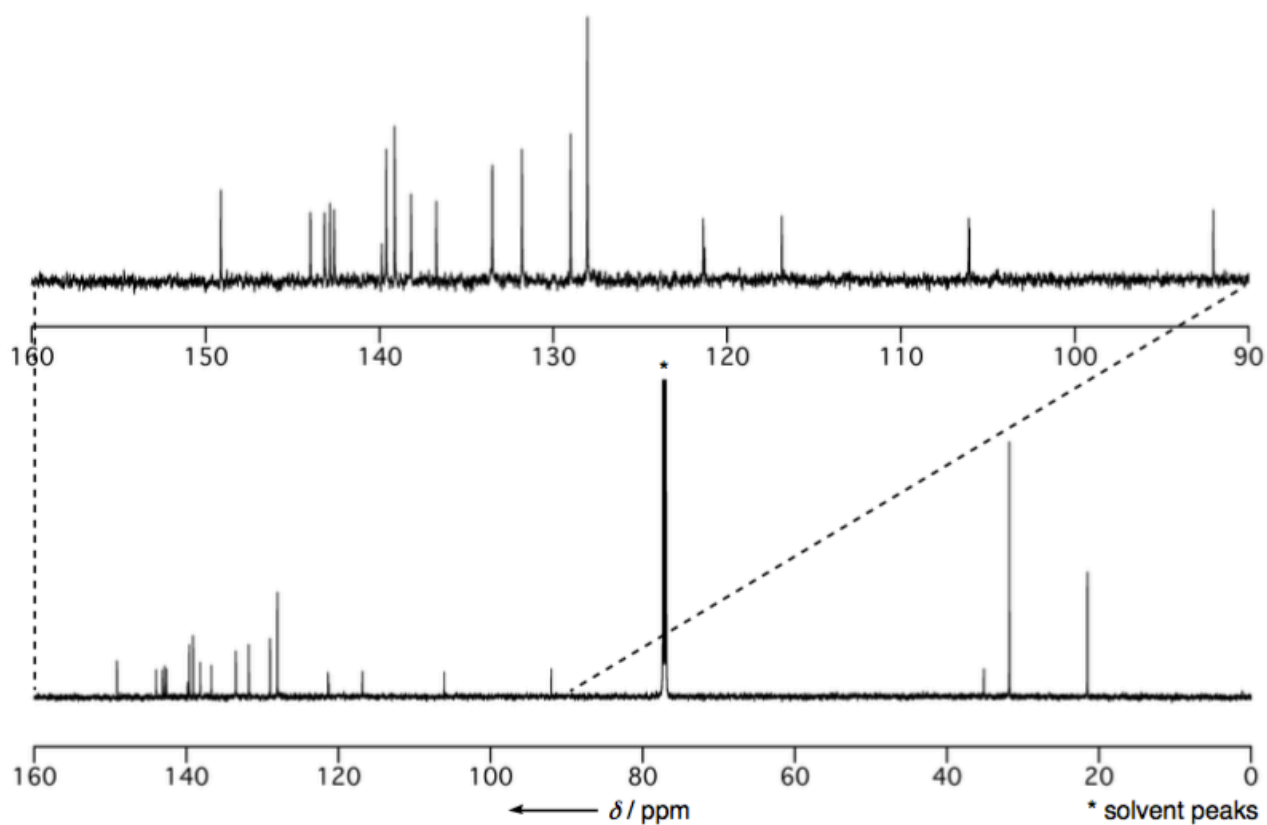


Figure S37. ^{13}C NMR spectrum of **16Ni** in CDCl_3 at 25 °C.

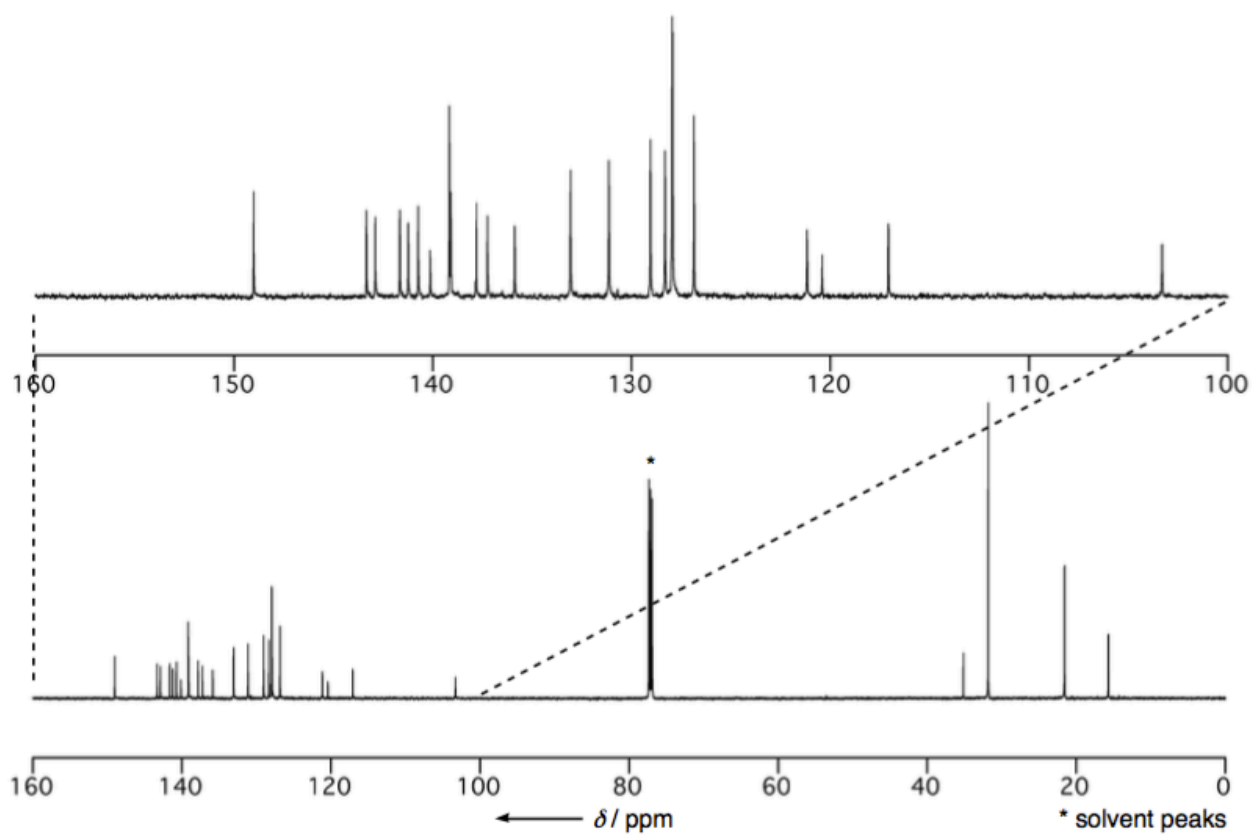


Figure S38. ^{13}C NMR spectrum of **17Ni** in CDCl_3 at 25 °C.

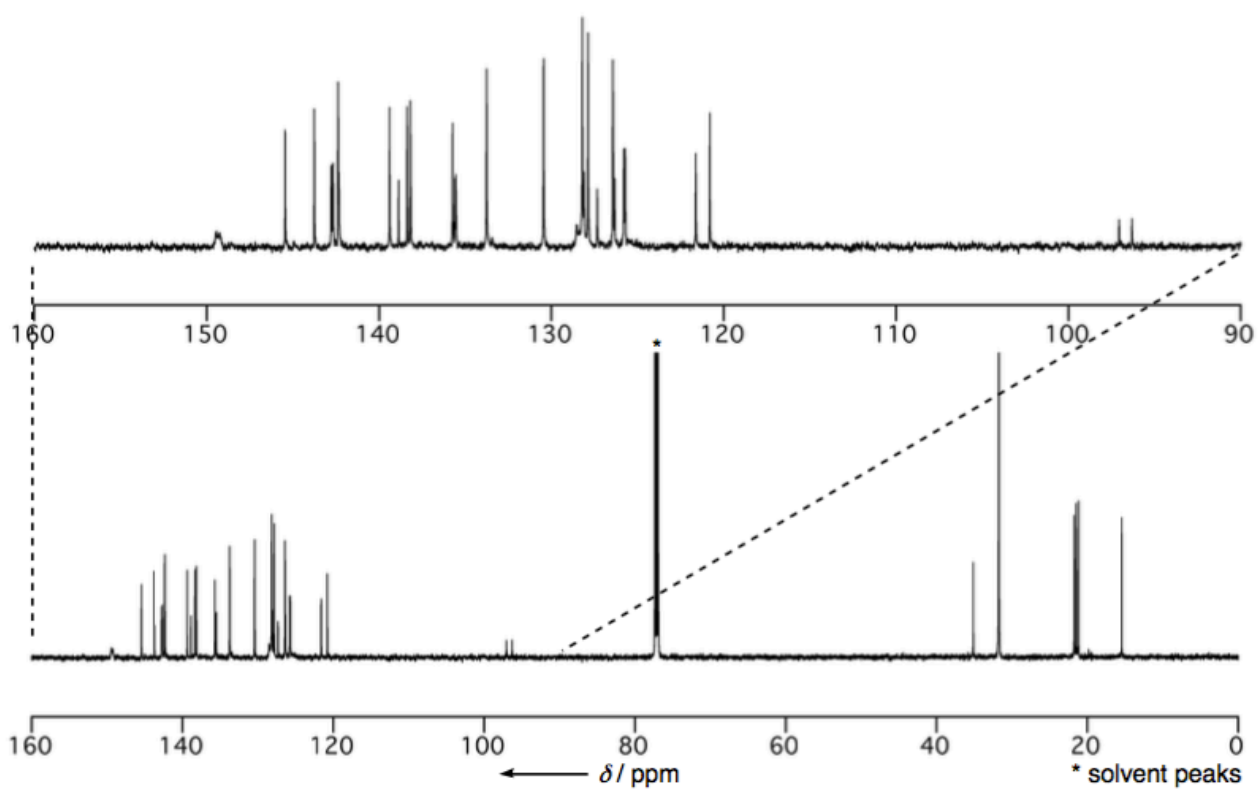


Figure S39. ^{13}C NMR spectrum of **18Ni** in CDCl_3 at 25 °C.

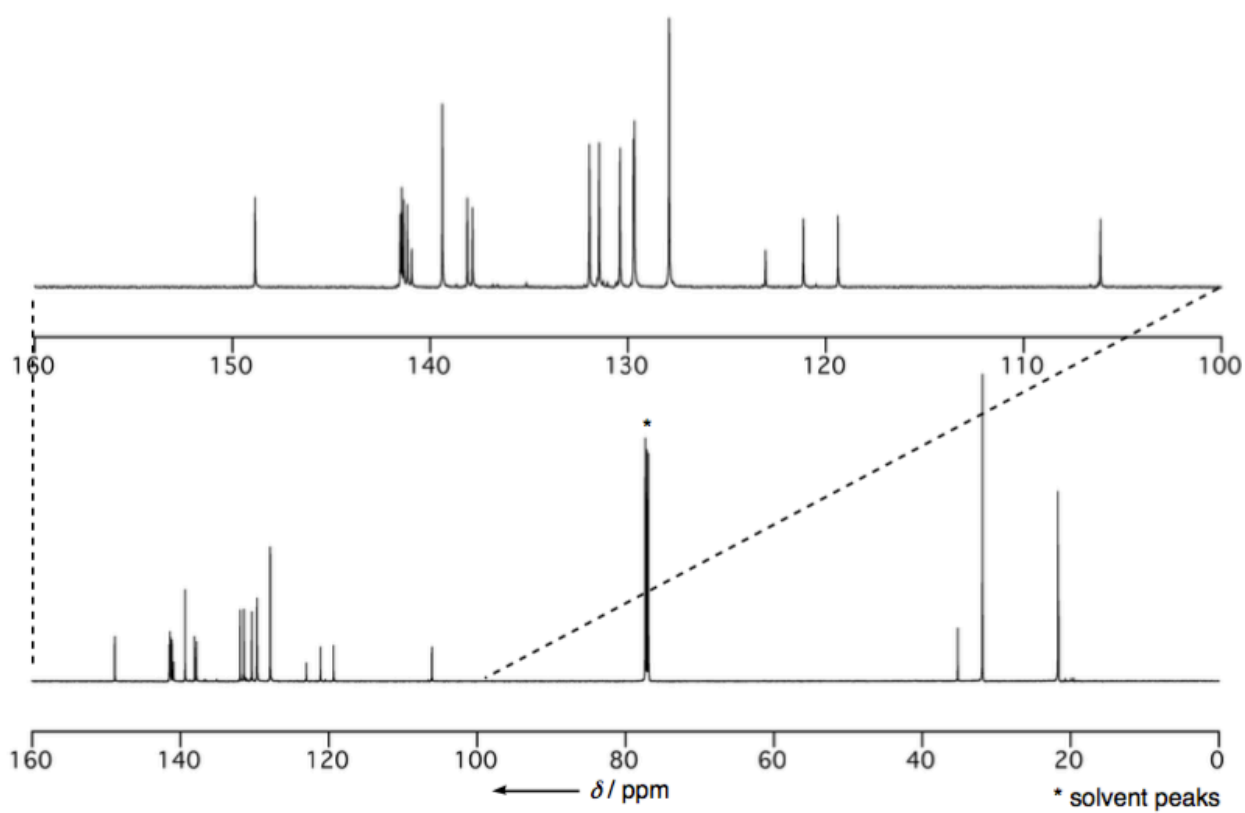


Figure S40. ^{13}C NMR spectrum of **S6** in CDCl_3 at 25 °C.

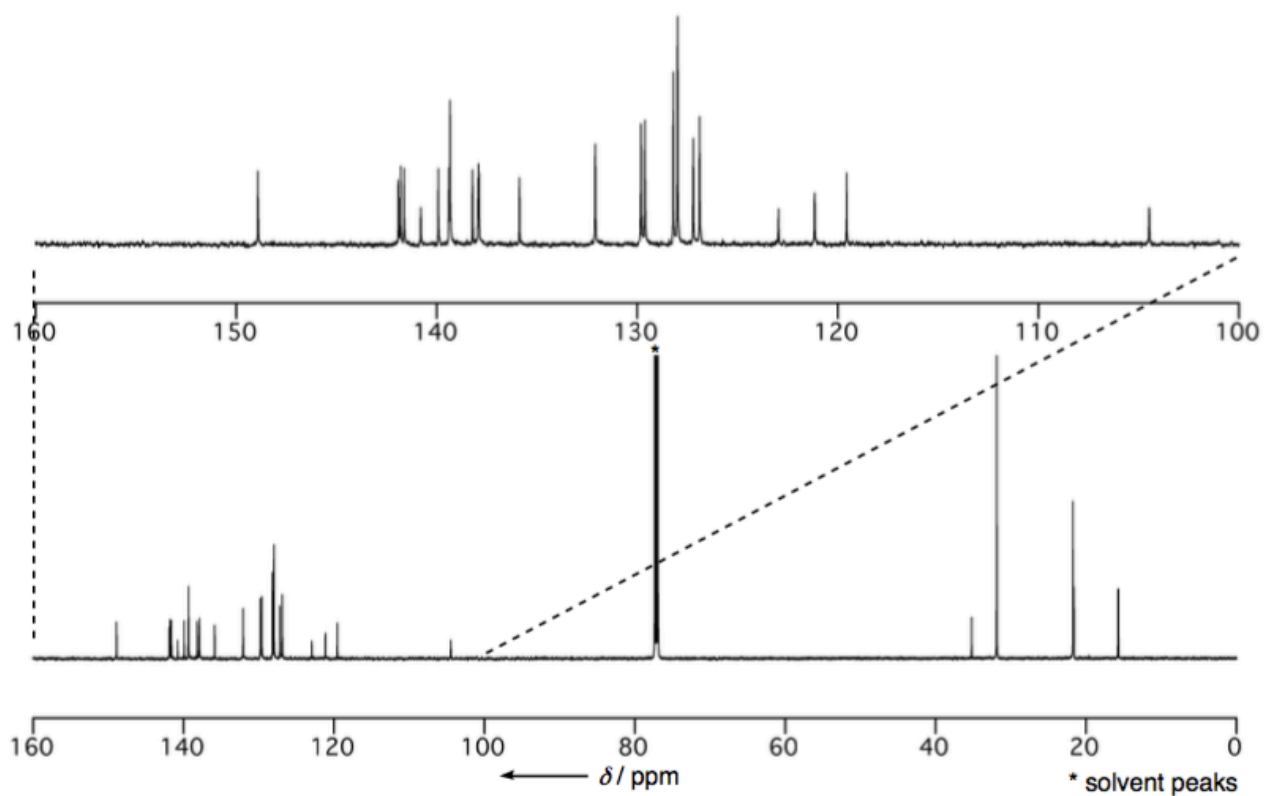


Figure S41. ^{13}C NMR spectrum of **17Pd** in CDCl_3 at 25 °C.

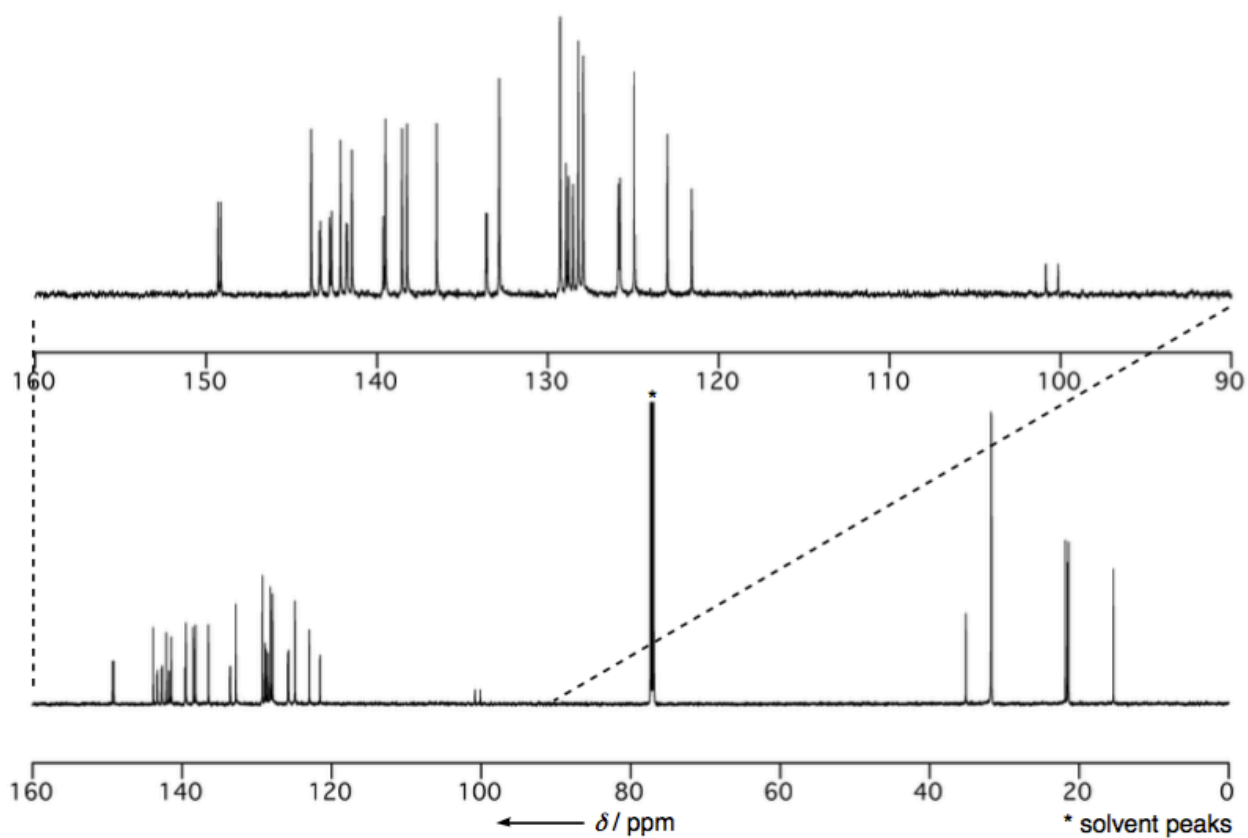


Figure S42. ^{13}C NMR spectrum of **18Pd** in CDCl_3 at 25 °C.

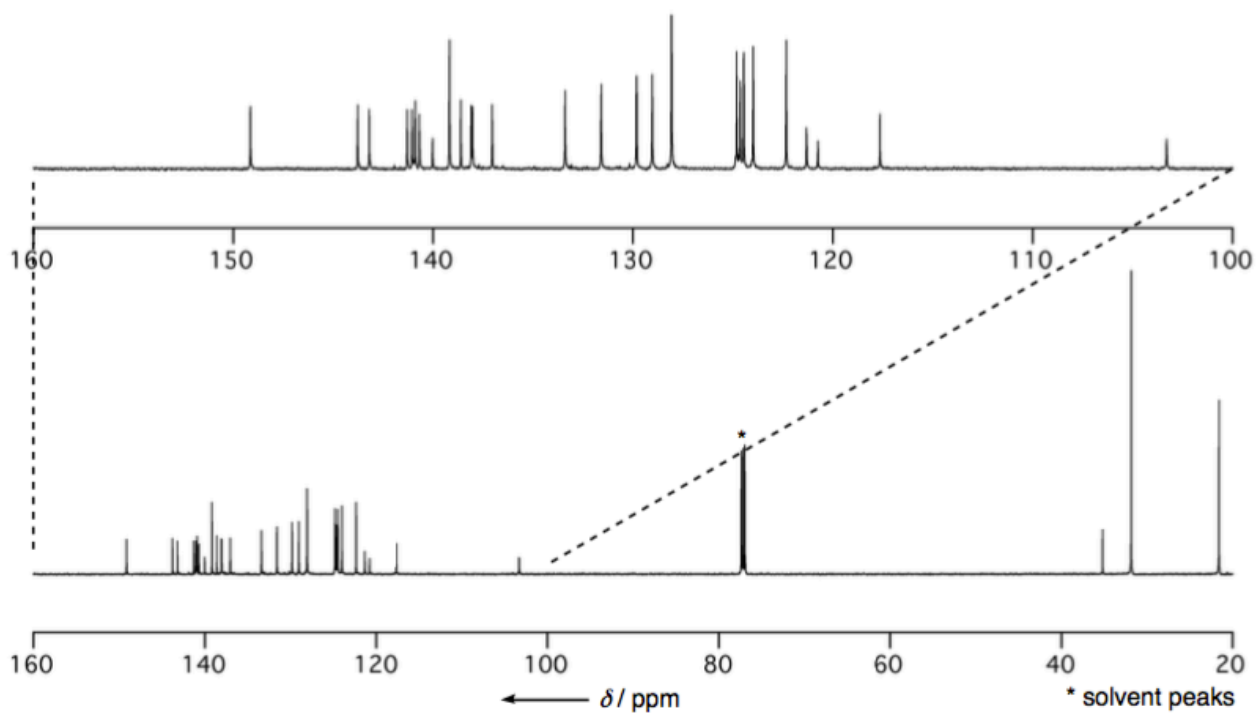


Figure S43. ^{13}C NMR spectrum of **19** in CDCl_3 at 25 °C.

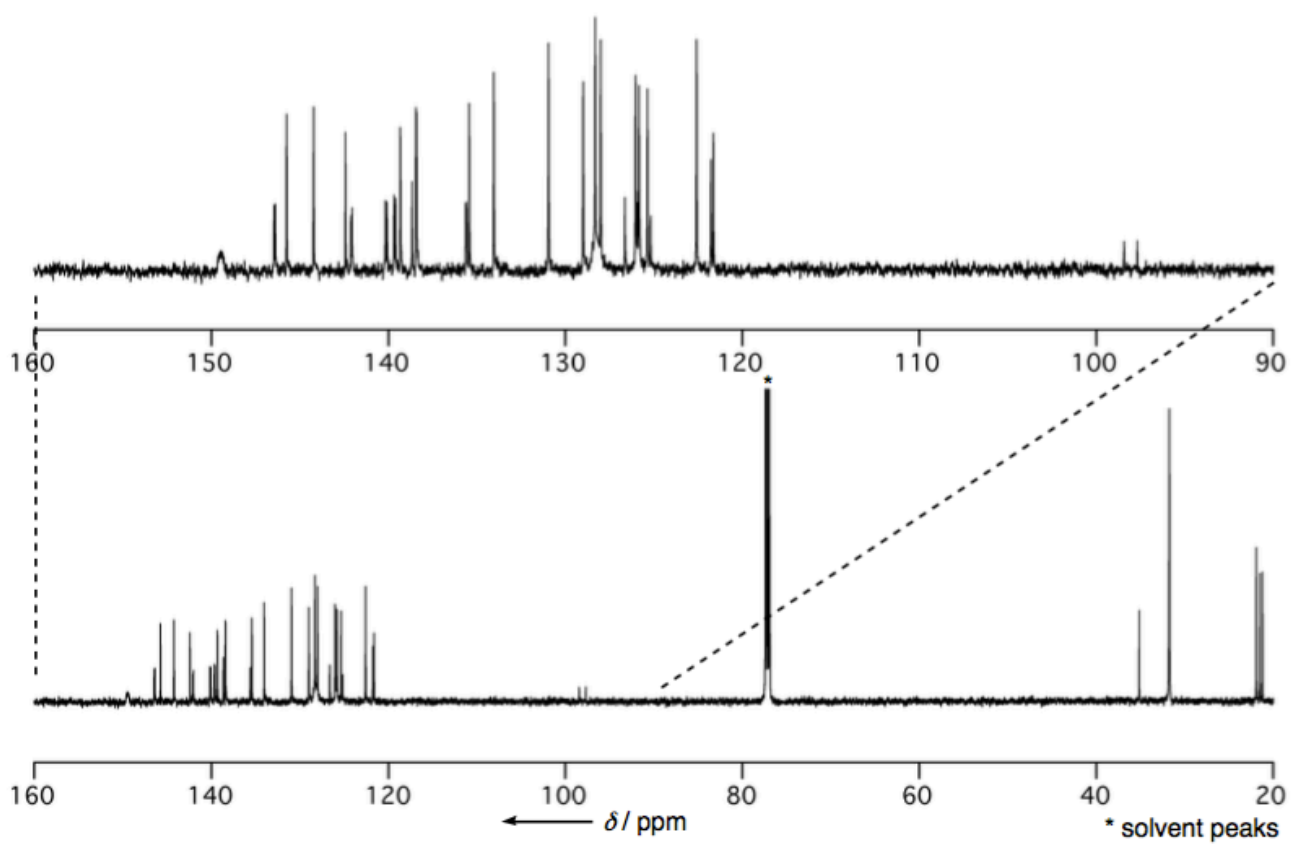


Figure S44. ^{13}C NMR spectrum of **20** in CDCl_3 at 25 °C.

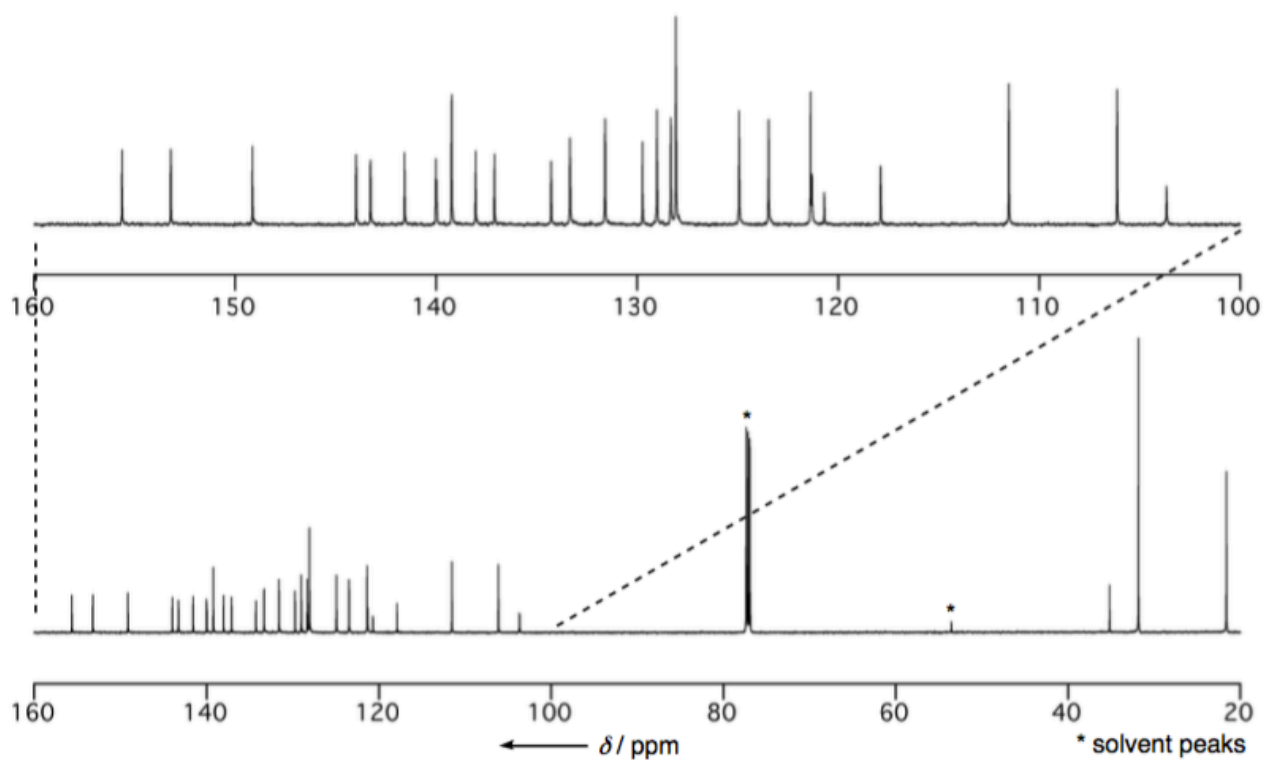


Figure S45. ^{13}C NMR spectrum of **21** in CDCl_3 at 25 °C.

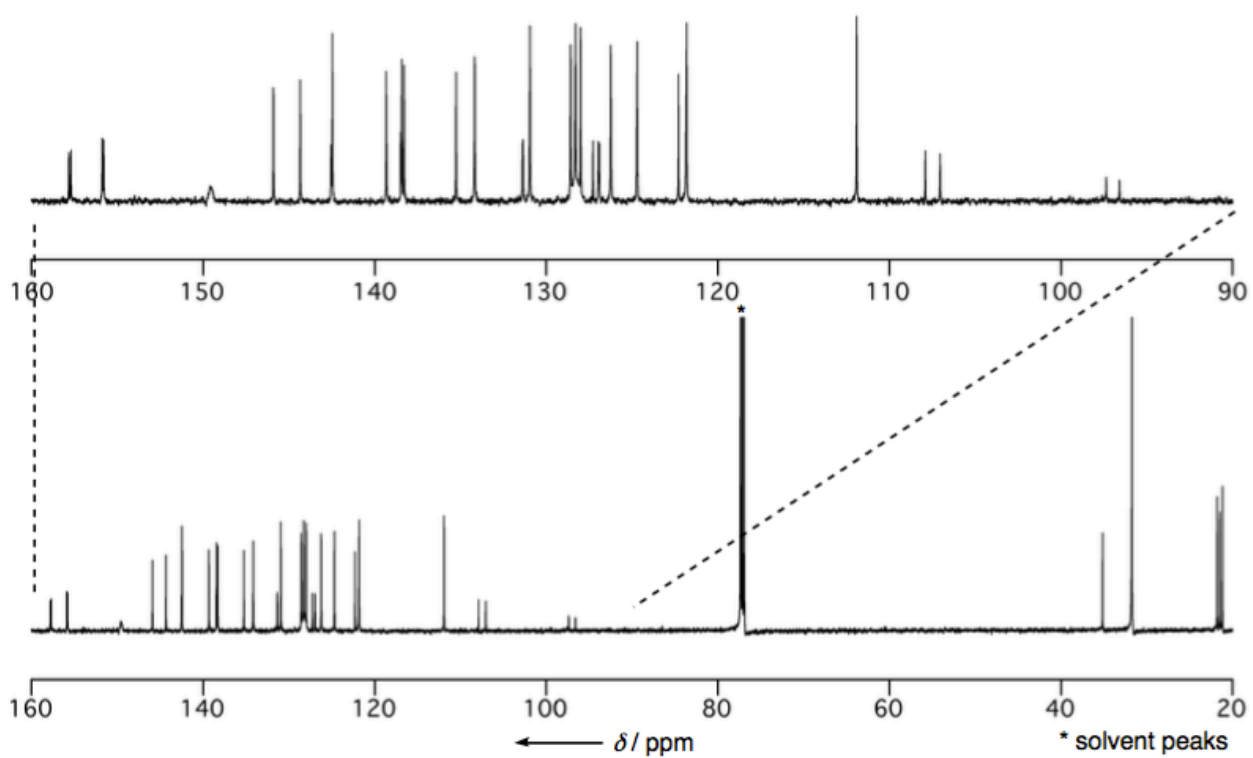


Figure S46. ^{13}C NMR spectrum of **22** in CDCl_3 at 25 °C.

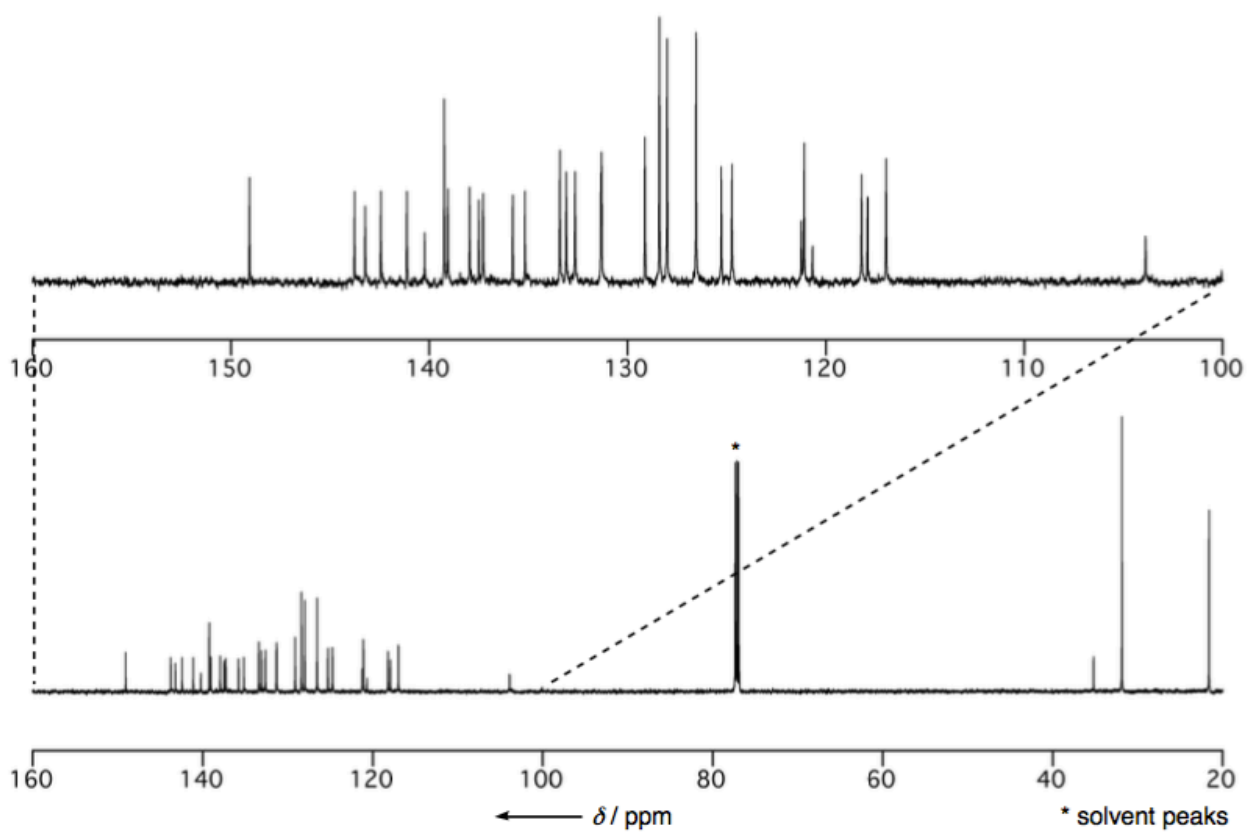


Figure S47. ^{13}C NMR spectrum of **23** in CDCl_3 at 25 °C.

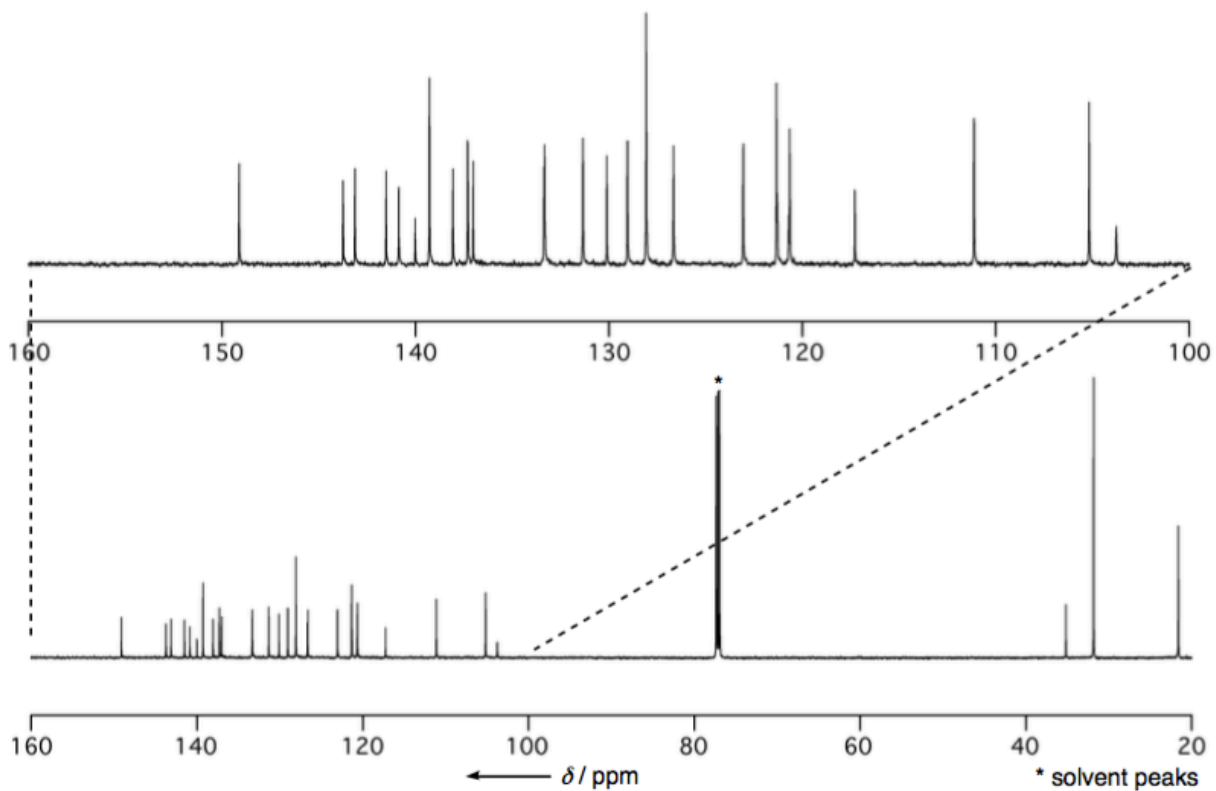


Figure S48. ^{13}C NMR spectrum of **25** in CDCl_3 at 25 °C.

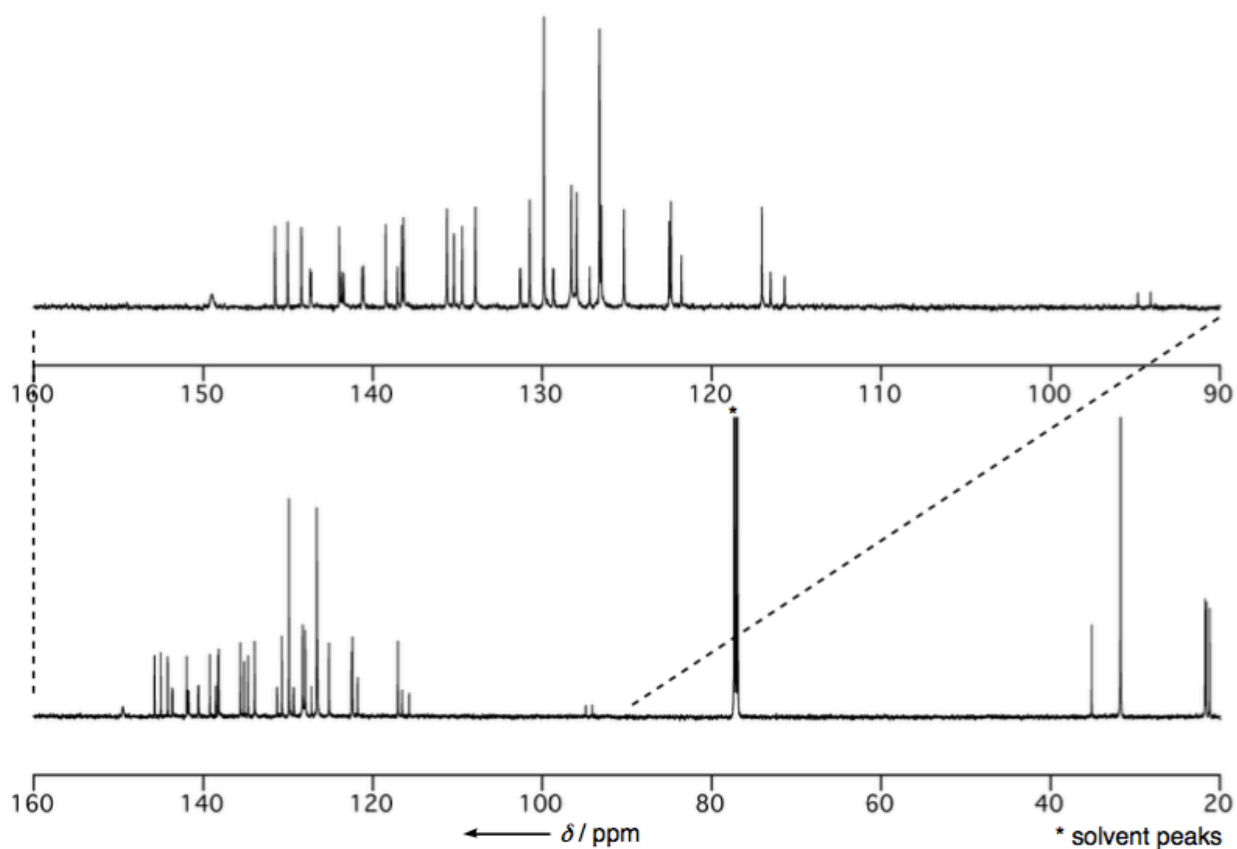


Figure S49. ^{13}C NMR spectrum of **26** in CDCl_3 at 25 °C.

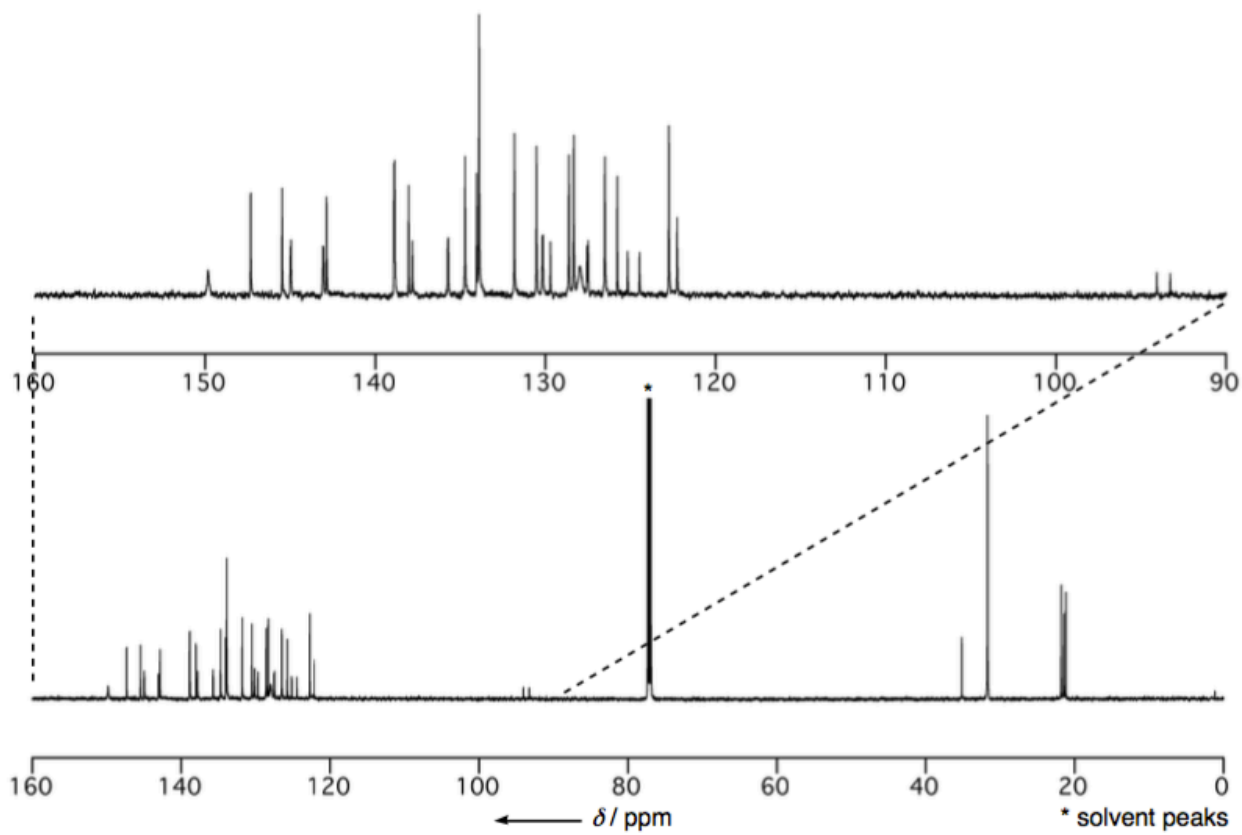


Figure S50. ^{13}C NMR spectrum of **27** in CDCl_3 at 25 °C.

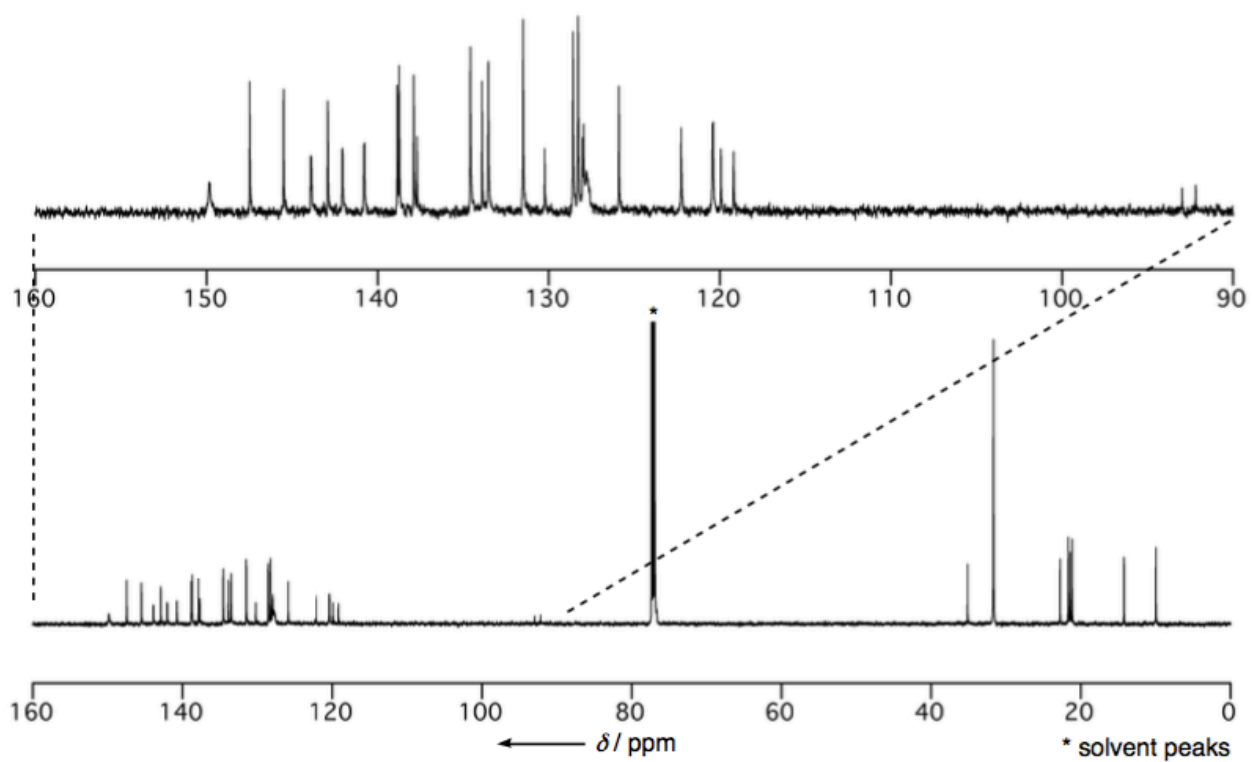


Figure S51. ^{13}C NMR spectrum of **28** in CDCl_3 at $25\text{ }^\circ\text{C}$.

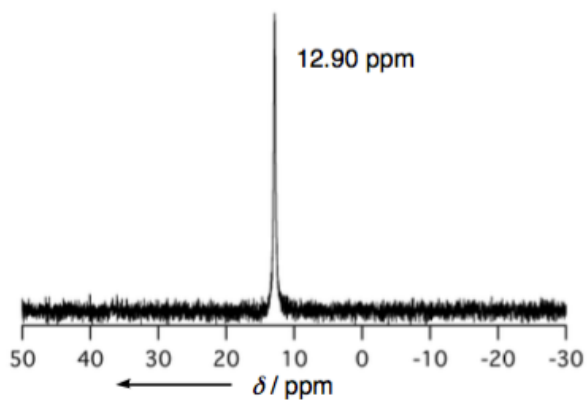


Figure S52. ^{31}P NMR spectrum of **8** in CDCl_3 at 25 °C.

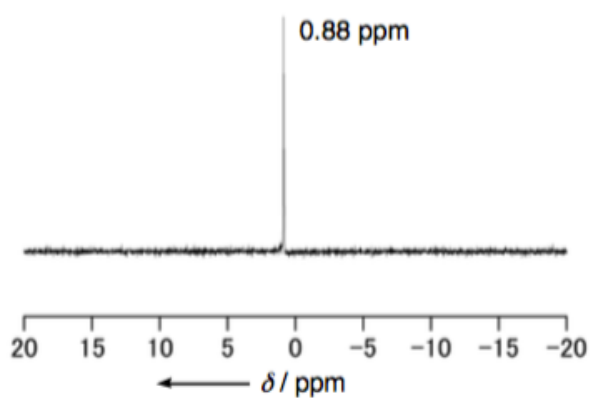


Figure S53. ^{31}P NMR spectrum of **9** in CDCl_3 at 25 °C.

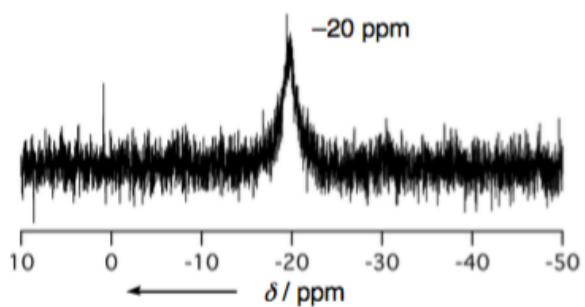


Figure S54. ^{31}P NMR spectrum of **6** in CDCl_3 at 25 °C.

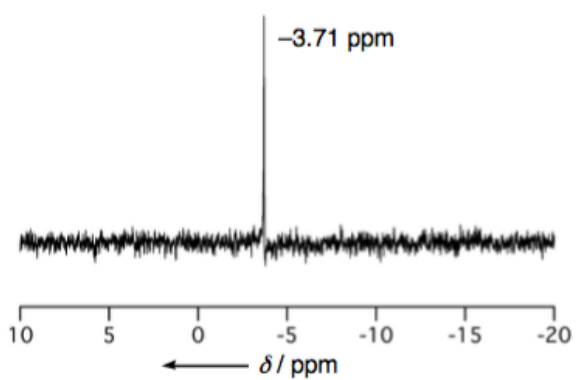


Figure S55. ^{31}P NMR spectrum of **18Ni** in CDCl_3 at 25 °C.

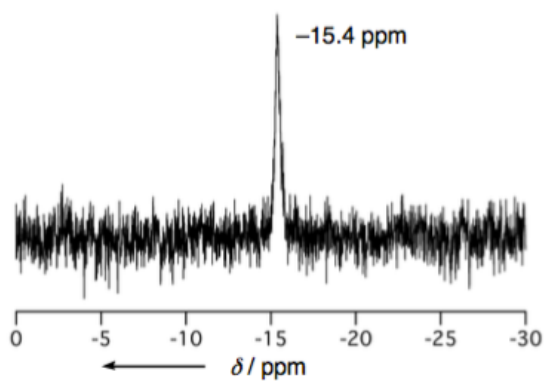


Figure S56. ^{31}P NMR spectrum of **10Ni** in CDCl_3 at 25 °C.

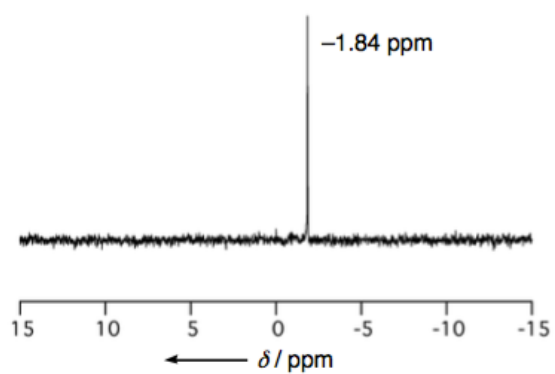


Figure S57. ^{31}P NMR spectrum of **18Pd** in CDCl_3 at 25 °C.

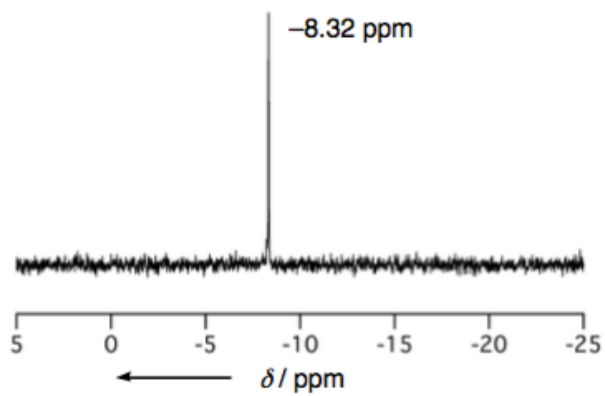


Figure S58. ^{31}P NMR spectrum of **10Pd** in CDCl_3 at 25 °C.

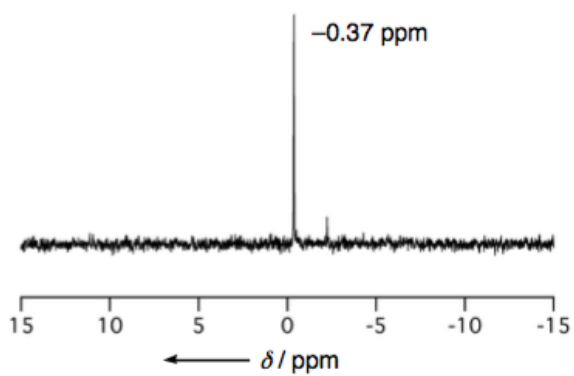


Figure S59. ^{31}P NMR spectrum of **20** in CDCl_3 at 25 °C.

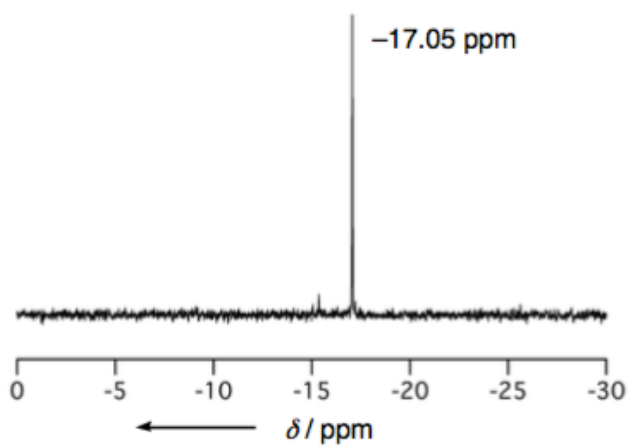


Figure S60. ^{31}P NMR spectrum of **11** in CDCl_3 at 25 °C.

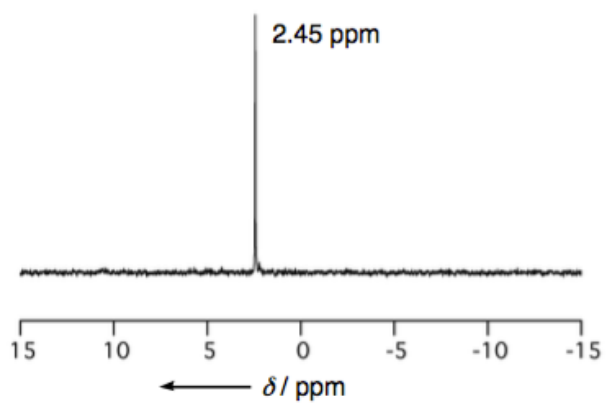


Figure S61. ^{31}P NMR spectrum of **22** in CDCl_3 at 25 °C.

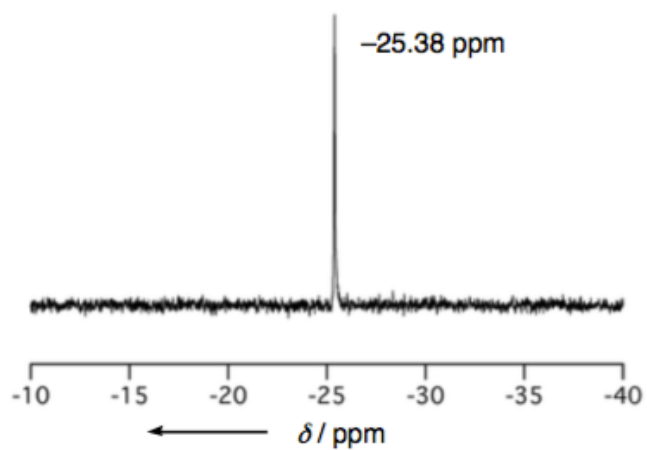


Figure S62. ^{31}P NMR spectrum of **12** in CDCl_3 at 25 °C.

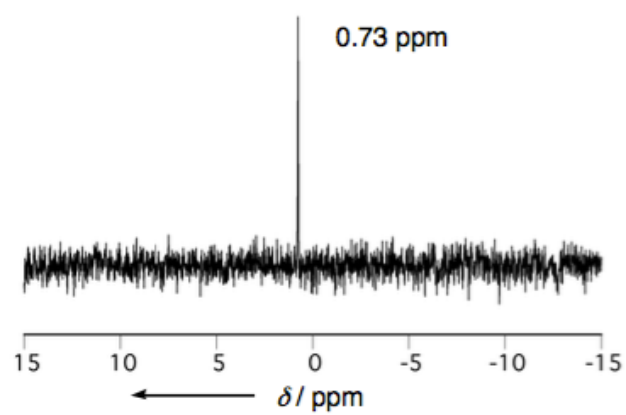


Figure S63. ^{31}P NMR spectrum of **25** in CDCl_3 at 25 °C.

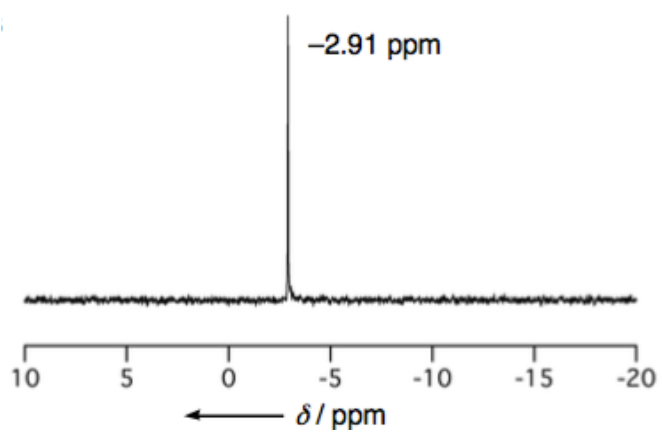


Figure S64. ^{31}P NMR spectrum of **26** in CDCl_3 at 25 °C.

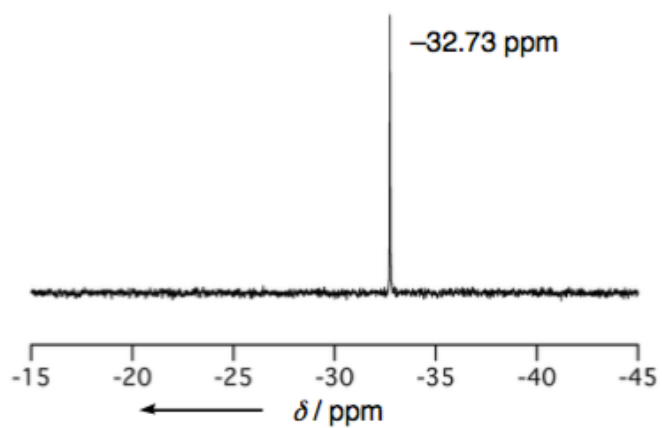


Figure S65. ^{31}P NMR spectrum of **13** in CDCl_3 at 25 °C.

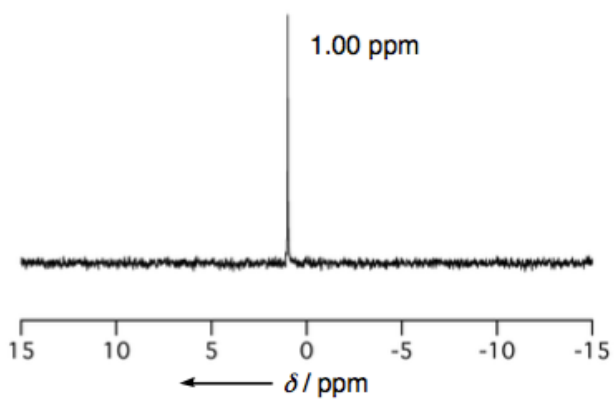


Figure S66. ^{31}P NMR spectrum of **27** in CDCl_3 at 25 °C.

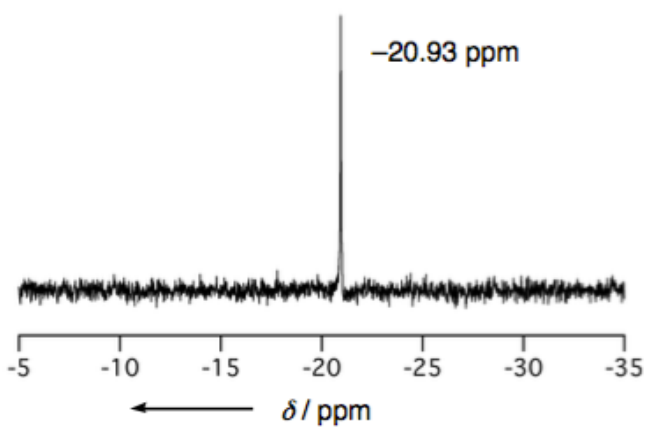


Figure S67. ^{31}P NMR spectrum of **14** in CDCl_3 at 25 °C.

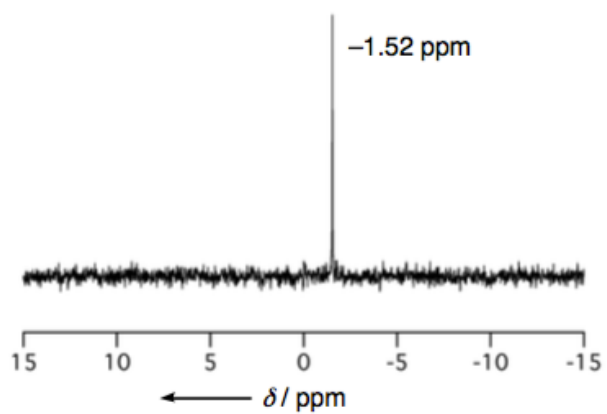


Figure S68. ^{31}P NMR spectrum of **28** in CDCl_3 at 25 °C.

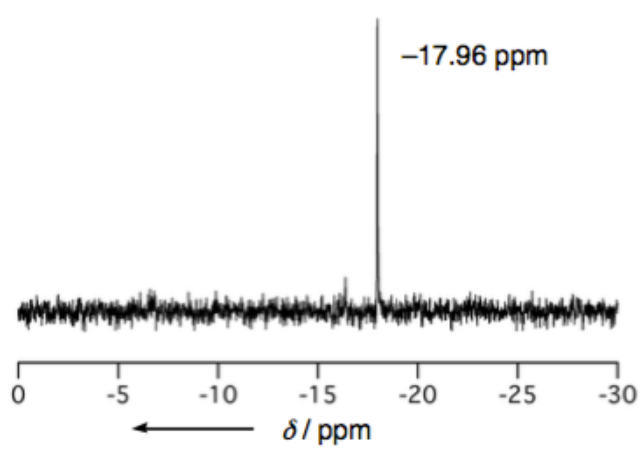


Figure S69. ^{31}P NMR spectrum of **15** in CDCl_3 at 25 °C.

4. High Resolution Mass Spectra

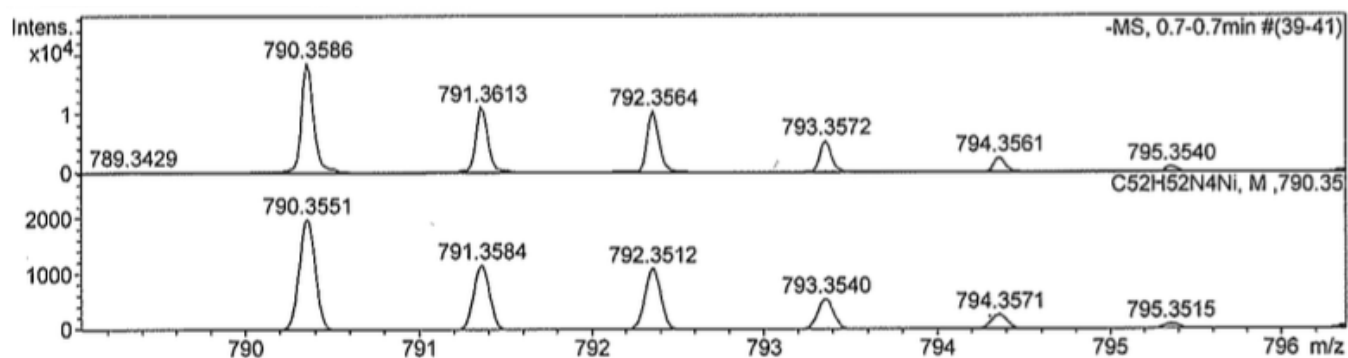


Figure S70. Observed (top) and simulated (bottom) HR-APCI-TOF MS of S3.

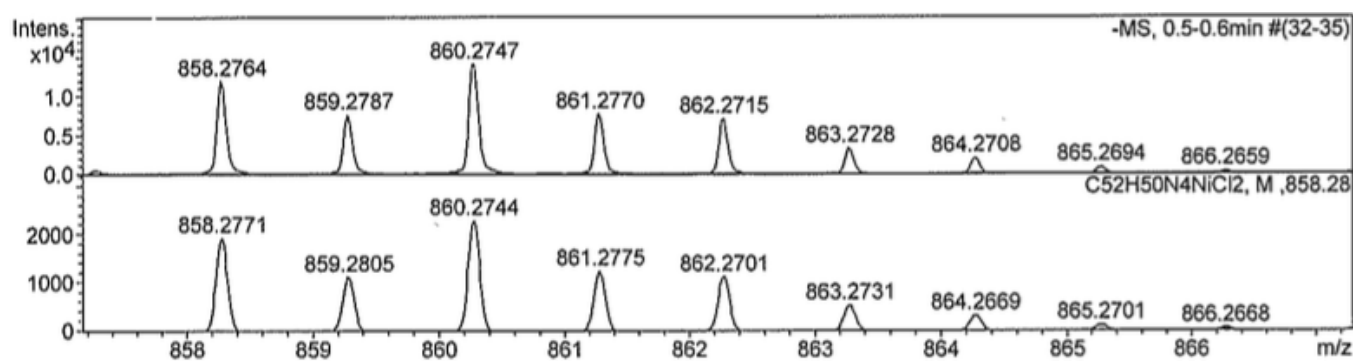


Figure S71. Observed (top) and simulated (bottom) HR-APCI-TOF MS of S5.

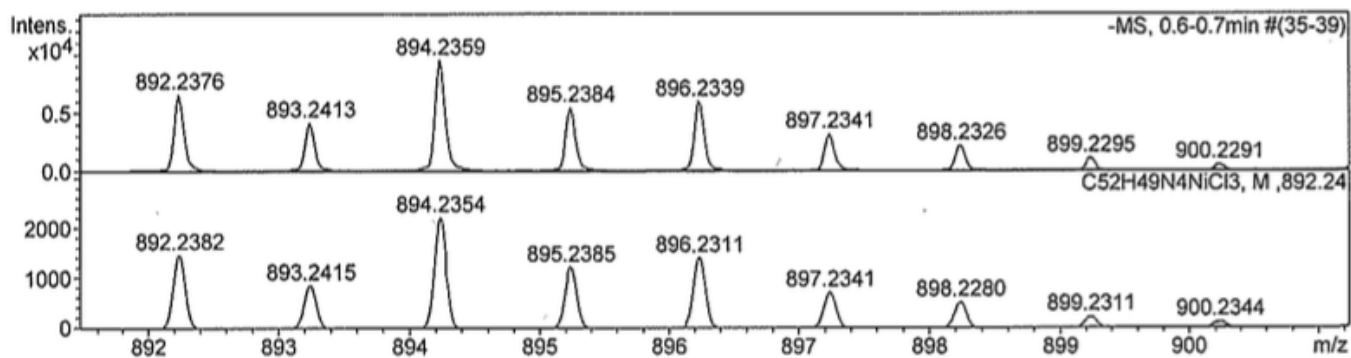


Figure S72. Observed (top) and simulated (bottom) HR-APCI-TOF MS of 7.

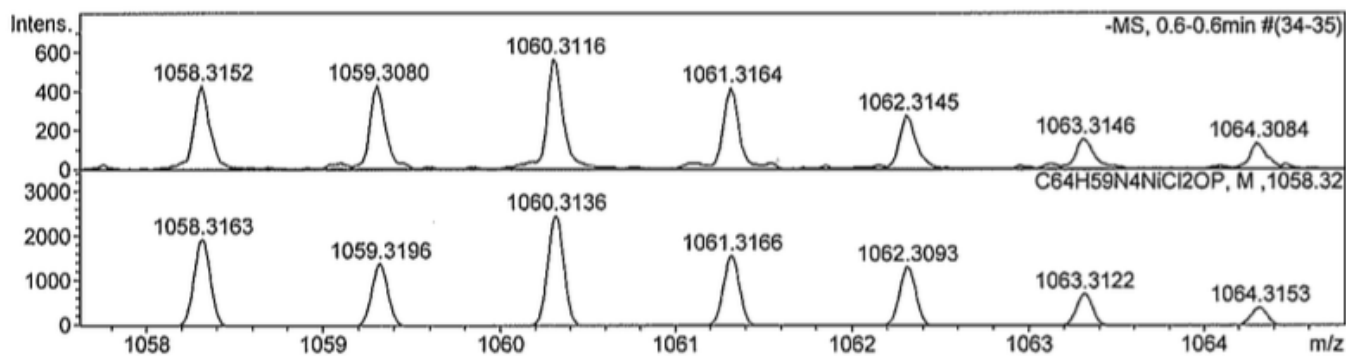


Figure S73. Observed (top) and simulated (bottom) HR-APCI-TOF MS of **8**.

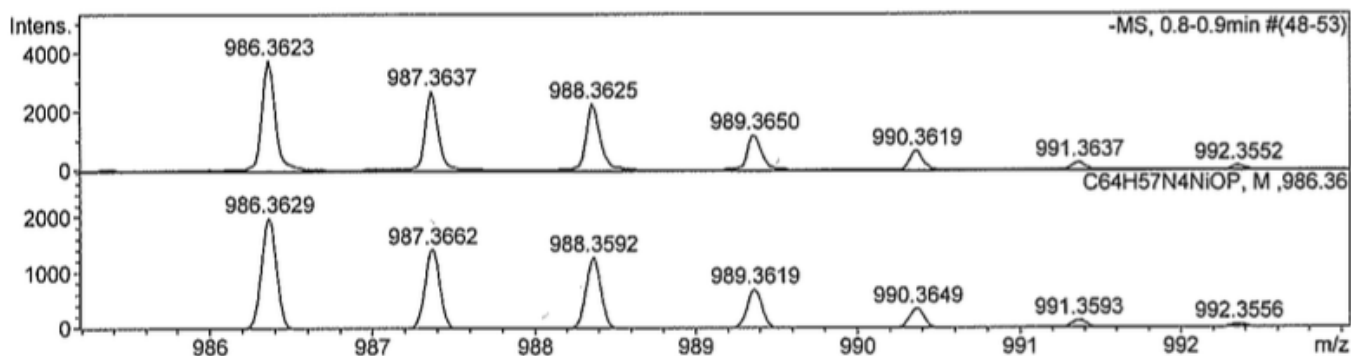


Figure S74. Observed (top) and simulated (bottom) HR-APCI-TOF MS of **9**.

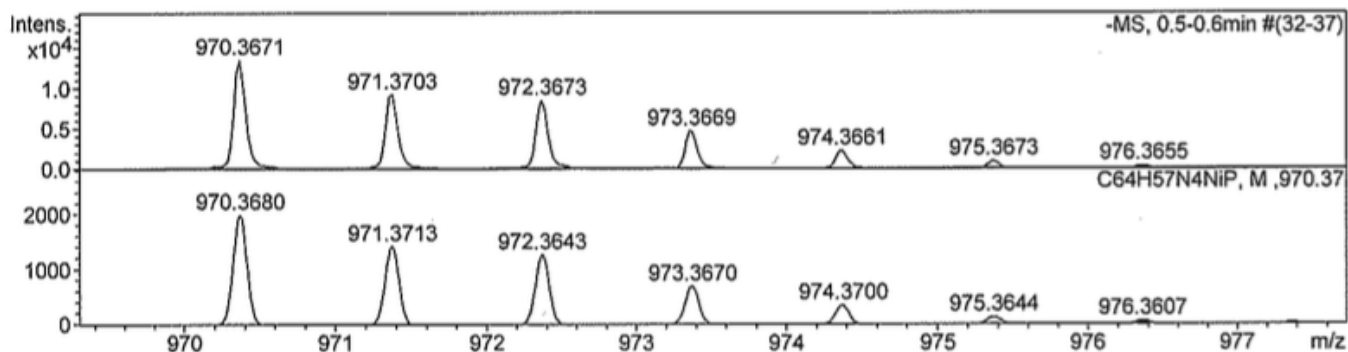


Figure S75. Observed (top) and simulated (bottom) HR-APCI-TOF MS of **6**.

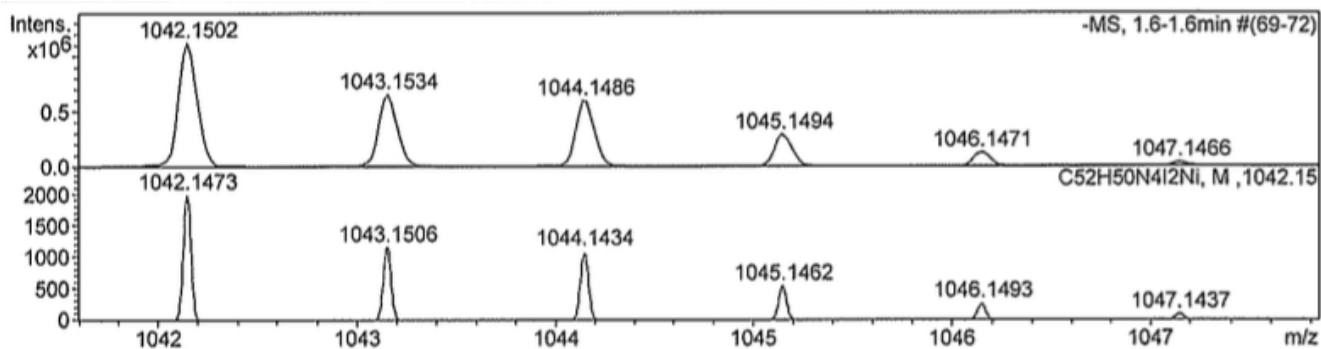


Figure S76. Observed (top) and simulated (bottom) HR-APCI-TOF MS of **16Ni**.

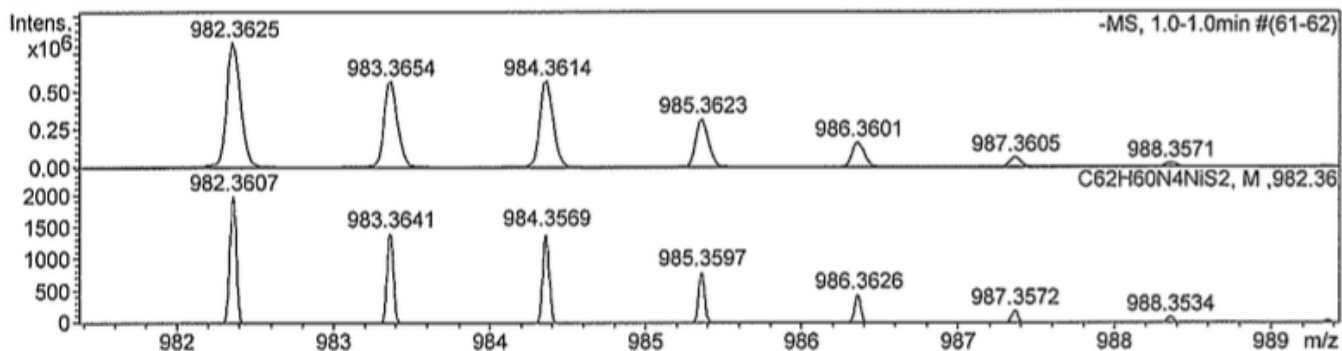


Figure S77. Observed (top) and simulated (bottom) HR-APCI-TOF MS of **17Ni**.

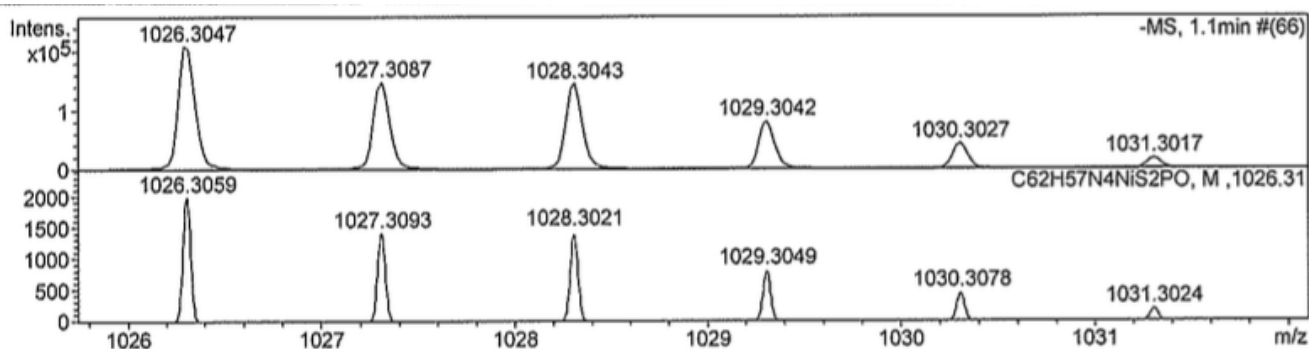


Figure S78. Observed (top) and simulated (bottom) HR-APCI-TOF MS of **18Ni**.

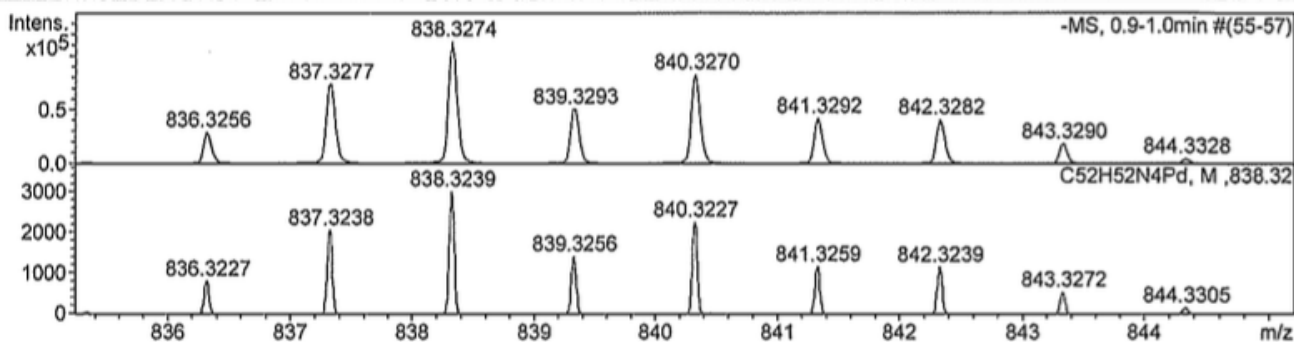


Figure S79. Observed (top) and simulated (bottom) HR-APCI-TOF MS of **S6**.

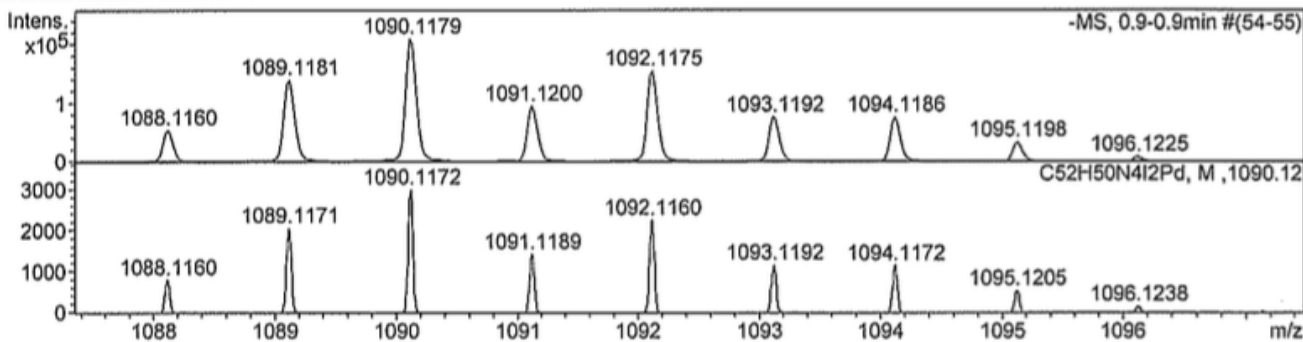


Figure S80. Observed (top) and simulated (bottom) HR-APCI-TOF MS of **16Pd**.

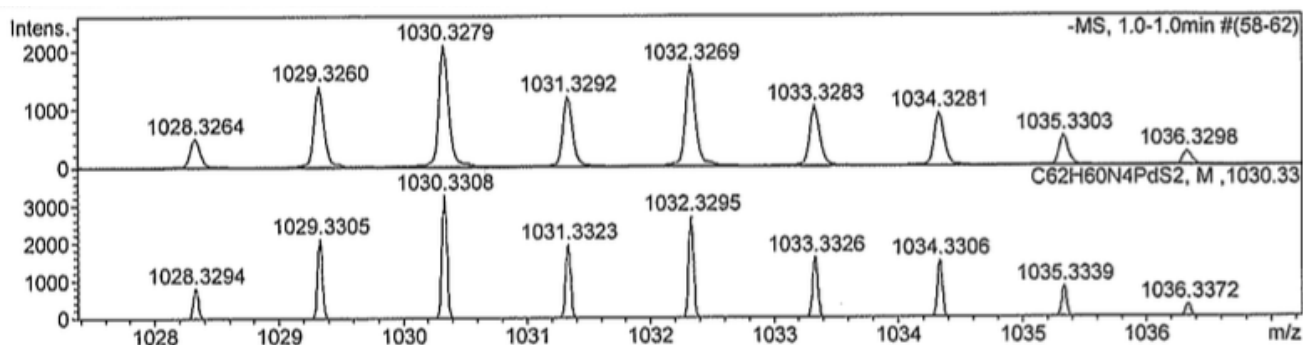


Figure S81. Observed (top) and simulated (bottom) HR-APCI-TOF MS of **17Pd**.

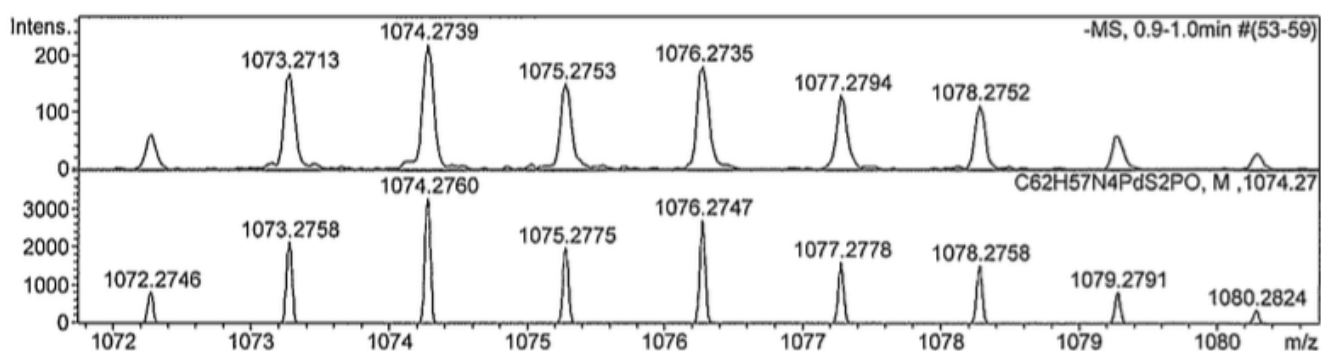


Figure S82. Observed (top) and simulated (bottom) HR-APCI-TOF MS of **18Pd**.

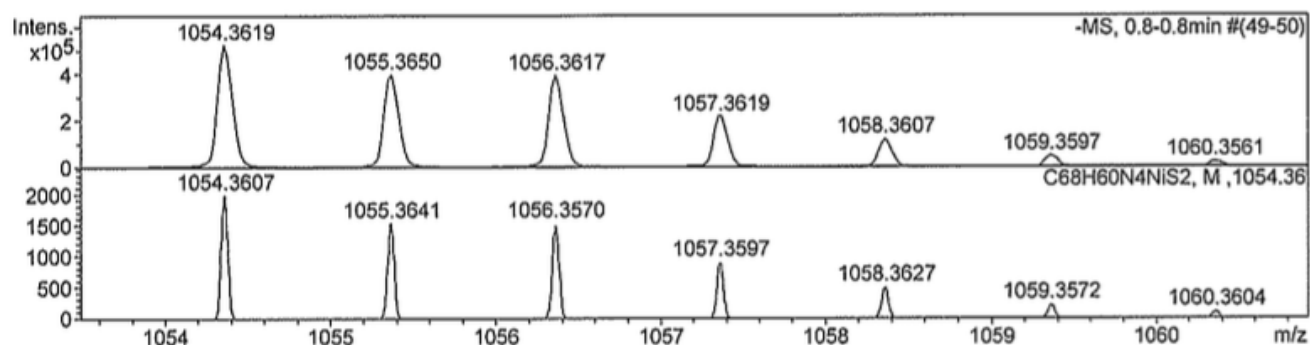


Figure S83. Observed (top) and simulated (bottom) HR-APCI-TOF MS of **19**.

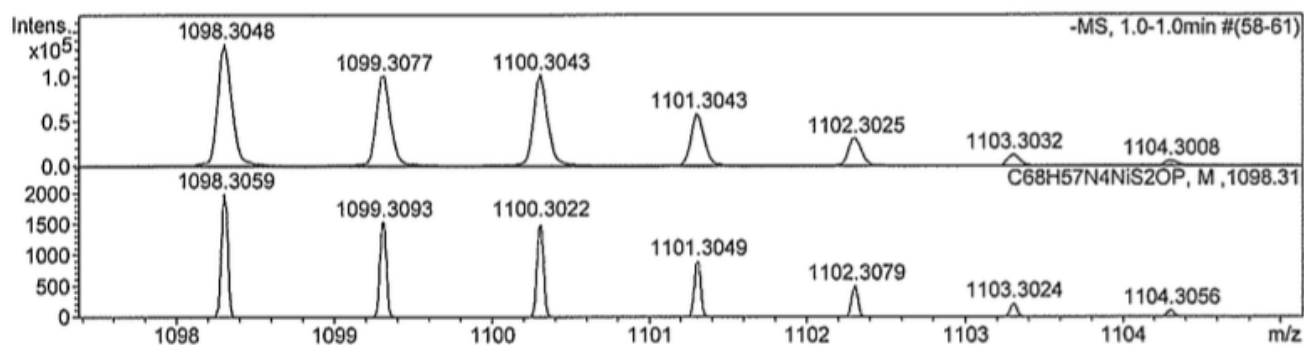


Figure S84. Observed (top) and simulated (bottom) HR-APCI-TOF MS of **20**.

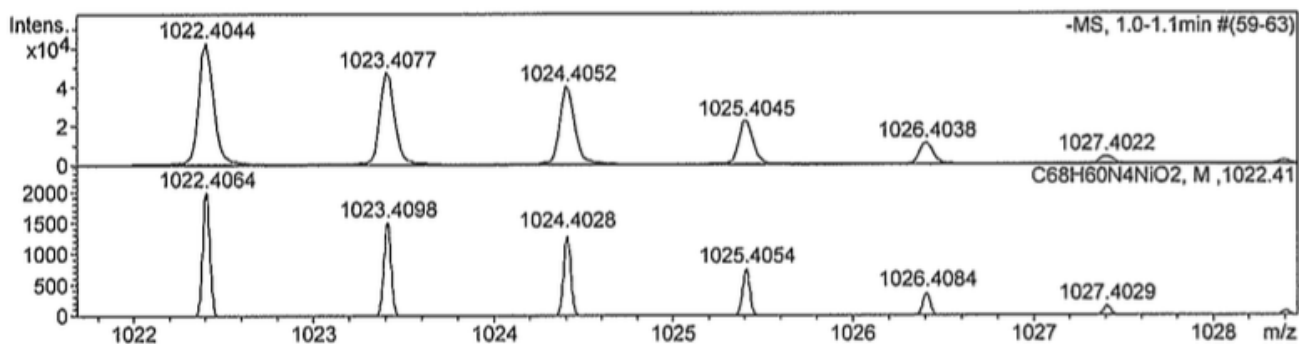


Figure S85. Observed (top) and simulated (bottom) HR-APCI-TOF MS of **21**.

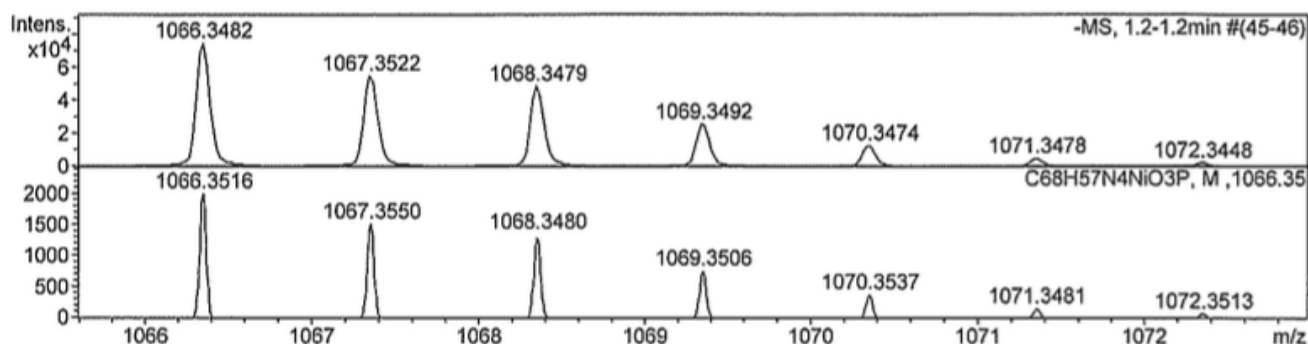


Figure S86. Observed (top) and simulated (bottom) HR-APCI-TOF MS of **22**.

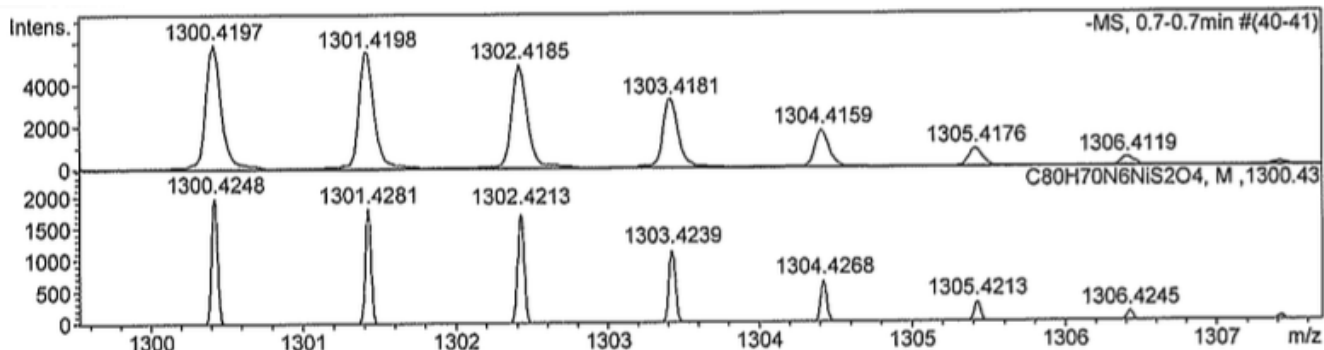


Figure S87. Observed (top) and simulated (bottom) HR-APCI-TOF MS of **23**.

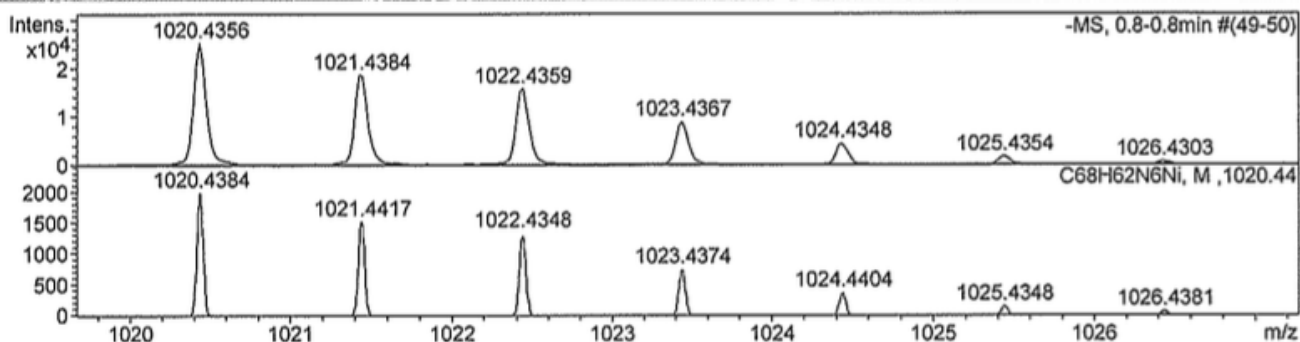


Figure S88. Observed (top) and simulated (bottom) HR-APCI-TOF MS of **24**.

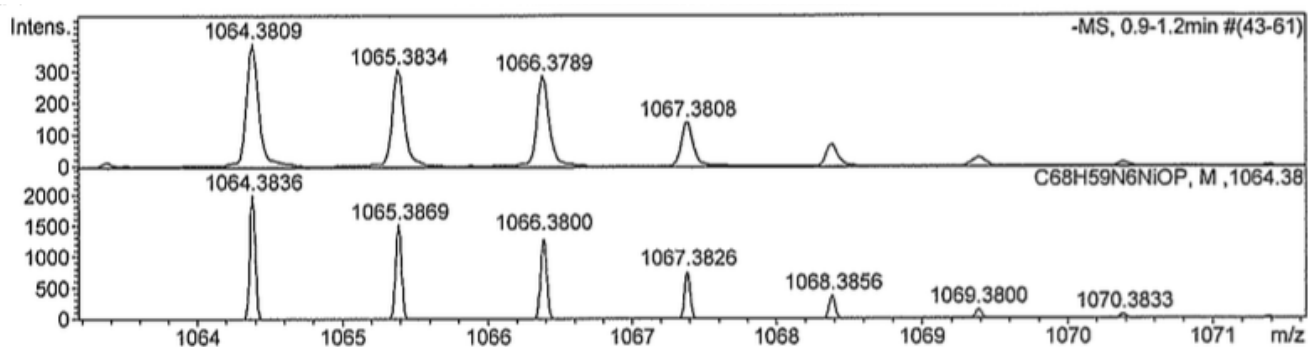


Figure S89. Observed (top) and simulated (bottom) HR-APCI-TOF MS of **25**.

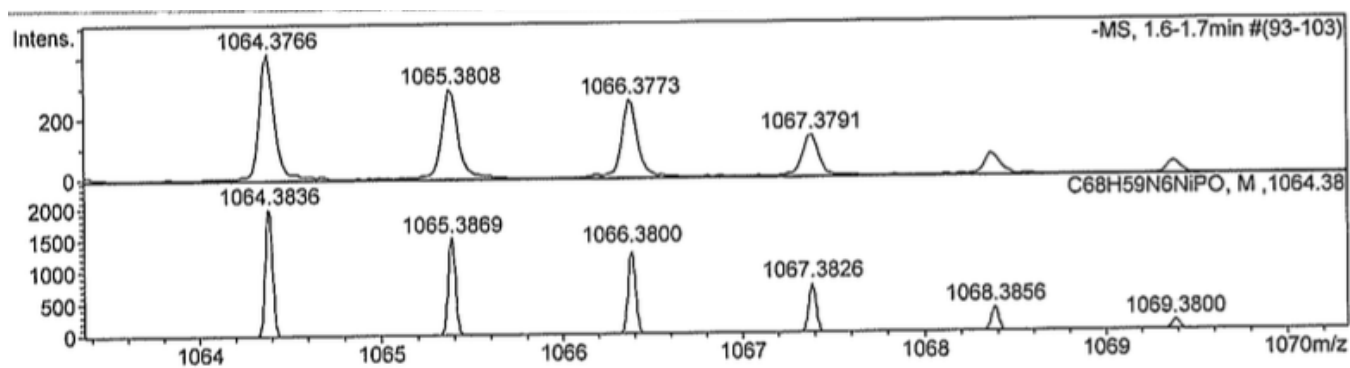


Figure S90. Observed (top) and simulated (bottom) HR-APCI-TOF MS of **26**.

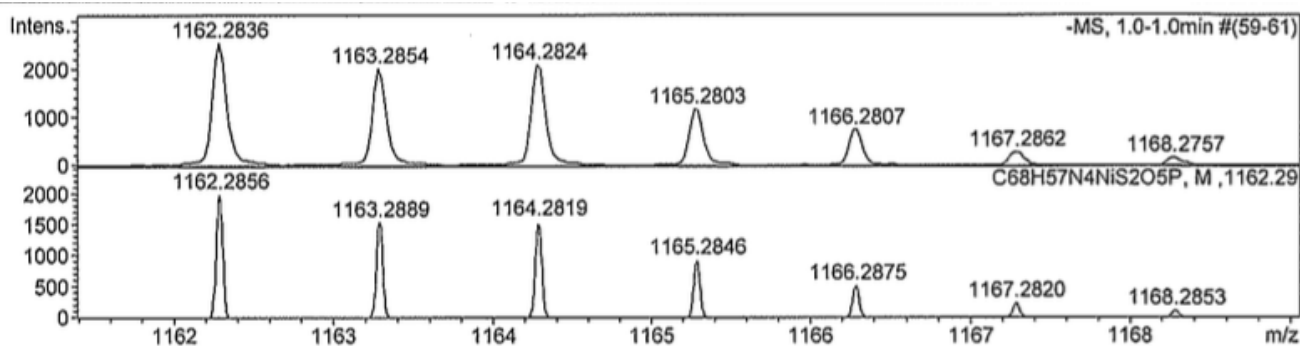


Figure S91. Observed (top) and simulated (bottom) HR-APCI-TOF MS of **27**.

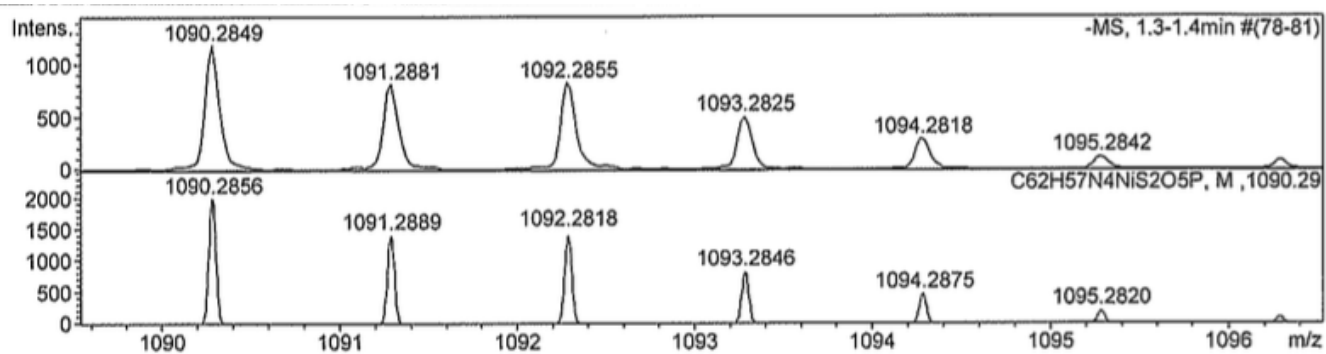


Figure S92. Observed (top) and simulated (bottom) HR-APCI-TOF MS of **28**.

5. X-Ray Crystal Structures

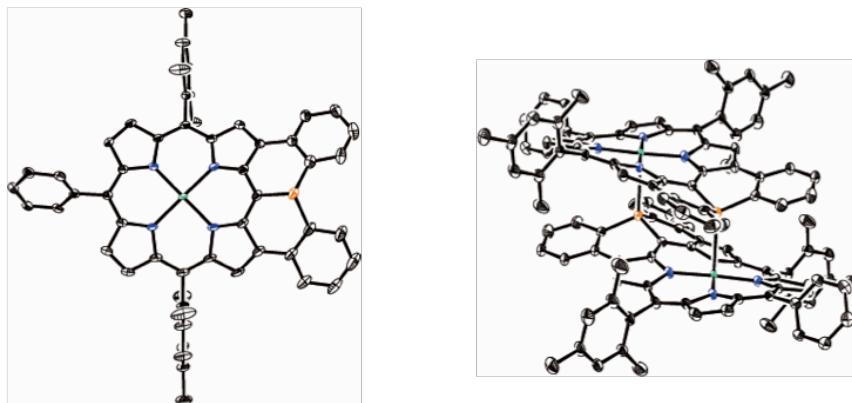


Figure S93. X-Ray crystal structure of **6**. Thermal ellipsoids are shown at the 50% probability level. Solvent molecules, *tert*-butyl groups, and hydrogen atoms are omitted for clarity.

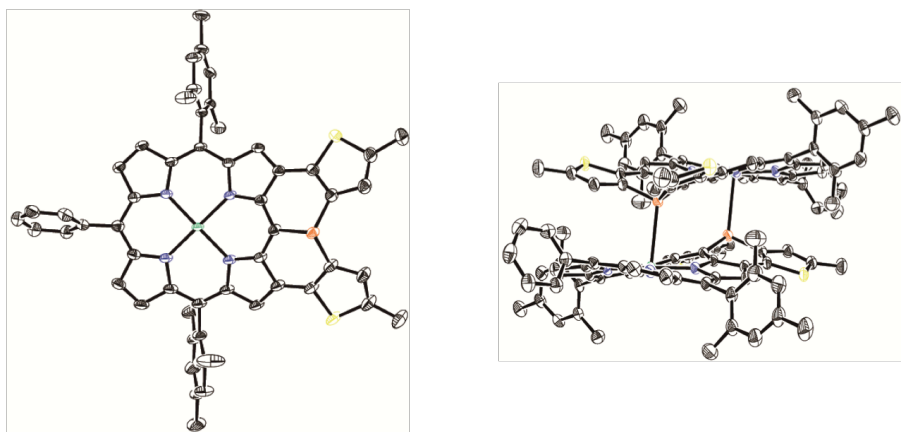


Figure S94. X-Ray crystal structure of **10Ni**. Thermal ellipsoids are shown at the 50% probability level. Solvent molecules, *tert*-butyl groups, and hydrogen atoms are omitted for clarity.

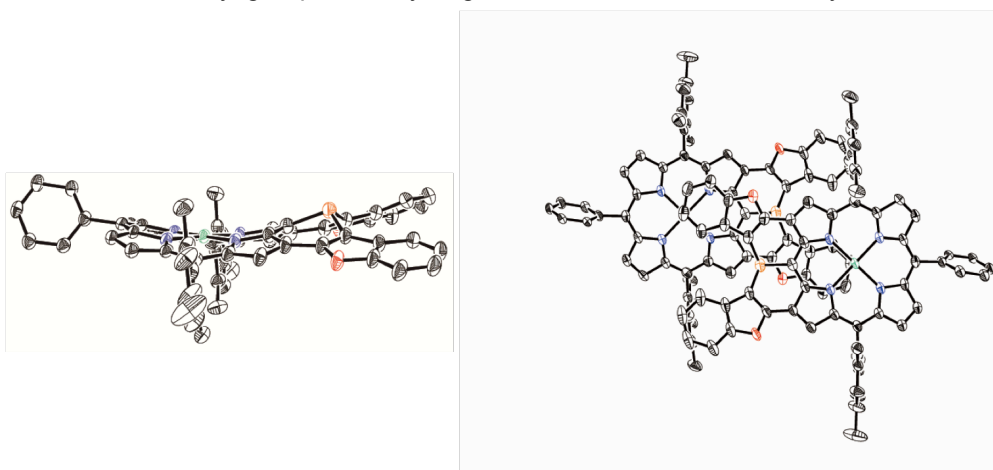


Figure S95. X-Ray crystal structure **12**. Thermal ellipsoids are shown at the 50% probability level. Solvent molecules, *tert*-butyl groups, and hydrogen atoms are omitted for clarity.

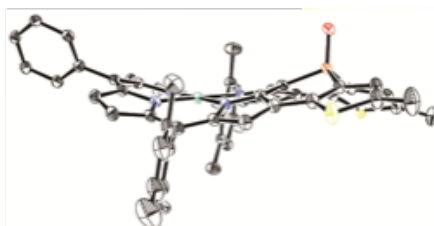
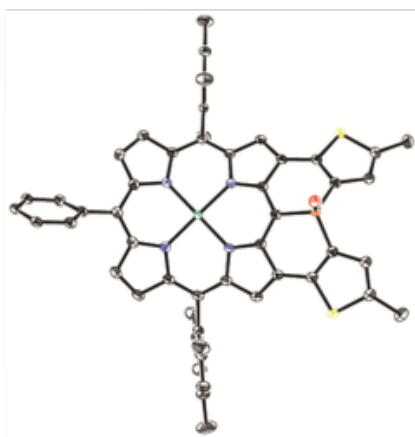


Figure S96. X-Ray crystal structure of **18Ni**. Thermal ellipsoids are shown at the 50% probability level. Solvent molecules, *tert*-butyl groups, and hydrogen atoms are omitted for clarity.

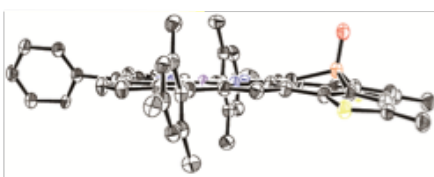
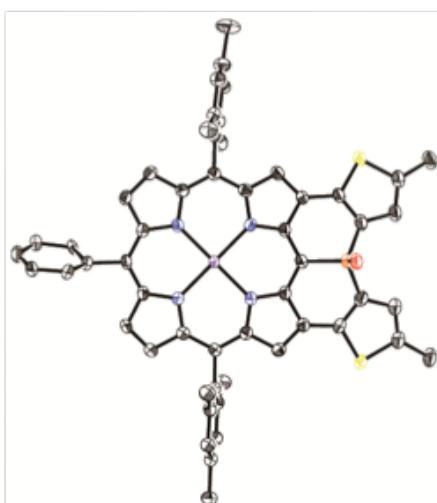


Figure S97. X-Ray crystal structure of **18Pd**. Thermal ellipsoids are shown at the 50% probability level. Solvent molecules, *tert*-butyl groups, and hydrogen atoms are omitted for clarity.

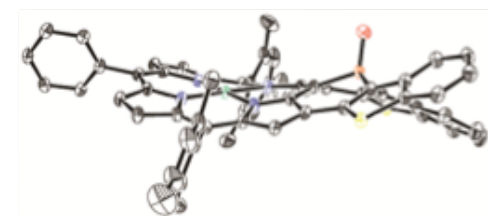
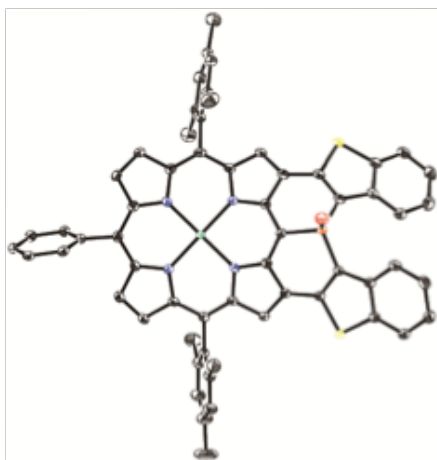


Figure S98. X-Ray crystal structure **20**. Thermal ellipsoids are shown at the 50% probability level. Solvent molecules, *tert*-butyl groups, and hydrogen atoms are omitted for clarity.

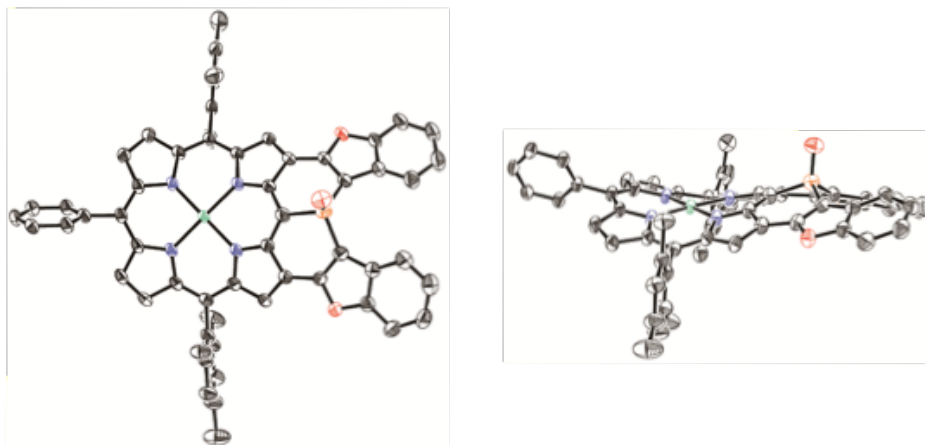


Figure S99. X-Ray crystal structure of **22**. Thermal ellipsoids are shown at the 50% probability level. Solvent molecules, *tert*-butyl groups, and hydrogen atoms are omitted for clarity.

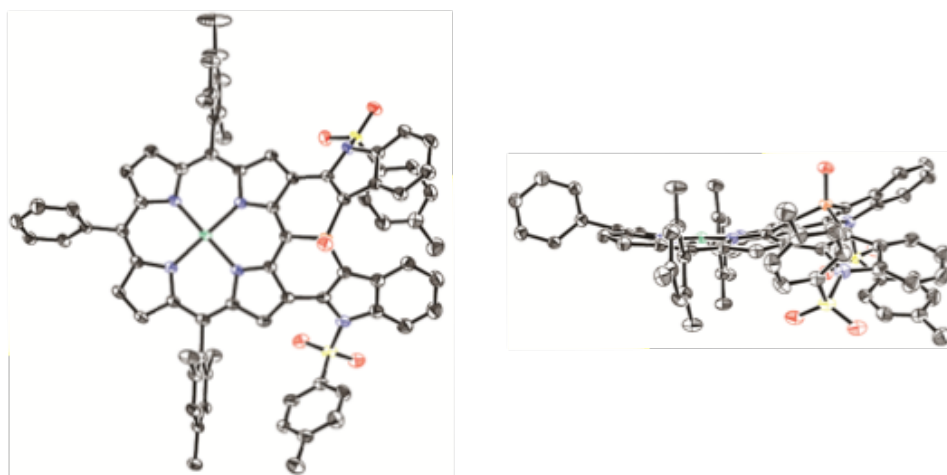


Figure S100. X-Ray crystal structure of **26**. Thermal ellipsoids are shown at the 50% probability level. Solvent molecules, *tert*-butyl groups, and hydrogen atoms are omitted for clarity.

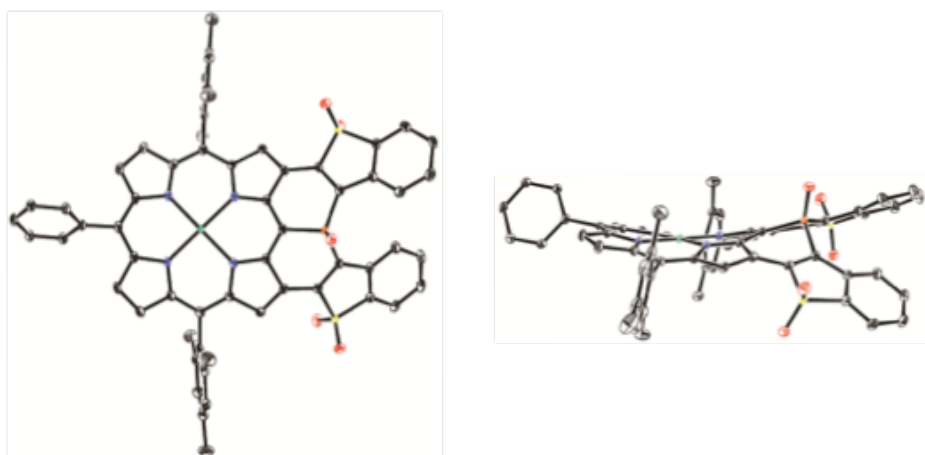


Figure S101. X-Ray crystal structure of **27**. Thermal ellipsoids are shown at the 50% probability level. Solvent molecules, *tert*-butyl groups, and hydrogen atoms are omitted for clarity.

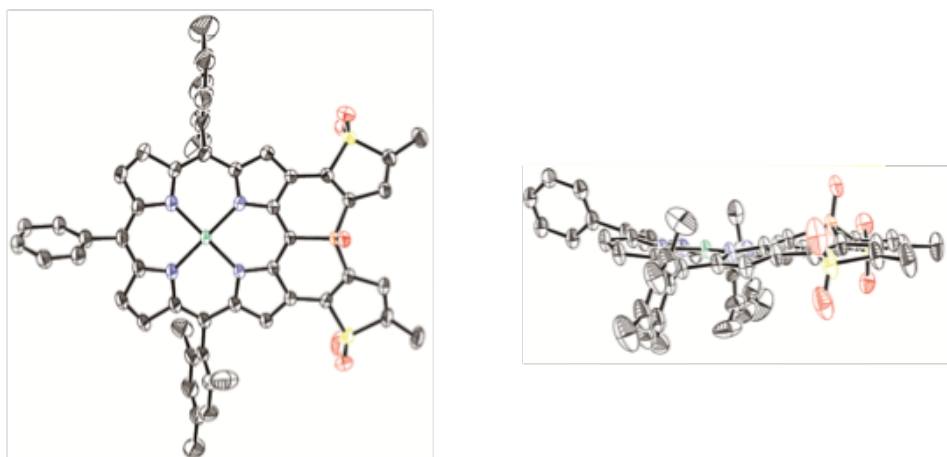


Figure S102. X-Ray crystal structure **28**. Thermal ellipsoids are shown at the 50% probability level. Solvent molecules, *tert*-butyl groups, and hydrogen atoms are omitted for clarity.

Table S1. Crystal data and structure refinements for **6**, **10Ni**, and **12**.

Compound	6	10Ni	12
Empirical Formula	C ₆₆ H ₅₉ N ₄ NiP	C ₇₄ H ₆₉ N ₄ NiPS ₂	C ₈₀ H ₆₉ N ₄ NiO ₂ P
<i>Mw</i>	1210.55	1168.13	1208.07
Crystal System	Monoclinic	Monoclinic	Monoclinic
Space Group	<i>P</i> 2 ₁ / <i>c</i> (No.14)	<i>P</i> 2 ₁ / <i>c</i> (No.14)	<i>P</i> 2 ₁ / <i>c</i> (No.14)
<i>a</i>	12.6212(19) Å	12.9016(19) Å	17.046(2) Å
<i>b</i>	16.578(2) Å	16.642(2) Å	11.8202(17) Å
<i>c</i>	27.567(4) Å	28.249(5) Å	31.451(5) Å
α	90°	90°	90°
β	95.009(3)°	95.324(6)°	97.756(4)°
γ	90°	90°	90°
Volume	5749.1(14) Å ³	6039.1(16) Å ³	6279.0(15) Å ³
<i>Z</i>	4	4	4
Density (calcd.)	1.399 g/cm ³	1.285 g/cm ³	1.278 g/cm ³
Completeness	0.985	0.989	0.978
Goodness-of-fit	1.079	1.010	1.085
<i>R</i> ₁ [<i>I</i> > 2σ(<i>I</i>)]	0.0723	0.0553	0.0768
<i>wR</i> ₂ [<i>I</i> > 2σ(<i>I</i>)]	0.2098	0.1562	0.1947
<i>R</i> ₁ (all data)	0.0835	0.0606	0.0910
<i>wR</i> ₂ (all data)	0.2218	0.1609	0.2023
Solvent System	CHCl ₃ /MeOH	C ₆ H ₆ /MeOH	C ₆ H ₆ /MeCN
CCDC No.	1572116	1572117	1572118

Table S2. Crystal data and structure refinements for **18Ni**, **18Pd**, and **20**.

Compound	18Ni	18Pd	20
Empirical Formula	C ₇₅ H ₇₂ N ₆ NiOPS ₂	C ₆₅ H ₆₀ N ₅ OCl ₄ NiPPdS ₂	C _{71.65} H ₅₇ N ₄ OCl _{14.59} NiPS ₂
<i>Mw</i>	1227.18	1270.47	1660.94
Crystal System	Monoclinic	Monoclinic	Triclinic
Space Group	C 2/c (No.15)	<i>P</i> 2 ₁ / <i>a</i> (No.14)	<i>P</i> -1 (No.2)
<i>a</i>	41.875(9) Å	13.476(3) Å	14.070(3) Å
<i>b</i>	12.116(2) Å	18.301(3) Å	15.707(3) Å
<i>c</i>	33.342(7) Å	25.301(5) Å	18.170(3) Å
α	90°	90°	96.635(3)°
β	127.805(4)°	103.474(6)°	103.033(7)°
γ	90°	90°	104.706(2)°
Volume	13366(5) Å ³	6068(2) Å ³	3719.8(12) Å ³
Z	8	4	2
Density (calcd.)	1.220 g/cm ³	1.391 g/cm ³	1.483 g/cm ³
Completeness	0.982	0.967	0.966
Goodness-of-fit	1.024	1.037	1.050
<i>R</i> ₁ [<i>I</i> >2σ(<i>I</i>)]	0.0435	0.0613	0.0674
<i>wR</i> ₂ [<i>I</i> >2σ(<i>I</i>)]	0.1173	0.1726	0.1875
<i>R</i> ₁ (all data)	0.0494	0.0696	0.0847
<i>wR</i> ₂ (all data)	0.1210	0.1789	0.1989
Solvent System	C ₆ H ₆ /MeCN	CCl ₄ /MeCN	CCl ₄ /MeCN
CCDC No.	1572119	1572120	1572121

Table S3. Crystal data and structure refinements for **22** and **26**.

Compound	22	26
Empirical Formula	C ₇₀ H _{58.89} N ₄ O ₃ Cl ₆ NiP ₂	C _{85.77} H _{73.77} N ₆ O _{7.59} Cl ₃ NiPS ₂
<i>Mw</i>	2266.44	1570.17
Crystal System	Monoclinic	Monoclinic
Space Group	<i>P</i> 2 ₁ / <i>n</i> (No.14)	<i>P</i> 2 ₁ / <i>c</i> (No.14)
<i>a</i>	15.250(2) Å	15.0591(17) Å
<i>b</i>	23.282(3) Å	27.873(3) Å
<i>c</i>	18.497(3) Å	18.771(2) Å
α	90°	90°
β	104.562(4)°	101.374(3)°
γ	90°	90°
Volume	6356.4(16) Å ³	7724.2(15) Å ³
<i>Z</i>	4	4
Density (calcd.)	1.365 g/cm ³	1.350 g/cm ³
Completeness	0.989	0.967
Goodness-of-fit	1.087	1.067
<i>R</i> ₁ [<i>I</i> >2σ(<i>I</i>)]	0.0687	0.0809
<i>wR</i> ₂ [<i>I</i> >2σ(<i>I</i>)]	0.1992	0.2261
<i>R</i> ₁ (all data)	0.0836	0.0941
<i>wR</i> ₂ (all data)	0.2087	0.2385
Solvent System	CHCl ₃ /MeOH	CH ₂ Cl ₂ /MeOH
CCDC No.	1572122	1572123

Table S4. Crystal data and structure refinements for **27** and **28**.

Compound	27	28
Empirical Formula	C ₇₃ H ₅₇ N ₄ O ₅ Cl ₂₀ NiPS ₂	C ₇₃ H ₆₈ N ₄ O _{5.5} NiPS ₂
<i>Mw</i>	1933.02	1243.11
Crystal System	Triclinic	Monoclinic
Space Group	<i>P</i> -1 (No.2)	<i>C</i> 2/ <i>c</i> (No.15)
<i>a</i>	14.5544(7) Å	28.316(5) Å
<i>b</i>	16.0580(5) Å	16.521(2) Å
<i>c</i>	19.2527(17) Å	32.462(6) Å
α	80.1620(10)°	90°
β	86.521(12)°	109.086(5)°
γ	67.319(8)°	90°
Volume	4090.5(5) Å ³	14351(4) Å ³
<i>Z</i>	2	8
Density (calcd.)	1.569 g/cm ³	1.151 g/cm ³
Completeness	0.959	0.985
Goodness-of-fit	1.007	1.025
<i>R</i> ₁ [<i>I</i> > 2σ (<i>I</i>)]	0.0422	0.0634
<i>wR</i> ₂ [<i>I</i> > 2σ (<i>I</i>)]	0.1225	0.1986
<i>R</i> ₁ (all data)	0.0474	0.0760
<i>wR</i> ₂ (all data)	0.1250	0.2087
Solvent System	CCl ₄ /MeOH	THF/hexane
CCDC No.	1572124	1572125

6. Absorption Spectra

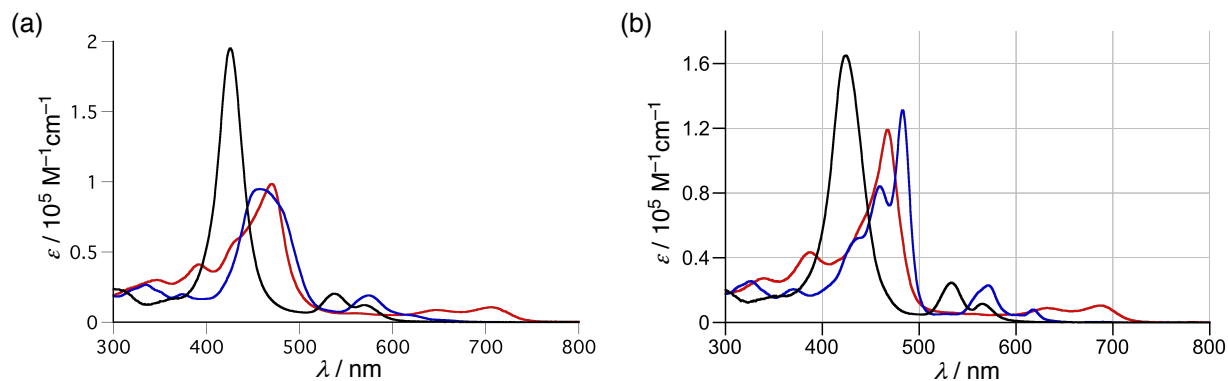


Figure S103. Absorption spectra of **17Ni** (a, black), **18Ni** (a, red), **10Ni** (a, blue), **17Pd** (b, black), **18Pd** (b, red), and **10Pd** (b, blue) in CH_2Cl_2 .

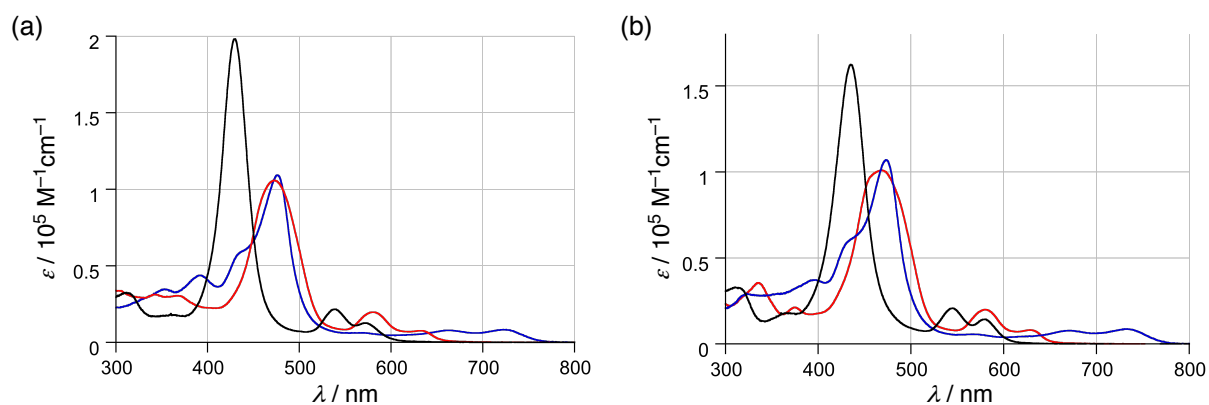


Figure S104. Absorption spectra of **19** (a, black), **20** (a, blue), **11** (a, red), **21** (b, black), **22** (b, blue), and **12** (b, red) in CH_2Cl_2 .

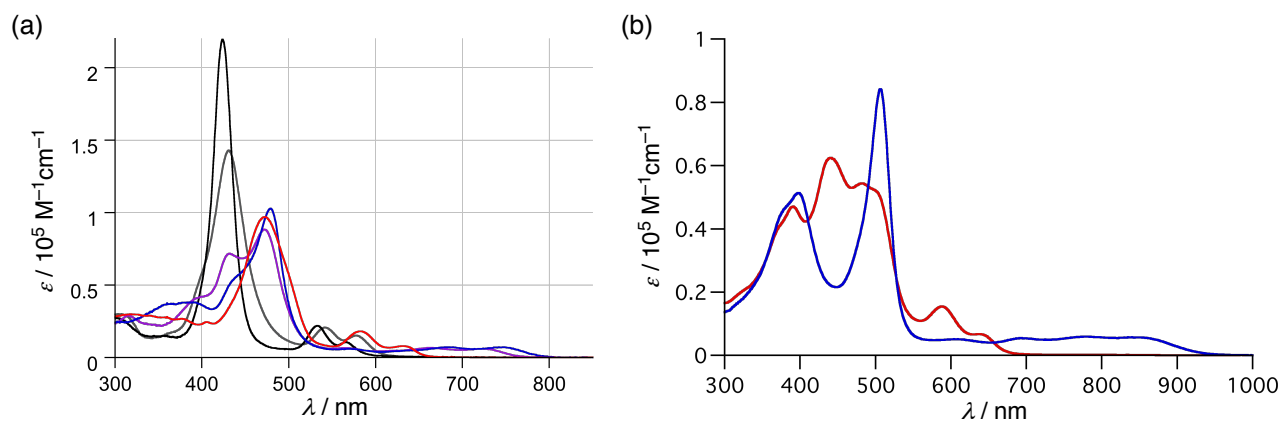


Figure S105. Absorption spectra of **23** (a, black), **24** (a, gray), **25** (a, violet), **26** (a, blue), **13** (a, red), **28** (b, blue), and **15** (b, red) in CH_2Cl_2 .

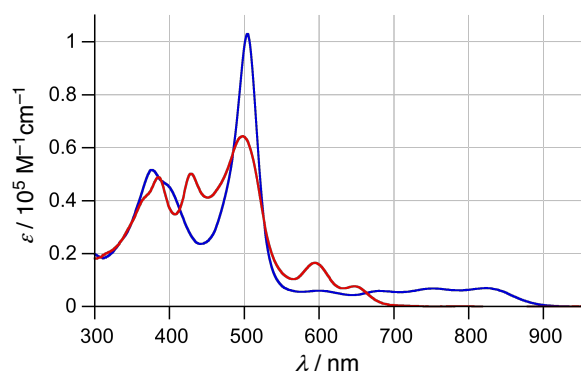


Figure S106. Absorption spectra of **27** (blue) and **14** (red) in CH_2Cl_2 .

7. Determination of Pyramidal Inversion Barriers

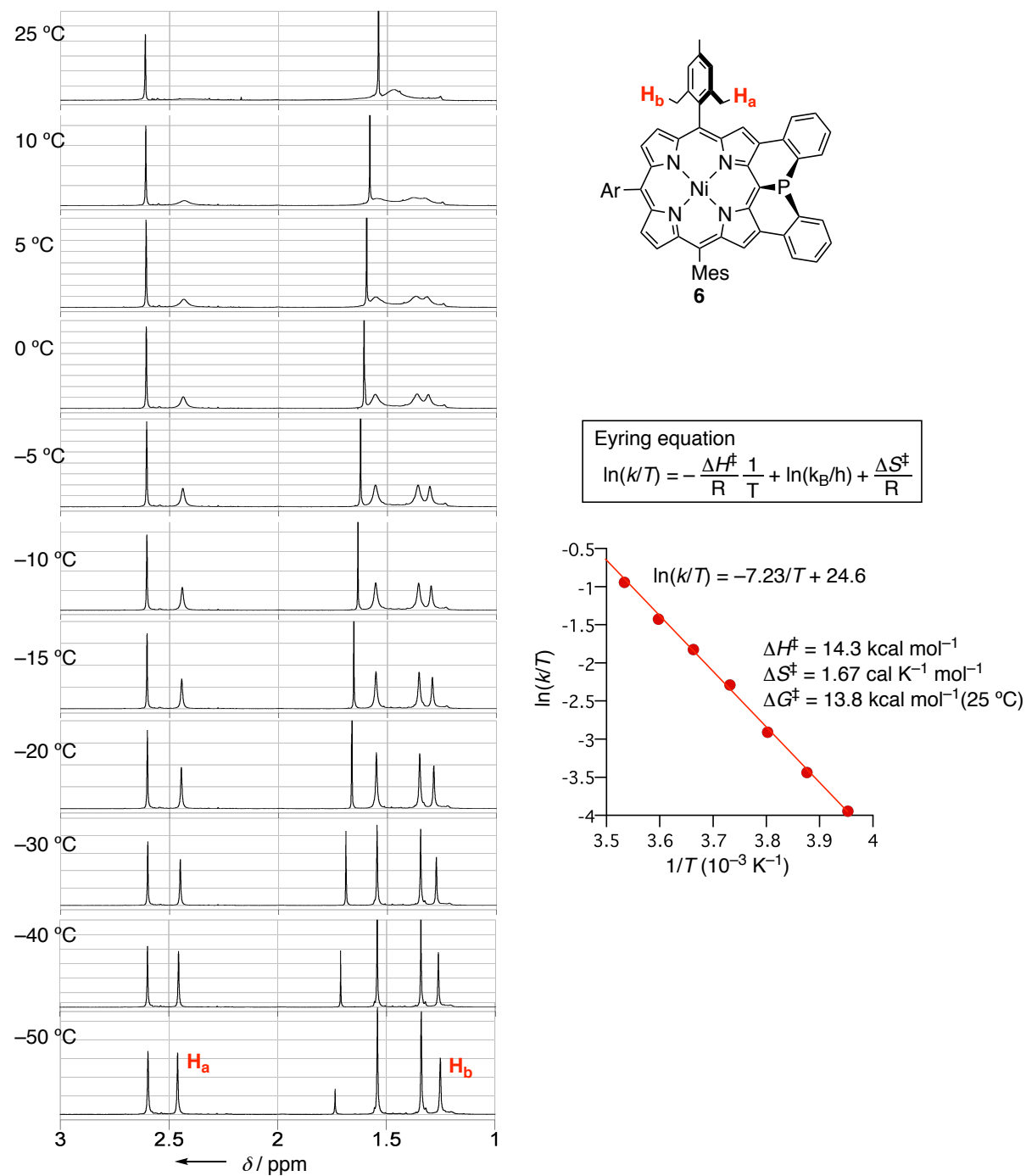
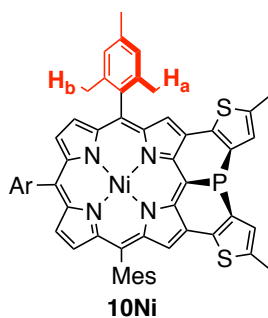
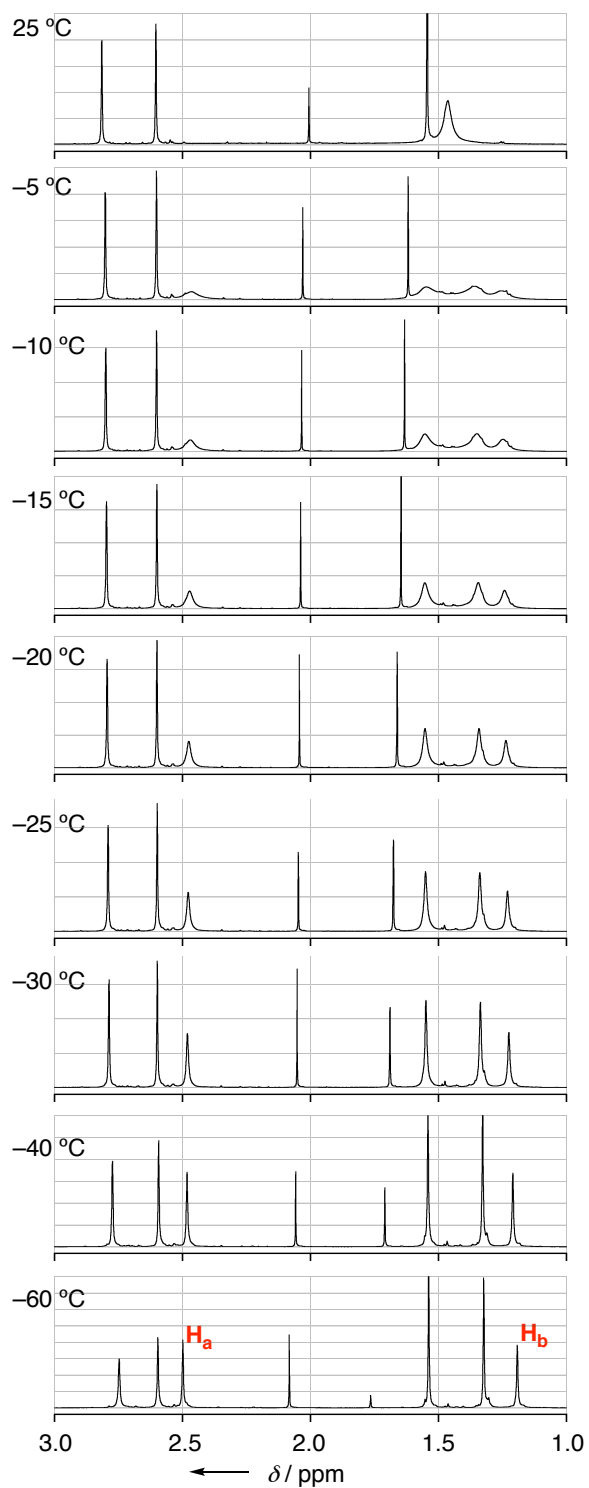


Figure S107. Temperature dependent ^1H NMR spectra of **6** in CDCl_3 and Eyring plot for determination of the pyramidal inversion barrier.



Eyring equation

$$\ln(k/T) = -\frac{\Delta H^\ddagger}{R} \frac{1}{T} + \ln(k_B/h) + \frac{\Delta S^\ddagger}{R}$$

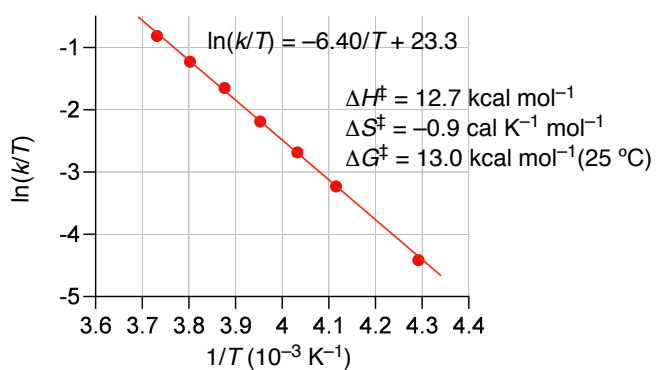
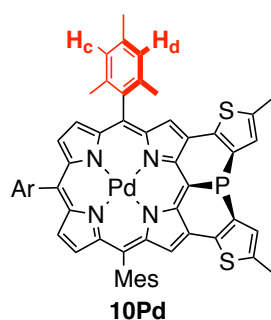
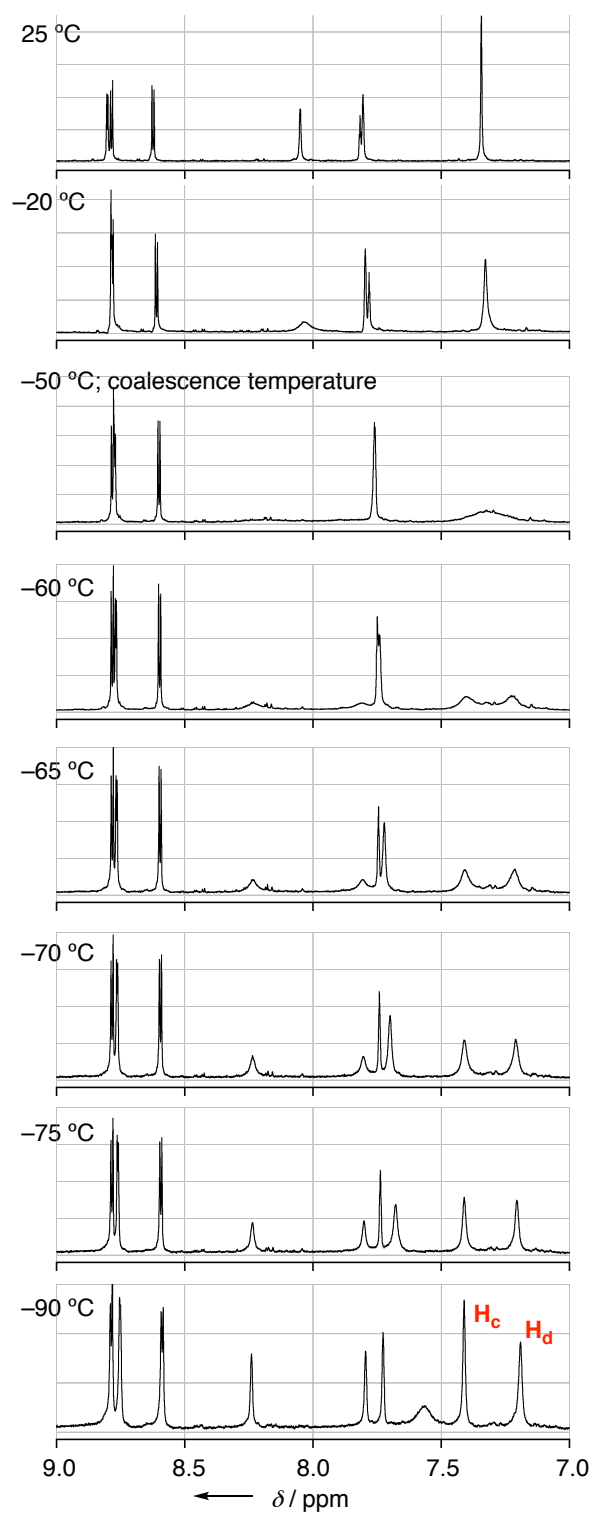


Figure S108. Temperature dependent ^1H NMR spectra of **10Ni** in CDCl_3 and Eyring plot for determination of the pyramidal inversion barrier.



Eyring equation

$$\ln(k/T) = -\frac{\Delta H^\ddagger}{R} \frac{1}{T} + \ln(k_B/h) + \frac{\Delta S^\ddagger}{R}$$

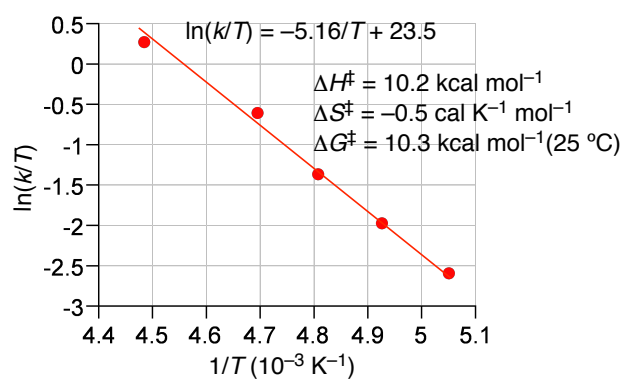
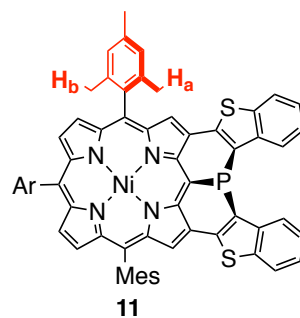
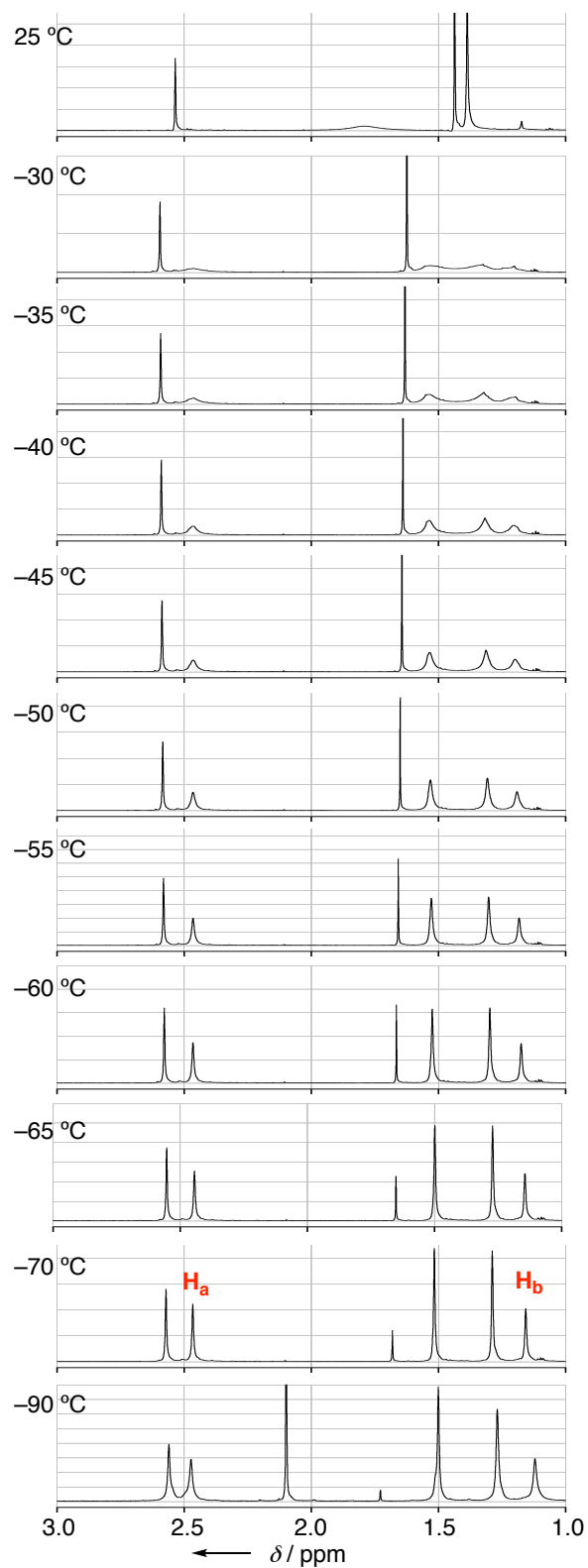


Figure S109. Temperature dependent ^1H NMR spectra of **10Pd** in CD_2Cl_2 and Eyring plot for determination of the pyramidal inversion barrier.



Eyring equation

$$\ln(k/T) = -\frac{\Delta H^\ddagger}{R} \frac{1}{T} + \ln(k_B/h) + \frac{\Delta S^\ddagger}{R}$$

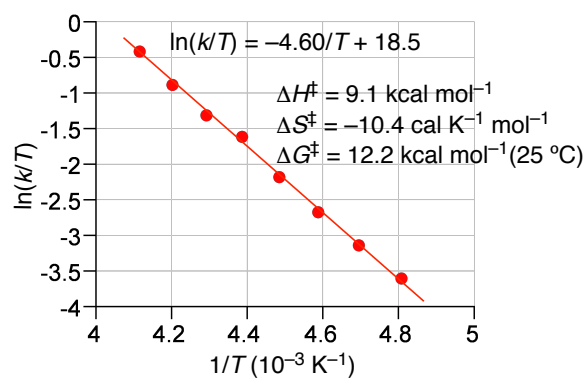
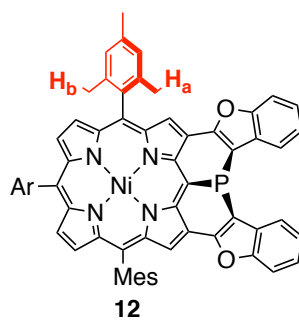
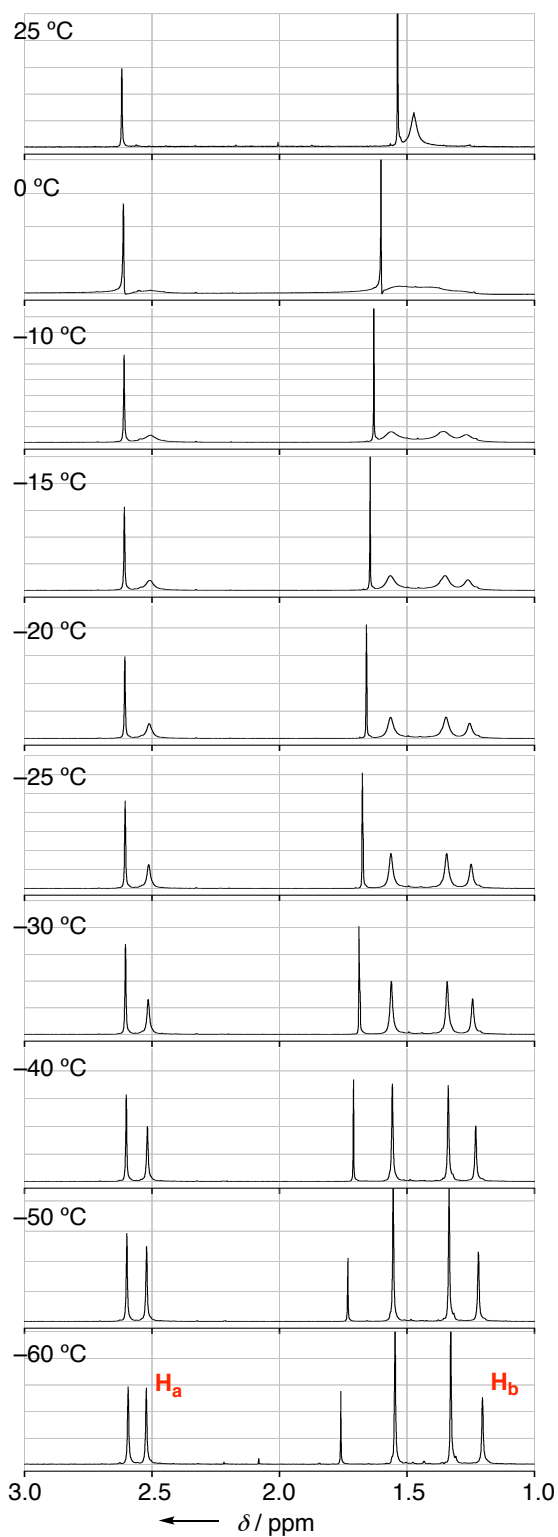


Figure S110. Temperature dependent ^1H NMR spectra of **11** in CD_2Cl_2 and Eyring plot for determination of the pyramidal inversion barrier.



Eyring equation

$$\ln(k/T) = -\frac{\Delta H^\ddagger}{R} \frac{1}{T} + \ln(k_B/h) + \frac{\Delta S^\ddagger}{R}$$

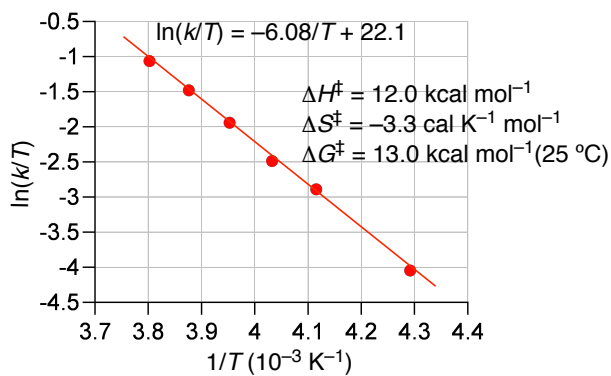
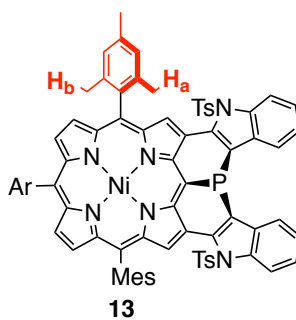
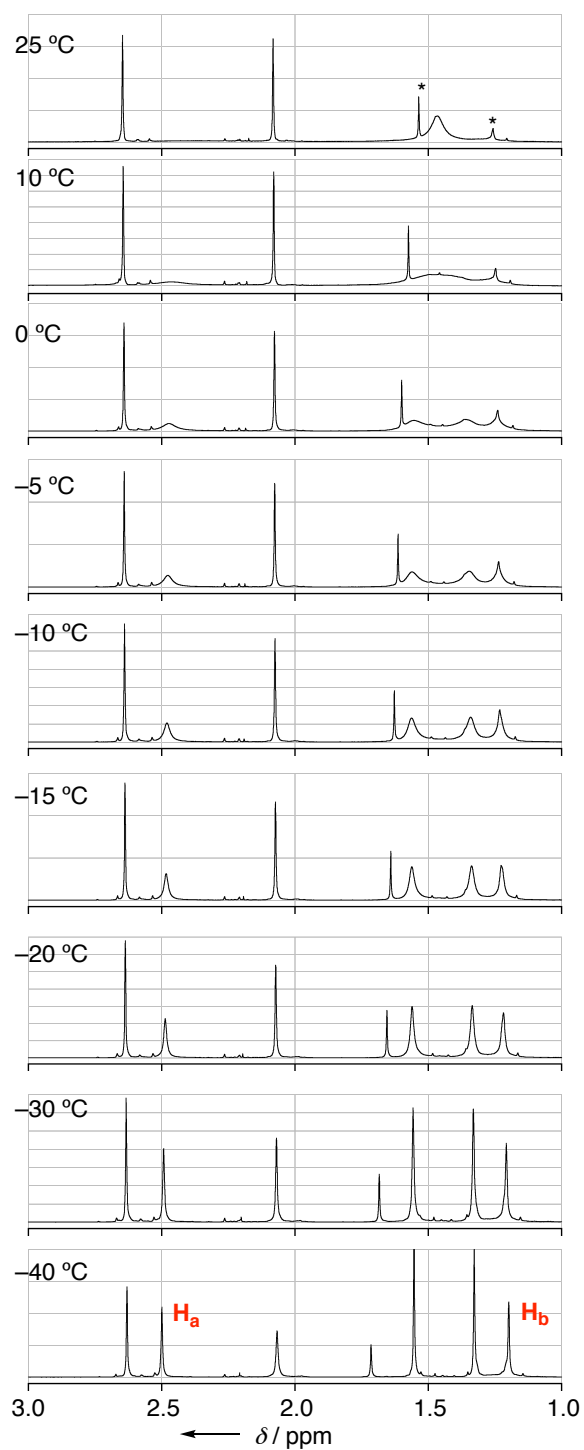


Figure S111. Temperature dependent ^1H NMR spectra of **12** in CDCl_3 and Eyring plot for determination of the pyramidal inversion barrier.



Eyring equation

$$\ln(k/T) = -\frac{\Delta H^\ddagger}{R} \frac{1}{T} + \ln(k_B/h) + \frac{\Delta S^\ddagger}{R}$$

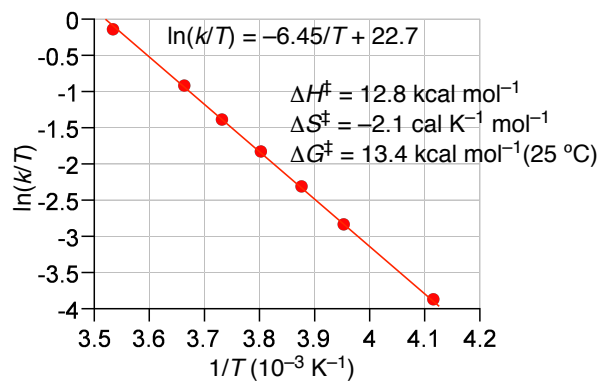
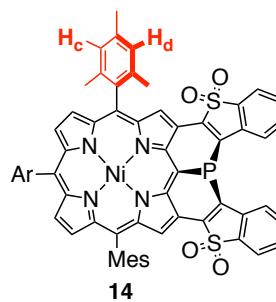
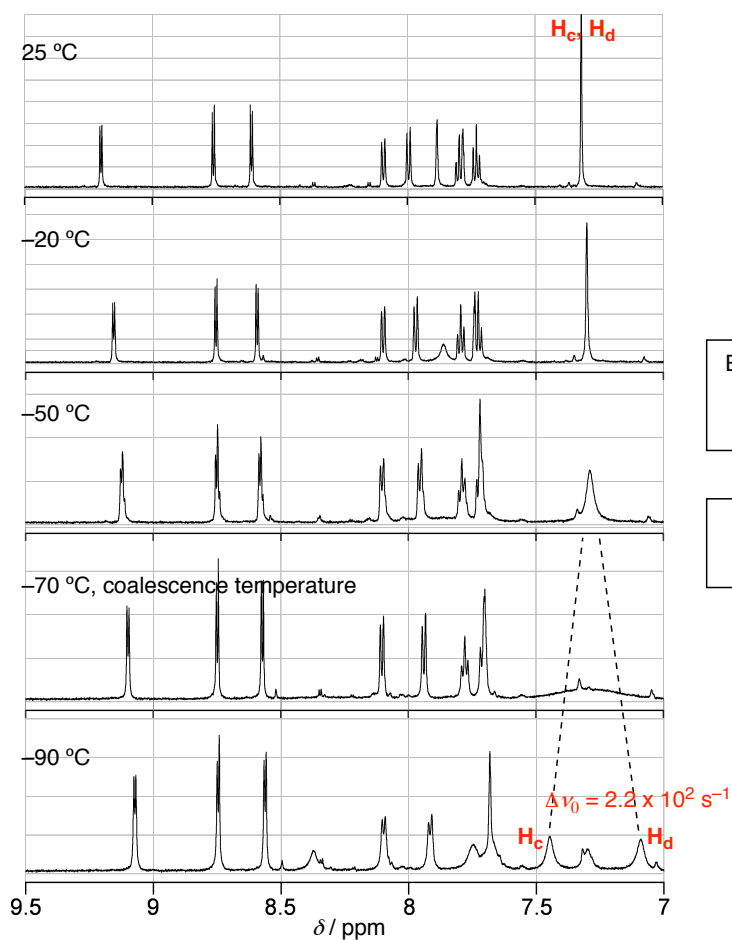


Figure S112. Temperature dependent ^1H NMR spectra of **13** in CDCl_3 and Eyring plot for determination of the pyramidal inversion barrier.



Eyring equation

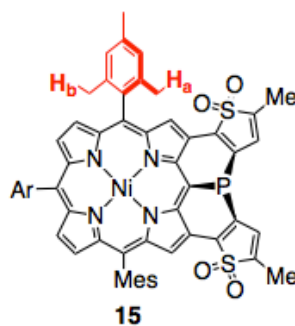
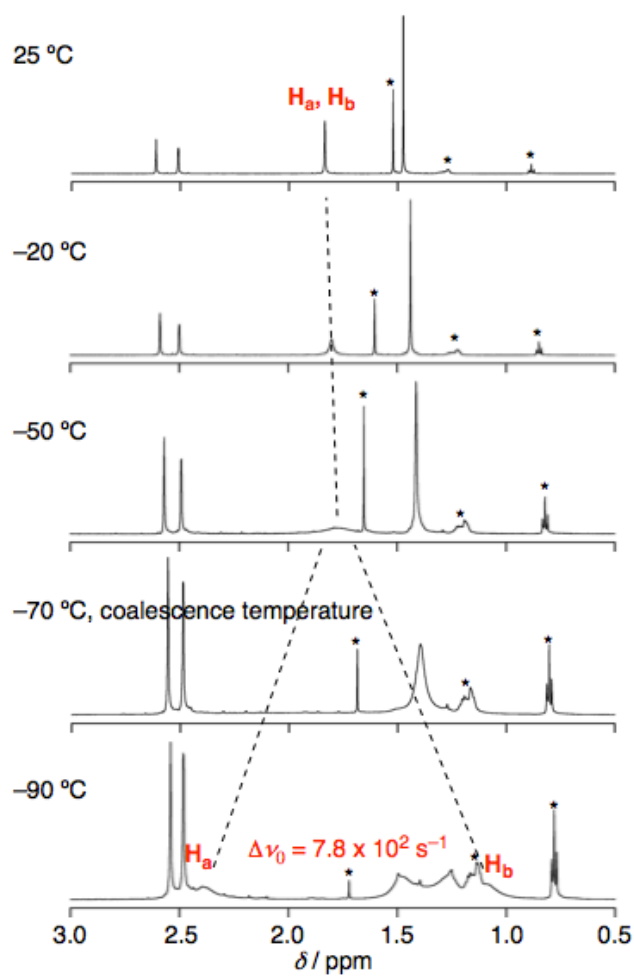
$$k_{T_C} = \frac{k_B T_C}{h} \exp\left(-\frac{\Delta G^\ddagger_{T_C}}{RT_C}\right) \quad \begin{array}{l} T_C: \text{coalescence temperature} \\ k_{T_C}: \text{rate constant at coalescence} \end{array}$$

$$k_{T_C} = 2.22 \times \Delta \nu_0 \text{ (s}^{-1}\text{)} \quad \Delta \nu_0: \text{peak separation}$$

J. Chem. Educ. **1977**, *54*, 258.

$$k = 4.9 \times 10^2 \text{ s}^{-1}, \Delta G^\ddagger_{203} = 9.2 \text{ kcal/mol}$$

Figure S113. Temperature dependent ^1H NMR spectra of **14** in CD_2Cl_2 and determination of the pyramidal inversion barrier.



Eyring equation

$$k_{T_C} = \frac{k_B T_C}{h} \exp\left(-\frac{\Delta G^\ddagger_{T_C}}{RT_C}\right)$$

T_C : coalescence temperature
 k_{T_C} : rate constant at coalescence

$$k_{T_C} = 2.22 \times \Delta \nu_0 \text{ (s}^{-1}\text{)}$$

$\Delta \nu_0$: peak separation
J. Chem. Educ. **1977**, *54*, 258.

$$k_{T_C} = 1.7 \times 10^3 \text{ s}^{-1}, \Delta G^\ddagger_{203} = 8.7 \text{ kcal/mol}$$

Figure S114. Temperature dependent ^1H NMR spectra of **15** in CD_2Cl_2 and determination of the pyramidal inversion barrier.

8. Electrochemical Properties

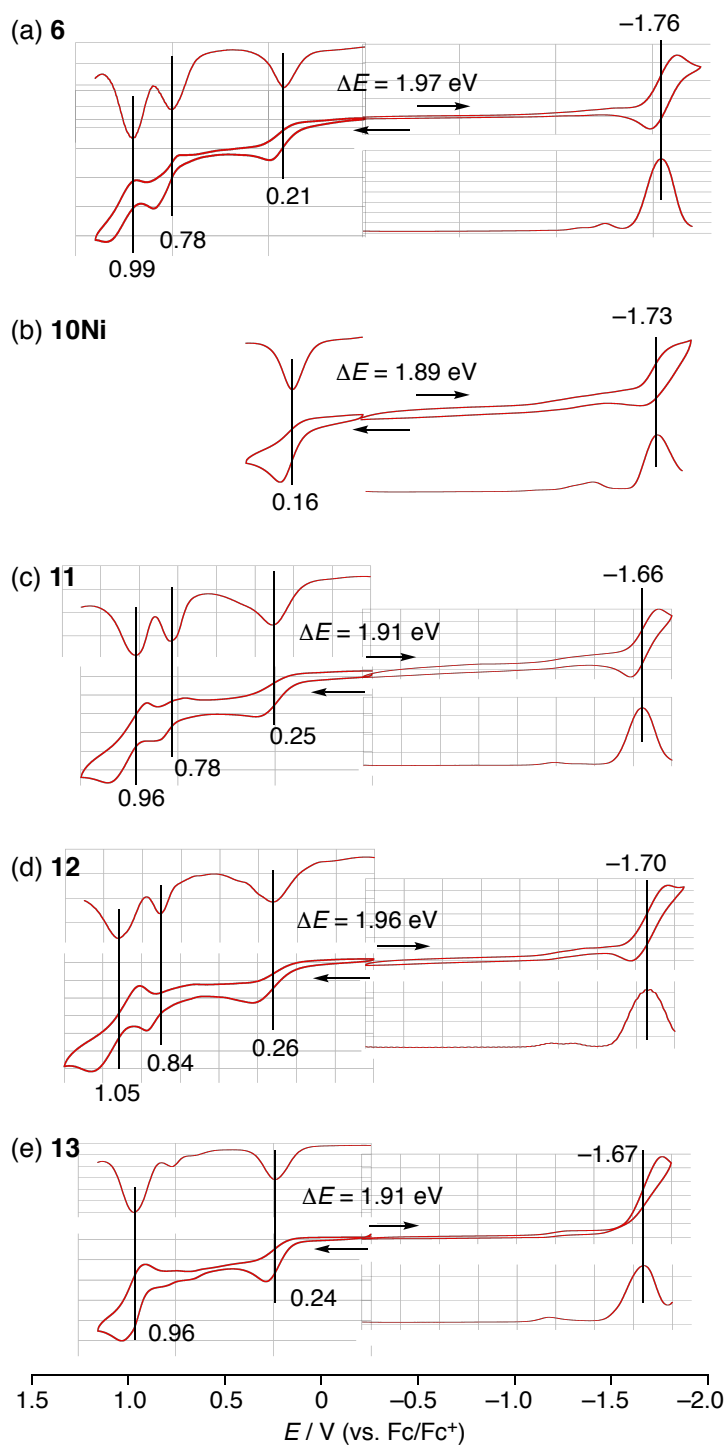


Figure S115. Cyclic voltammograms and differential pulse voltammograms of (a) **6**, (b) **10Ni**, (c) **11**, (d) **12**, and (e) **13** in anhydrous CH_2Cl_2 . Potentials [V] vs ferrocene/ferrocenium cation. Scan rate, 0.05 Vs^{-1} ; working electrode, glassy carbon; counter electrode, Pt wire; supporting electrolyte, 0.1 M Bu_4NPF_6 .

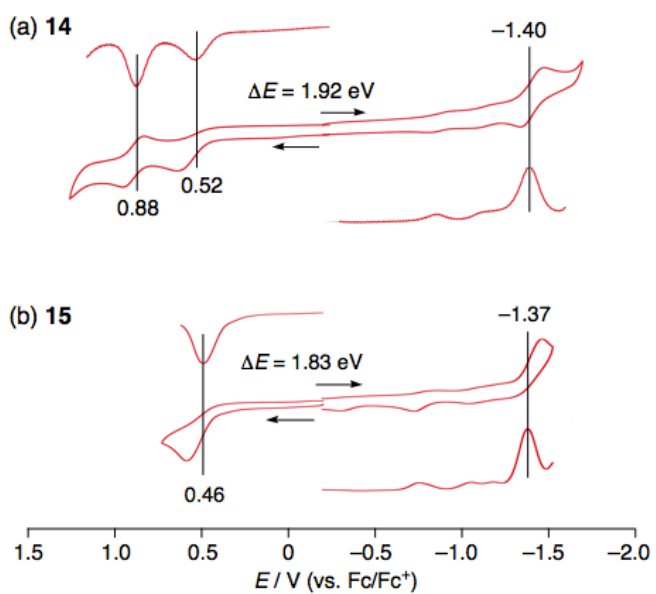


Figure S116. Cyclic voltammograms and differential pulse voltammograms of (a) **14** and (b) **15** in anhydrous CH_2Cl_2 . Potentials [V] vs ferrocene/ferrocenium cation. Scan rate, 0.05 Vs^{-1} ; working electrode, glassy carbon; counter electrode, Pt wire; supporting electrolyte, $0.1 \text{ M Bu}_4\text{NPF}_6$.

9. Temperature Dependent Magnetic Susceptibility

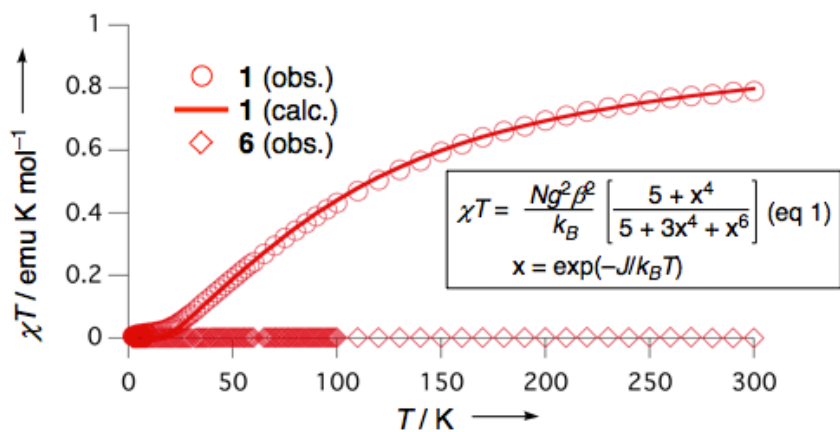


Figure S117. Temperature dependent magnetic susceptibility of **1** (circles), **6** (diamonds), and simulated χT value for **1** (solid line) which was calculated from eq 1 with fitted parameter of $J_1/k_B = -44.7$ K.

10. DFT Calculations

The calculations were performed by the density functional theory (DFT) method with restricted B3LYP (Becke's three-parameter hybrid exchange functionals and the Lee-Yang-Parr correlation functional)^[S2] level, employing basis sets 6-31G(d) for C, H, O, N, S, and P and LANL2DZ for Ni and Pd using the *Gaussian 09* program.^[S2] The initial geometries for optimization of **6**, **10Ni**, and **12**, were obtained from the X-ray structures. The initial geometries for optimization of **10Pd**, **11**, **14**, and **15** were obtained from X-ray structures of the corresponding phosphine oxide. *meso*-Aryl groups were replaced with phenyl groups to simplify the calculation. The planar transition structure was also calculated in the same level and is confirmed by one imaginary frequency corresponding to the pyramidal inversion. The nucleus independent chemical shift (NICS) values^[S3] were obtained with the GIAO method at the B3LYP/6-31G(p) level.

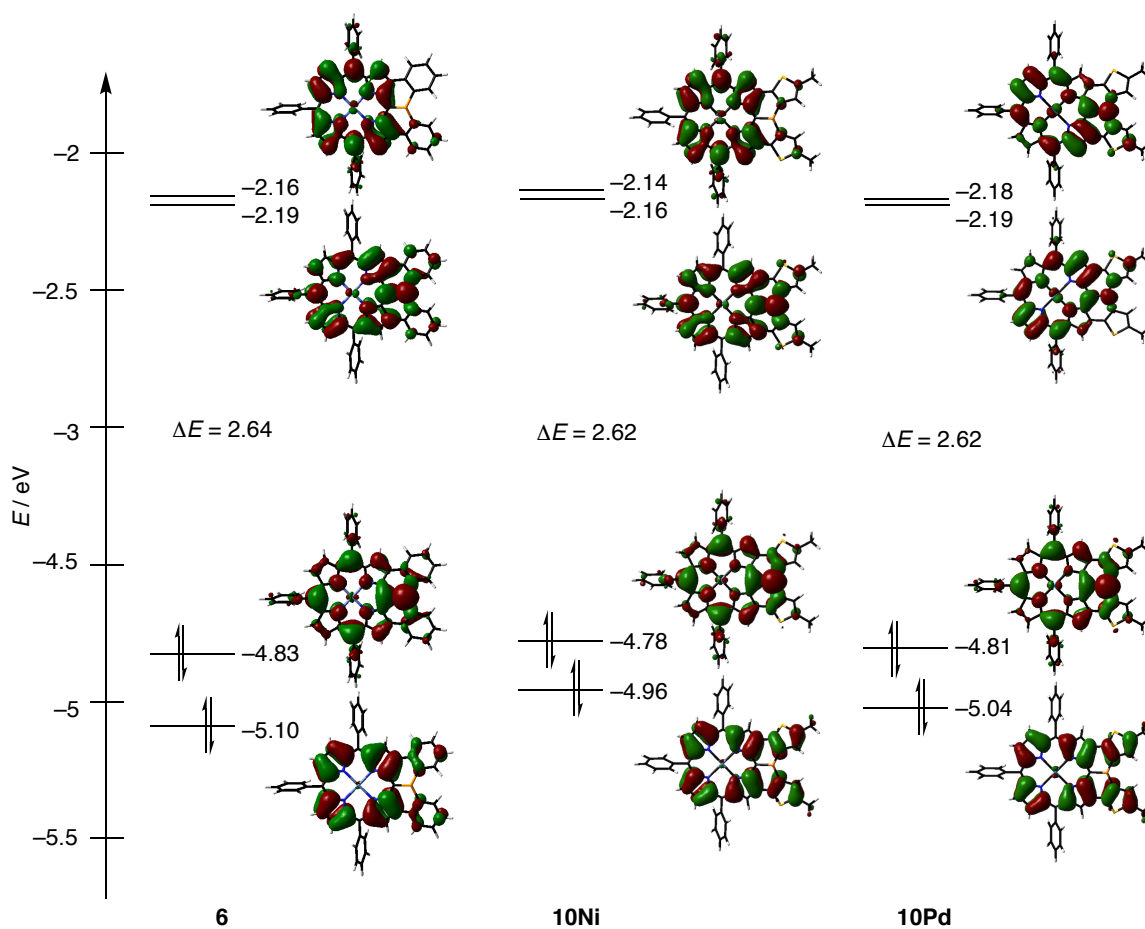


Figure S118. Energy diagram and representative Kohn-Sham orbitals of **6**, **10Ni**, and **10Pd**.

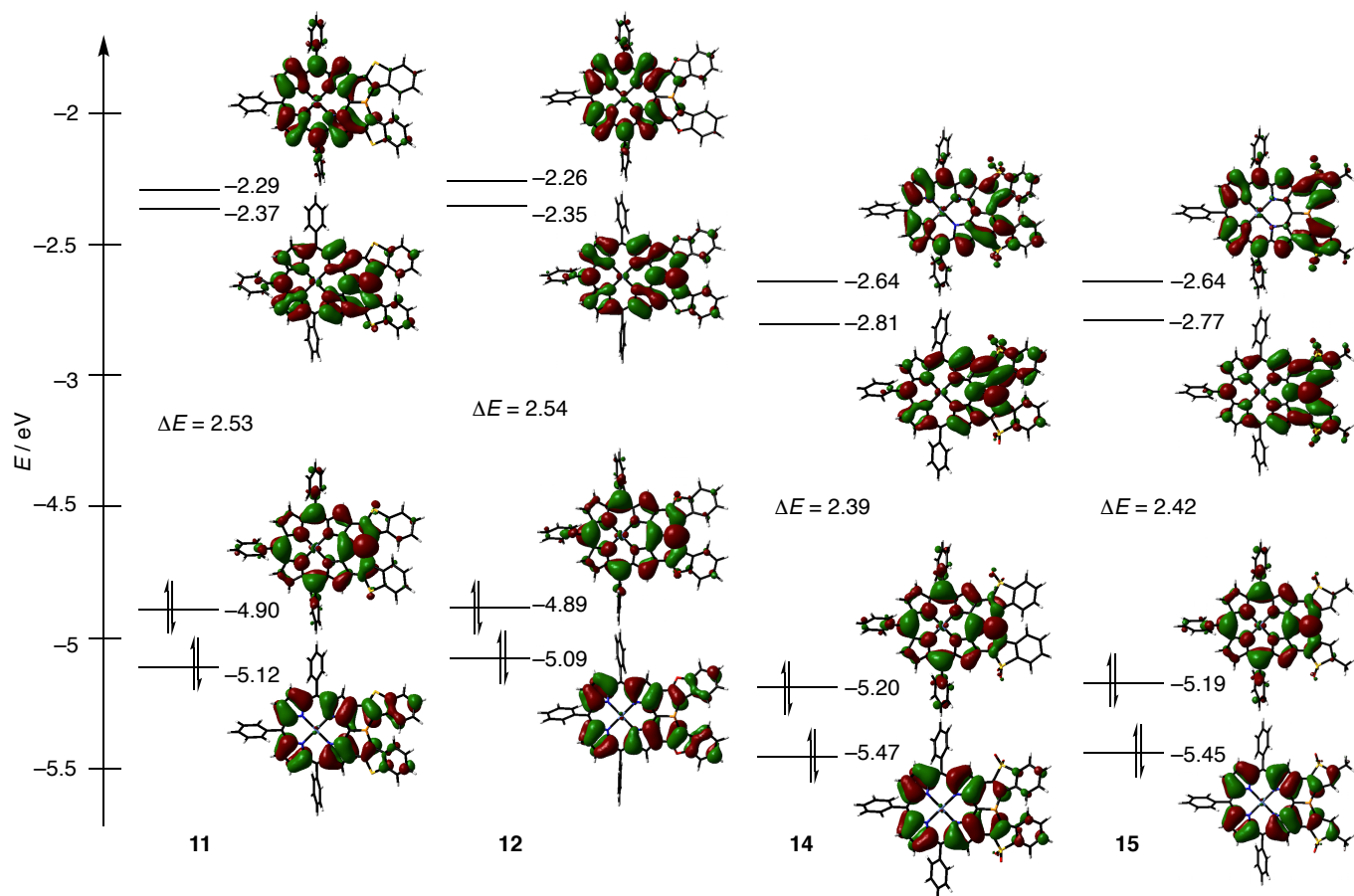


Figure S119. Energy diagram and representative Kohn-Sham orbitals of **11**, **12**, **14**, and **15**.

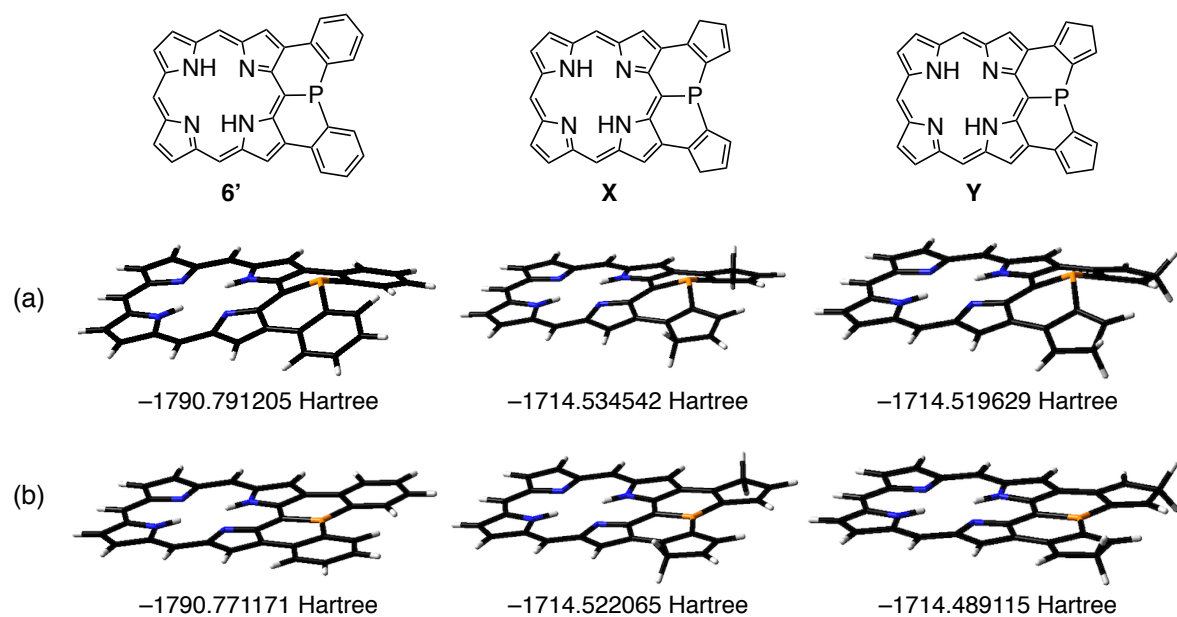


Figure S120. Optimized structures of **6'**, **X**, and **Y** (a) without symmetric restriction and (b) with symmetric restriction to C_s and sum of total energy and zero-point energy.

Compound (structure)	NICS(0) ppm								
	1	2	3	4	5	6	7	8	9
6' (pyramidal)	-14.18	-13.67	-2.85	-12.53	-5.80	+4.37	+2.97	-7.47	-7.80
6' (planar)	-11.78	-17.99	-2.43	-11.37	-14.09	-3.91	-5.92	-9.29	-10.20
X (pyramidal)	-14.28	-15.61	-2.98	-12.80	-9.45	+0.20	-1.12	+0.34	+0.73
X (planar)	-11.40	-19.67	-2.53	-11.26	-17.71	-10.15	-11.99	+0.43	+1.04
Y (pyramidal)	-14.13	-12.80	-2.82	-12.62	-2.91	+5.52	+5.59	-1.74	-2.05
Y (planar)	-11.45	-13.45	-2.63	-11.32	-4.35	+3.67	+3.62	-3.07	-3.35

Figure S121. NICS(0) values at various positions of **6'**, **X**, and **Y** in the pyramidal ground state and planar transition state.

11. References

- [S1] SHELXL-97 and SHELXS-97, program for refinement of crystal structures from diffraction data, University of Goettingen, Goettingen (Germany); Sheldrick, G.; Schneider, T. *Methods Enzymol.* **1997**, *277*, 319.
- [S2] (a) Gaussian 09, Revision A.02, Frisch, M. J.; Trucks, G. W.; Schlegel, H. B.; Scuseria, G. E.; Robb, M. A.; Cheeseman, J. R.; Scalmani, G.; Barone, V.; Mennucci, B.; Petersson, G. A.; Nakatsuji, H.; Caricato, M.; Li, X.; Hratchian, H. P.; Izmaylov, A. P.; Bloino, J.; Zheng, G.; Sonnenberg, J. L.; Hada, M.; Ehara, M.; Toyota, K.; Fukuda, R.; Hasegawa, J.; Ishida, M.; Nakajima, T.; Honda, Y.; Kitao, O.; Nakai, H.; Vreven, T.; Montgomery Jr., J. A.; Peralta, J. E.; Ogliaro, F.; Bearpark, M.; Heyd, J. J.; Brothers, E.; Kudin, K. N.; Staroverov, V. N.; Kobayashi, R.; Normand, J.; Raghavachari, K.; Rendell, A.; Burant, J. C.; Iyengar, S. S.; Tomasi, J.; Cossi, M.; Rega, N.; Millam, J. M.; Klene, M.; Knox, J. E.; Cross, J. B.; Bakken, V.; Adamo, C.; Jaramillo, J.; Gomperts, R.; Stratmann, R. E.; Yazyev, O.; Austin, A. J.; Cammi, R.; Pomelli, C.; Ochterski, J. W.; Martin, R. L.; Morokuma, K.; Zakrzewski, V. G.; Voth, G. A.; Salvador, P.; Dannenberg, J. J.; Dapprich, S.; Daniels, A. D.; Farkas, O.; Foresman, J. B.; Ortiz, J. V.; Cioslowski, J.; Fox, D. J. Gaussian, Inc.: Wallingford, CT, 2009. (b) Becke, A. D. *J. Chem. Phys.* **1993**, *98*, 1372; (c) Lee, C.; Yang, W.; Parr, R. G. *Phys. Rev. B* **1998**, *37*, 785.
- [S3] (a) Schleyer, P. v. R.; Maerker, C.; Dransfeld, A.; Jiao, H.; Hommes, N. J. R. v. E. *J. Am. Chem. Soc.*, **1996**, *118*, 6317. (b) Chen, Z.; Wannere, C. S.; Corminboeuf, C.; Puchta, R.; Schleyer, P. v. R. *Chem. Rev.* **2005**, *105*, 3842.